An investigation of cellulose nitrates and double based propellant by spectroscopic techniques with particular reference to E.S.C.A

Stephenson, Peter John

AN INVESTIGATION OF CELLULOSE NITRATES AND DOUBLE BASED PROPELLANT BY SPECTROSCOPIC TECHNIQUES WITH PARTICULAR REFERENCE TO E.S.C.A.

by

PETER JOHN STEPHENSON, B.TECH.

A Candidate for the Degree of Doctor of Philosophy

Graduate Society,
University of Durham

September 1981

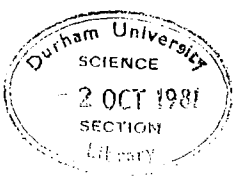

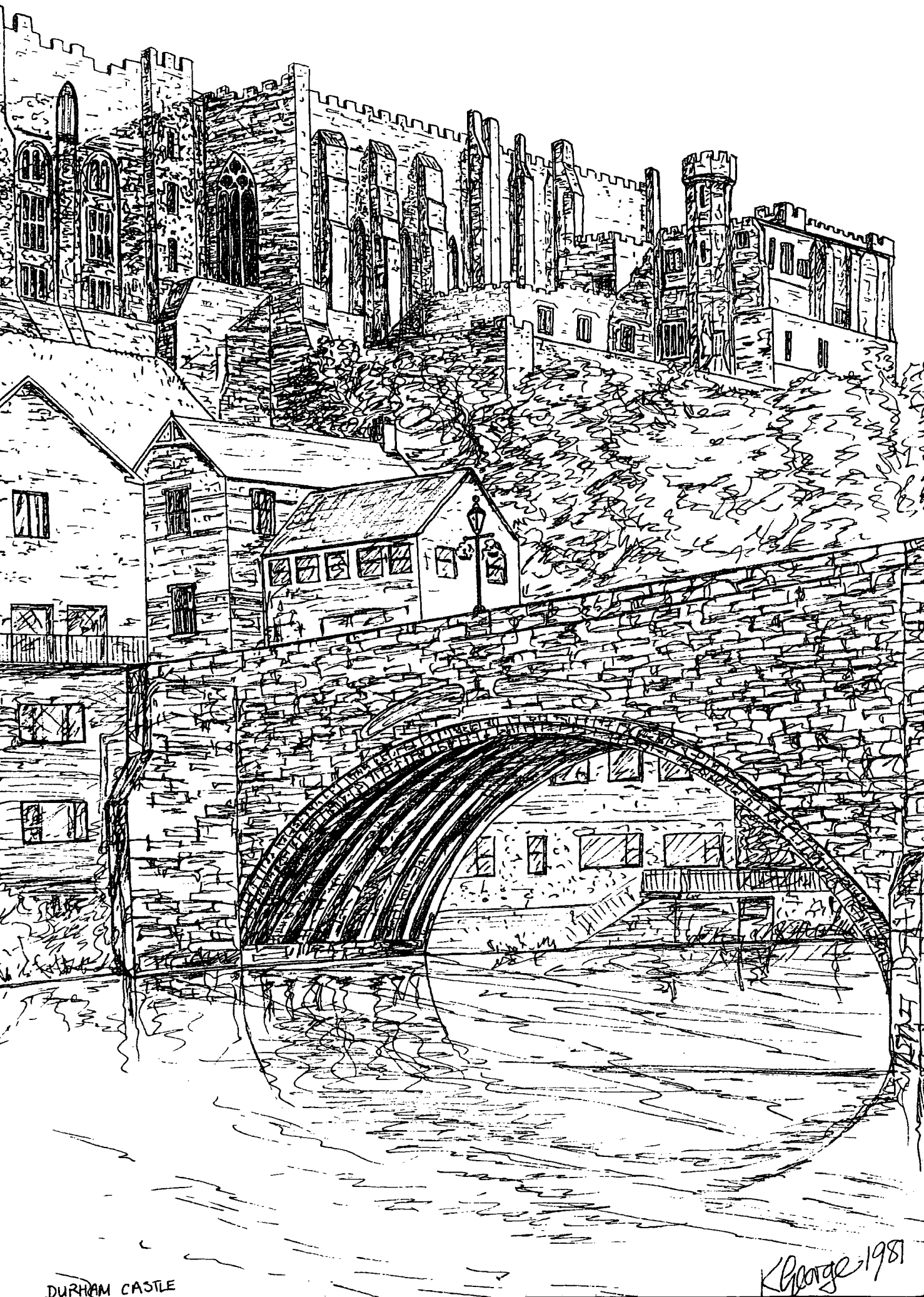

DURHAM CASTLE

To Kirstin and my parents

"There is no such thing as a problem without a gift for you in its hands - we seek problems because we need their gifts"

Richard Bach

"There is no such thing as a problem without a gift for you in its hands - we seek problems because we need their gifts"

Richard Bach

CONTENTS

ABSTRACT

X-ray photoelectron spectroscopy, (E.S.C.A.), has been used to investigate the surface chemistry of cellulose nitrates and double based propellant. The nitration and denitration of cellulose nitrates has been studied and important conclusions drawn on the complex equilibria established at the surface, ($<50^{o}A$), of cellulose fibres particularly with respect to sulphate ester formation in mixed acid nitrations. The degradation of double based propellants and cellulose nitrate, (a major component), on exposure to U.V. light has also been studied by E.S.C.A. and new information on the build up of degradation products at the surface is presented. The migration of stabiliser, (diethyldiphenyl-urea), to the surface regions of double based propellant has also been monitored using E.S.C.A. and is found to be greatest in those propellants containing a large percentage of nitroglycerin.

75.5 MHz, proton decoupled, ^{13}C n.m.r. spectra of a series of cellulose nitrates have been assigned and partial degrees of substitution established at individual sites of a β-d glucopyranose rings. This important distribution data is supplemented by sequence distribution data extracted from the anomeric region of the ^{13}C spectrum which allows rough models of sections of cellulose nitrate chains to be constructed for particular degrees of substitution. Important correlations are drawn between these substitution patterns and the mean (101) interchain spacings in cellulose nitrates and the accuracy of birefringence measurements for the estimation of degree of substitution in cellulose nitrates is assessed. Using all the data levels available from the various techniques

employed arguments are presented in favour of a nitration equilibrium rather than an accessibility theory.

MEMORANDUM

The work outlined in this thesis is wholly original except where referenced and this thesis contains material which forms part or whole of the following publications:

1. Clark, D.T., Stephenson, P.J. "Proceedings of the Waltham Abbey Conference", Ed. T.J. Lewis at PERME Waltham Abbey, 1980, Plenum Press.

2. Clark, D.T., Stephenson, P.J. and Heatley, F. Polymer, 1981, 22, 1112-1117

3. Clark. D.T., Stephenson P.J., Polymer Communications 1981, in press.

4. Clark D.T.. Stephenson, P.J., Polymer, submitted 1981.

5. Clark D.T., Stephenson, P.J., J.Polym.Sci.. submitted 1981.

The work described in Chapter Five also makes reference to early work described in-

6. Baker, F.S., Clark, D.T. and Stephenson, P.J., 'Proceedings of the Waltham Abbey Conference, Ed. T.J. Lewis, PERME Waltham Abbey, Essex, 1980, Plenum Press.

ACKNOWLEDGEMENTS

The greatest thanks in this acknowledgement must be offered to my Supervisor, Professor David T. Clark for help and advice throughout the three years. I am also indebted to Drs. Tom Lewis and Frank Baker of the Ministry of Defence, Waltham Abbey, for advice and criticism and in the case of the birefringence studies for the results referenced in Chapter Seven. For their help with the N.M.R. studies I would first like to thank Dr. Frank Heatley of the University of Manchester for running many of the excellent spectra used in this thesis. Also of great importance was the assistance of Tony Cunliffe (M.O.D.), Jim Peeling (Saudi Arabia) and Ray Matthews (Durham).

I have also drawn on the skill and experience of Ron Hardy for the X-ray diffraction measurements and Colin Percival, friend and soccer ruffian, for X-ray diffraction and all microscope work.

In the U.V. degradation work acknowledgement is due to Hugh Munro for help and advice and use of his apparatus. The theoretical work which supports the assignments of E.S.C.A. peaks in this thesis was carried out by Alan Harrison, friend, fellow Geordie and the best theorist in Stanley. Thanks are also due to John Warwicker of the Shirley Institute for early advice and to Alan Dilks, now of Xerox Co. Webster, New York, for early inspiration. Acknowledged too are all members of the research group who grow too numerous to mention. Lastly, I would like to pay tribute to Marion Wilson, my typist. whose skill and correction of spelling was of great help.

CHAPTER ONE

THE CHEMISTRY OF CELLULOSIC MATERIALS

1.1 INTRODUCTION

Vegetation is thought to produce an estimated 100 billion tons of cellulose a year, that is, approximately twenty-five tons of cellulose for every person on earth.[1] This vast quantity of naturally occurring, readily available fibre has helped to maintain cotton as the most important textile fibre in the world. Enormous research effort has been directed towards the study of cellulosic materials and this has led to a wealth of information in the literature pertaining to the morphology, biosynthesis and varied reactions of this important substance.[136]

The structure and synthesis of its main derivatives such as the cellulose nitrates and acetates has also been well documented and the variety of properties available by derivatisation has led to a diversification in the market outlets for cellulosic materials. Cellulose nitrate, first reported by Schönbein[2] has developed into the major component of most propellants and blasting explosives and was originally employed in the production of cine film and even billiard and snooker balls. Today the nitrate ester of cellulose is still utilised in the formulation of many lacquers and surface finishes. The cellulose acetates however have been widely studied essentially for their textile properties whereas the more unusual derivatives such as carboxymethylcellulose have been developed for use in ion exchange columns and separation techniques.[45] Several esters of cellulose, but notably the nitrates, are cast from suitable solvents to produce semi-permeable membranes used in osmotic measurements and dialysis experiments. Thus it can be appreciated

that cellulose is a valuable natural resource which has been exploited by several major industries, in particular the pulp and paper making concerns, the textile producers and in the case of cellulose nitrates by government bodies for military applications.

Despite the voluminous literature,[136,137] however, available on the chemistry and structure of cellulose and its nitrates which has accumulated over the past century a number of important questions remain unanswered and some interesting areas of research are still comparatively unexplored. These aspects will be further discussed in a later section but it is the purpose of this chapter to present a brief review of the relevant literature pertaining to the chemistry and morphology of cellulose and of its important ester cellulose nitrate. Obviously it would be beyond the scope and purpose of this thesis to present a full review but it is hoped that the following pages contain a concise history of the major contributions which relate directly or indirectly to the research program outlined in this thesis.

1.2 COTTON

1.2.1 Basic Morphology and Dimensions of Cellulose Fibres

Raw cotton is 85-95% cellulose with the major non cellulosic components being waxes and pectins which are generally located in the outer layers of the fibre.[3] After the scouring and bleaching processes (see section 1.6) a 98% pure cellulose can be obtained either as free linters or pressed into a paper form. The general morphology of

cotton has been the subject of intense investigation over the years and a knowledge of its unique structure is required before considering its reactions in detail. The cellulose fibre has an outer layer or primary wall which in the raw cotton is in close association with the waxes and pectins which form the so-called cuticle. The cuticle has been shown by Whistler[4] to be a continuous membrane of insoluble pectic salts which can be destroyed by pectinase. Dewaxed and depectinised cellulose therefore has the primary cellulose wall as its outer layer, the structure of which is still under investigation. However Roelofsen[5] showed that there are at least two sets of fibrils in the outer wall, one running axially and one transversely to the axis of the fibre. Similar views have been put forward by Tripp.[6]

The secondary thickening which develops in the young plant has been studied by Sisson[7,8] and found to be highly crystalline cellulose which is laid down in fibrils that form a spiral with regular reversals along its length. The secondary wall is subdivided into S_1, S_2 and S_3 layers although there is some doubt about the latter.[3] The hollow lumen forms the core of the fibre and can vary in size according to the maturity of the fibre. This layered structure is shown in figure 1. The fibrillar nature of cotton was first observed by Ruska[9,10] using the electron microscope and since then it has become clear that cotton has a structure that is built up from basic fibrillar units. Hess[11,12] has observed fibrils of 150A° diameter which he termed elementary fibrils. Preston[13,14] working with algae reported that microfibrils vary in width from 80-300A° and are approximately half as thick as they are wide. Hodge

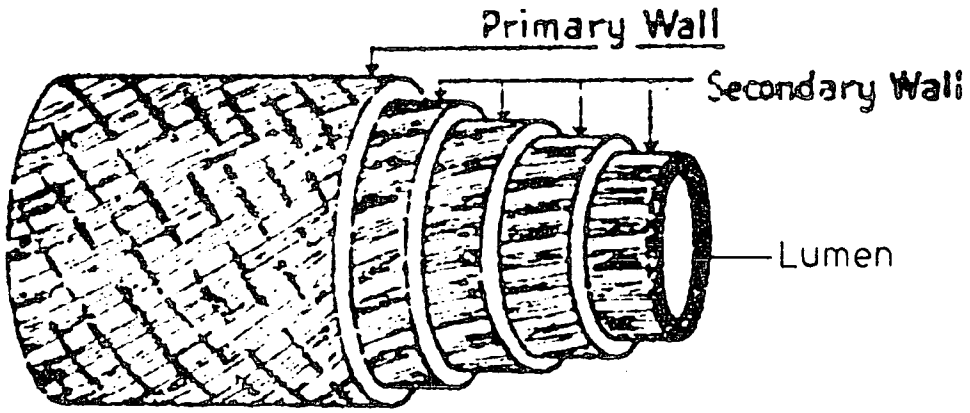

Diagram of Structure
of Cotton Hair.

Figure One Schematic of a cellulose fibre

and Wardrop[15] found a range of 5-10nm for wood and Vögel[16] found a 17-20nm span for ramie microfibrils. Frey-Wyssling[17] recognised fibrillar strands down to 60A° whereas Muhlethaer[18] claims to have seen 35A° units. There is still doubt however whether or not the ultrasonic techniques used to isolate the material for electron microscopy does in fact cause fibrillation. It is assumed for the purpose of this work that the basic fibril is between 100-200A° in width. A complete list of observed dimensions has been gathered together by Warwicker.[3] It has been suggested that there exist within the glucose chains weak links which are acid labile. Das Mitra[19] has claimed to have detected xylose in hydrolysates of purified Egyptian cotton which he believes to be the cause of weak links which cause transverse cleavage across a fibre. The width of elementary fibrils has also been estimated by low angle X-ray techniques. Kratky[20] has deduced that fibrils

are ribbon shaped with cross section 28 x 93A°. However despite the vast amount of data relating to basic dimensions no absolute values can be presented since the size of the elementary fibril may well depend on the source of cellulose, a factor not always reported in the literature.

1.2.2 Fibrillar Structure

Early concepts about the fine structure of microfibrils have been reviewed by several authors and will only be briefly mentioned here as a background for a description of later developments. In 1858 Nägeli[21] proposed the micellar theory; this assumed the presence of distinct brick-like crystalline micelles within cellulose fibres (see figure 2) to explain the birefringence observed with a polarised microscope. Many years elapsed before the crystalline structure of cellulose was proved by X-ray diffraction methods. The ensuing investigations showed that with the possible exception of the Halicystis plant[22] the cellulosic materials from all sources including bacteria and animals have the same crystalline structure (cellulose I).

These studies resulted in the description by Meyer and Misch[23] of the crystallographic unit cell for cellulose I, with antiparallel orientation of the neighbouring molecular chains. When the crystalline structure was confirmed the micellar theory was expanded to accommodate new observations including the diffuse X-ray diagrams of cellulose having broad diffraction lines. This broadening is assumed to be due to discontinuity resulting from small crystal size or other factors. The size of the micellar crystallites was estimated at 5-10nm in diameter and 50-60nm in length.[128] The X-ray scattering resulting in a diffuse diagram was attributed to

the presence of amorphous materials. It is proposed that these materials acted as a cementing compound between the crystalline micelles and were responsible for the swelling of the cellulose fibres.[24]

The micellar theory which assumed that straight chains of cellulose molecules 60nm in length form the crystalline particles was supported to some extent by determination of the degree of polymerisation of the polysaccharide. End group analysis at the time indicated for different types of cellulose a d.p. of 100-200 that was in close agreement with a minimum value of 120 estimated from the X-ray data.[25] However these values were soon found to be low and the development of newer physical techniques such as viscosity measurements, e.g. by Staudinger[26] and Mohr indicated for native cellulose a d.p. of about 3000 which corresponds with the chain length of 1.5nm. Gralen and Svedberg[27] obtained by ultracentrifugation d.p. values of about 10,000 for native celluloses and it soon became clear that the early micelle theory was untenable. At the same time an argument was presented for the existence of a continuous structure in which long molecules are arranged parallel with some interdispersed discontinuities. However the presence of amorphous and crystalline regions in cellulose was supported by X-ray studies which showed no change in diagram on swelling with water; this it was argued was due to water being absorbed into the amorphous regions only between micelles.[28] These apparently conflicting ideas were reconciled in the fringed micelle theory postulated by Kratky[129] and Frey-Wyssling.[29] According to this theory the microfibrils are composed of statistically distributed crystalline and amorphous regions

formed by the transition of the cellulose chain from an orderly arrangement in the crystalline regions and less orderly orientation of the amorphous area.

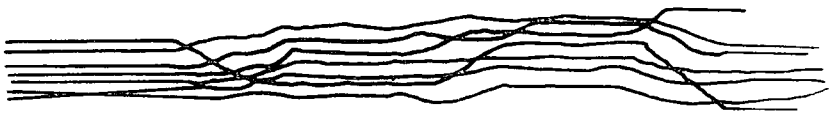

(a) FRINGED MICELLE THEORY

(b) CRYSTALLINE MICROFIBRIL MODEL

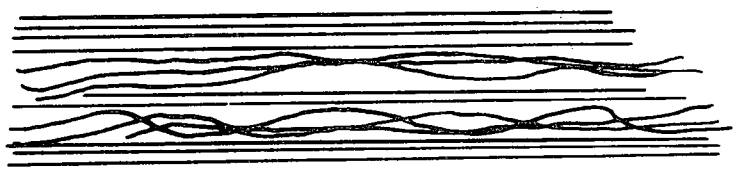

(c) VEINED MODEL

Figure Two Three proposed models for cellulose

The presence of amorphous and crystalline regions has been investigated by a number of physical and chemical methods. The density of cellulose was found to be lower than the theoretical density calculated from the unit cell; this seemed to show the presence of material less densely packed or amorphous. This method can be used for estimation of percentage crystallinity. Chemical methods such as deuterium exchange,[30] periodate oxidation,[31] hydrolysis and thallation with thallium ethoxide[32,133] have also been used. It should be noted that these methods are effectively measuring inaccessibility rather than crystallinity. The reactive

groups positioned at the surface of the fibrils (it has been estimated that 39% of all the macromolecules in cellulose fibrils lie at the surface) are obviously more accessible than those in the bulk. It may be that the extent of reaction of such reagents may be a function of the surface area available and will be greatly influenced by such factors as swelling. This important question is further addressed in Chapter Three. Recent work presented by Vanderhart[33] has used ^{13}C n.m.r. to distinguish between a primary hydroxyl in crystalline regions and hydroxyls in an amorphous region. However it is apparent that the molecules at the surface may contribute to accessibility and other properties of microfibrils which have previously been attributed to amorphous materials. These molecules which represent structural discontinuity cause small particle scattering thus increasing the width of X-ray deflections and decreasing the resolution. These simulate or give the illusion of the presence of amorphous materials. Briant[34] and co-workers have also reported that X-ray scattering in cellulose analysis is due to lattice distortion rather than to amorphous regions. Muhlethaler[35] used a staining technique where the cellulose is treated with phosphotungstic acid which is thought to penetrate the capilliary spaces. The elementary fibrils appear to be crystalline along the whole length, he estimated 35 x 35A^{o}. He proposed a new structure to accommodate the new data in which 16 of the 18 pairs of antiparallel chains lay at the surface. Furthermore the only disorder or disturbance in the structure is caused by chain end dislocation which could cause as much scattering of X-ray as the amorphous regions. A folded chain model for cellulose has been proposed

by Dolmetsch[130] and Manley.[36] One of the notable features of the chain folded conformation is that it readily explains the antiparallel arrangement of the cellulose molecules within the crystalline structure of the microfibrils.

A compromise between the fringed micelle theory and the totally crystalline microfibril has been recently suggested[37] the main feature of the model being that voids run between basically crystalline fibrils and that these voids will vary in width and accessibility according to the swelling power of the reagent. The interest in swelling reagents and the effect of morphology on the reactivity arises from numerous observations that samples which appear chemically identical differ in fact in ease of reaction. The next section will therefore summarise the relevant data which has accumulated on the swelling phenomenon.

1.3 SWELLING

The swelling behaviour of cellulosic materials is well known and the available literature has been reviewed by Warwicker.[3] Sodium hydroxide is known to swell cellulose in certain concentrations and to alter parameters in the unit cell in a process referred to as mercerisation. The general effect of mercerisation is to increase the sorption of various reagents and thus is a valuable means of modifying structure. The swelling behaviour in other reagents and in particular in acids is of special relevance to the work presented in this thesis and will be considered further here.

Bracconot[38] was the first to indicate that sulphuric acid had a swelling and dissolving effect on cellulose; the

greatest swelling taking place between 63-72% and dissolution occurring above this value. There is evidence that swelling is interfibrillar[3] and does not affect lattice constants over a range of swelling conditions. Phosphoric acid on the other hand is known to induce intrafibrillar swelling in concentrations above 90%.[3] This high swelling generally causes rupture of the primary wall. Nitric acid is extremely complex in its swelling behaviour since below 60% only a small amount of interfibrillar swelling occurs, but above this value there is evidence for the formation of the Knecht[39] compound which indicates intrafibrillar swelling. There is no evidence for nitration at this stage and only in concentrations above 70% is there data[40] to suggest nitration and extensive swelling. There are some authors who believe that nitrations in mixed acids of nitric acid/sulphuric acids proceed by initial interfibrillar swelling by sulphuric acid followed by penetration of nitric acid into the crystalline fibrils.[41] The sulphuric acid is not thought to enter the crystalline regions in the initial stages. This important point is further considered in Chapter Three.

1.4 OXIDATION OF CELLULOSE

The oxidation of celluloses by a variety of oxidising agents have been widely reported in the literature.[42] The interest in oxidised cellulosic materials lies mainly in the manufacture of ion exchange celluloses for separation techniques. However it is also known that the capacity of acidic cellulose (i.e. those with carboxyl groups usually at the C_6 position) to bind with ions will accordingly influence the electrical conductivity, the dyeing and the

finishing of fabrics.[42] The further reaction of carboxy-celluloses to form acid esters with alcohols, and ring compounds such as ethylene oxide and propionlactone is also much investigated.[42] The general effects of introducing carboxylic acids into cellulose in terms of solubility hydrogen bonding, water absorbency and other properties are well covered in an excellent review by Allen.[45] The determination of carboxyl groups is therefore of great interest and many methods have been developed for this purpose. A comparison of the available methods is presented by Wilson and Mandel[46] but essentially they fall into two categories; the absorption of methylene blue, (or other dyes). or ion exchange techniques using calcium acetate[134] or other similar reagents. Davidson[53] reported that the absorption of certain dyes was related to the carboxyl content whereas Putnam,[48] Sookne[126] and Harris[49] have all experimented with ion exchange methods following the general scheme:

$$\text{CELL - COOH} + \text{MA} \longrightarrow \text{CELLCOOM} + \text{HA}.$$

Ion exchange celluloses and their uses are discussed by Davidova and Rachinskii[50] in a lengthy review. Guthrie and Bulbeck[51] have also reported their uses for the separation of proteins, enzymes and nucleic acids. Ion exchange celluloses may be made by attaching substituent groups with basic or acidic properties to the cellulose molecule. The D.O.S. of such materials is generally low since the various uses of ion exchange celluloses require that they do not dissolve or swell in various dilute acids or bases.[45] They include cellulose phosphate used for the sorption of thorium from acidic solutions, sulfoethylcellulose and carboxymethyl-cellulose.[42] Sodium metaperiodate is a common glycol cleaving

agent[125] which is, (along with lead tetra-acetate), used for crystallinity measurements. Head has found that the cleavage is accelerated by the action of light and has also investigated the reduction of the aldehyde groups[52] so formed by the action of sodium borohydride. It is also possible to convert the aldehydic groups to carboxyls using chlorous acid.[47] Aldehydic groups in cellulose are generally determined by the copper number method[54] which estimates a quantity of copper reduced from salt solutions.

1.5 CELLULOSE SOLVENTS

It is appropriate at this point to mention that, in comparison to its nitrate and acetate derivatives, cellulose is extremely insoluble. It will dissolve in strong acids of certain concentrations but the degradation due to hydrolysis on regeneration by dilution is too great to allow the use of such acids as cellulose solvents. In contrast to strong mineral acids, metal complexes have attained much greater importance as solvents for cellulose containing materials.[42] Sweiger[55] has established that a solution of Copper II oxide in concentrated ammonia solution is an excellent solvent for unsubstituted cellulose. Cadmium[59], iron[61] and cobalt[60] have also been complexed and are in regular use for this purpose.[42] More recently hydrazine[56] has been reported to dissolve cellulose without causing excessive degradation and the use of N_2O_4 in association with various organic compounds is well substantiated.[37] Sweiger[131] has also reported the use of N_2O_4 and dimethyl formanide (D.M.F.) for the dissolution and subsequent conversion to cellulose nitrite.

1.6 PULPING AND BLEACHING

Pulping can be considered to involve the steps of fibre separation, removal of undesirable components and the tailoring of the pulp for desired chemical and physical properties. Commercial pulping procedures which are more fully discussed elsewhere[62] may be considered to be composites of general pulping classifications. The acid-sulphite process[58] for example is a hydrolytic method whereas the nitric acid process is a mixture of both oxidative and hydrolytic processes.[42] The commercial sulphite procedure is based on the fact that lignin will react with sulphur dioxide or solutions of its salts at different pH levels to form a soluble derivative which can be removed from the wood. There is always some degradation, mainly due to hydrolysis and lowering of D.P., as a result of these processes.

1.7 DRYING OF CELLULOSE

Cellulose exists as a porous material with a large capilliary surface area; this area may range up to 200 sq. metres per gram[63] depending on the history of the sample. Cellulose also has a great affinity for water and in an air dry condition it will contain about 5% by weight of water. Removal of this water as water vapour will cause collapse of this capilliary structure and may affect adversely the reactivity of the cellulose to subsequent reaction systems.[64] Although some people advise the use of miscible organic liquids[65] to replace the water in the capillaries in a process called solvent exchange, this is not a generally

applied method and drying is more often carried out in ovens at low temperatures. It is particularly important in the nitration of cellulose to have less than 2% moisture.[41] a level that is more conveniently achieved by oven drying. However it is believed, from electron micrograph studies, that solvent exchange can preserve the lumen[65] and prevent its collapse, a factor that may be important in structural studies. The condition of the lumen, i.e. whether preserved or collapsed may also affect the birefringence of fibres, a point which is further addressed in Chapter Seven.

1.8 STRUCTURAL STUDIES

1.8.1 Infra Red

In those fields of chemistry where one deals with a number of compounds of similar chemical and physical properties infra-red spectroscopy is a very useful tool for analysis and identification. Hence in carbohydrate chemistry it has been widely applied and in the case of cellulose and cellulose derivatives the technique is well established.[66] The I.R. spectra of cellulose, nitrocellulose and oxidised cellulose as well as various other derivatives have been recorded[138] and in the case of oxidation of cellulose it has proved especially useful in monitoring the increase in carboxyl and aldehydic groups.[66] In most cases the dry ground fibres are analysed as KBr discs as proposed by Kuhn[67] and the many absorbtion bands have been assigned by Rowen[68]. The near infra-red region has been of particular interest and a number of workers have studied the nature of the hydroxyl bonds in the 3 μ region.[69] Marrian and Munn[70] have

attributed specific bonds to various types of hydrogen bonds by the use of deuteration techniques, whereas Barker[71] *et al* have studied cellulose and discussed the nature of bands at 112μ. The important transition between cellulose I to cellulose II crystal forms has also received some attention.[72] Higgins[73] has reviewed the application of the technique to cellulosic materials and Kuhn[74] has attempted to assess the nitrate ester groups in nitrocellulose using I.R.

1.8.2 E.S.C.A. Analysis of Cellulose

Despite the fact that the surface reactions of cellulosic materials and those of other natural fibres are of immense interest to many industries very little is known in this important area. The advent of E.S.C.A.,[75] (X-ray photoelectron spectroscopy), as a powerful technique for the delineation of surface and subsurface has allowed such investigations to commence for the first time. Millard.[76] for instance, has made preliminary studies of cellulose fibres but has concentrated his research on the surface properties of wool[123] and studied changes as a result of low temperature plasma treatment at the surface of such fibres.

Soignet[77] has used E.S.C.A. to determine the nature of the reaction of cotton fibres with flame retardant agents[122] and oil repellant finishes. Gray[78,124] has made some attempt to deconvolute C_{1s} and O_{1s} core level spectra of cellulose and obtained area ratios consistent with that expected for cellulosic material. However no assignments have been given and the application of E.S.C.A. particularly to derivatives of cellulose is comparatively new.

In conclusion, then, to this initial introduction to cellulose chemistry it is readily apparent that cellulose is a unique polymer. The ease of its reactions may well depend on the morphology and hence upon the age and source of the cellulose. It is important to specify both the source and the type of cellulose used. i.e. whether it is in the form of linters which are the waste cellulose from the seed hairs or whether the purer fibres are utilised.

With a greater understanding of the structure and morphology of cellulose it is now possible to go on to examine the history, preparation, and properties of cellulose nitrate upon which this thesis is primarily concerned.

1.9 CELLULOSE NITRATE

1.9.1 Brief History of Cellulose Nitrate Production

The study of the esterification or so called nitration of cellulose has a long and interesting history. The discovery in 1833 by Bracconot[79] that the reaction of nitric acid with cotton produced highly inflammable material and the subsequent patent granted to Schönbein[80] in 1846 specifying the production of the material from cellulose and mixed acids can be said to have materially changed the course of history. After the first unscheduled large scale explosion in 1847, work on the technical production of nitrocelluloses was somewhat restrained; after this mishap however the possibility of modifying burn rate for propulsion purposes was recognised[41] and by 1867 the basis of the production of smoke-

less propellants for guns, rifles and shells was established and altered the course of modern warfare. The innovative use of camphor as a plasticiser for nitrocellulose by Parkes[81] in 1862 in the production of celluloid represents an important landmark in the emergence of polymer science and the observation of the solubility of nitrocelluloses and the production of colloidan and thin films undoubtedly accelerated the development of photography as we know it. However despite the wide usage of nitrocellulose in surface lacquers and finishes it is for military purposes that the main interest lies. In the coming pages, then, the literature reviewed is that concerned directly with nitrocellulose or double based propellant.

1.9.2 Production Methods

By far the greater part of raw material used for the manufacture of nitrocellulose is either cotton linters or woodpulp.[41] Cotton linters receive special preliminary treatment principally by heating under pressure with dilute sodium hydroxide. By regulation of this 'kiering' process the viscosity of the cotton can be reduced although kiering after nitration is more effective in reducing total viscosity. There are two basic nitration processes used which will be considered in turn.

(i) Mechanical Nitration[135,41]

The nitrating vessels are upright oval cylinders of stainless steel in each of which operate two paddles on vertical shafts and a centrifuge is situated below the vessels. The acid is pumped into the vessels with a charge of cotton linters. After the nitration period, during which time the

temperature does not rise by more than 2°C. the contents are despatched to the centrifuge and the waste acid is spun off and passed to an acid plant for reconcentration. Phosphoric acid is not used in industrial processes because of difficulties in recycling and the nitric acid/sulphuric mix is widely utilised for nitration purposes. The spun nitrocotton has its own weight of spent mixed acid adhering to it and it is necessary to drown the material in a jet of water. This is done rapidly to obviate denitration effects. The resultant nitrocellulose is then washed in several changes of hot water before stabilisation.

(ii) The Displacement Process[135,41]

This process which was a development from the original pot nitration was introduced to Waltham Abbey in 1905. The displacement pans are usually shallow square vessels with a central bottom outlet. A perforated false bottom is included into the vessel. About 800 lbs. of fresh acid is run into the pan and from 24-27 lbs. of cotton is dipped into the acids with stainless steel forks. Heavy tiles are laid over the cotton to exclude air for periods of up to one hour when the acid is displaced with a regulated flow of water while the spent acid is slowly run out of the bottom outlet. The water-wet but acid-free nitrocellulose is removed from the pan and is ready for stabilisation. There is evidence that the nitrocellulose from this process is more likely to suffer denitration, a fact that has been more recently inferred by Lewis[82] from birefringence measurements.

1.9.3 Laboratory Preparation

(i) In Nitric Acid: Water Mixes

These mixes are generally unsatisfactory for nitration purposes and according to Miles[41] the products dissolve in acids of up to 85% concentration. (This is in some doubt however since both in this work and that of Trommel[83] such acids have been used to denitrate high D.O.S. nitrocelluloses). The nitration is also believed to be uneven but the evidence for this is scanty, what is evident however is that the viscosity of NC prepared by this method is very low indeed and gelatinisation of the fibre may also occur. The gelatinisation problem can be circumvented by the use of potassium and sodium nitrates[84] in the acid baths, although a full explanation of this phenomenon has never been given.

(ii) In Phosphoric-Nitric Acid Mixes

Of the many types of acid mixes the nitric-phosphoric system is considered the most useful next to the industrially important nitric-sulphuric mix. Stabilisation is particularly easy for the nitrated products but the attack of the reagent on steel and glass precludes its use on a large scale.

(iii) Nitric Acid with Organic Liquids

Acetic anhydride[85] is a common partner for nitric acid for nitrating purposes. Very high degrees of nitration have been achieved although little is known of the kinetics of the reaction. Similar high percentage nitrogen material can be obtained using chloroform[86] acetic acid,[87] propionic acid[88] and butyric acid[89] with fuming nitric.

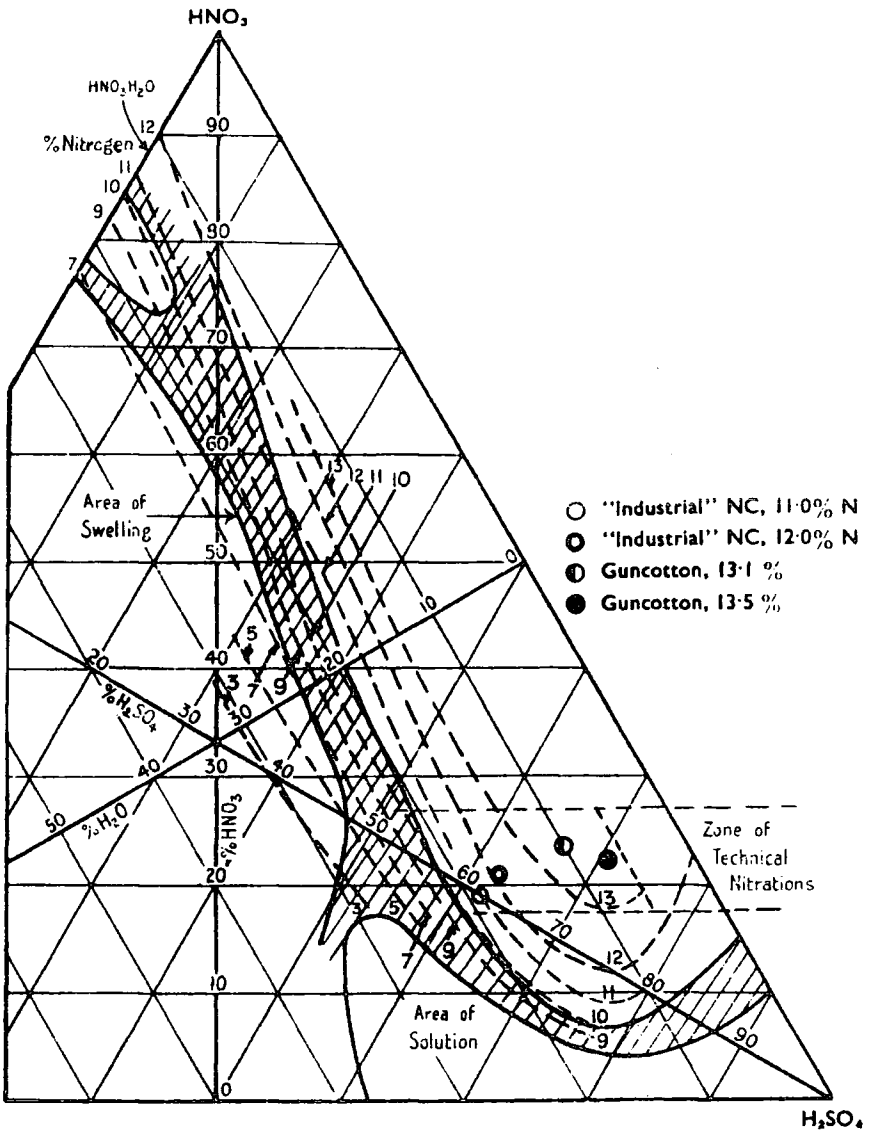

Mixed acid chart. Lines of constant nitrogen and areas of swelling and solution

Figure Three Three-way composition diagram for nitration of cellulose[41]

(iv) Nitration in Mixed Acid

Due to the enormous interest in industrial manufacture of cellulose nitrate almost every possible ratio of nitric acid and sulphuric acid has been investigated and the results of such work have enabled a three-way nitration diagram to be drawn up where the expected degree of substitution can be read off for a particular acid mix,[41] (Figure 3). Although experience has shown that the diagram is not particularly accurate (because it has been argued that it takes no account of the effect of starting material on the final degree of substitution attained), the diagram can be used to give an approximate value. The technical zone is so situated on the graph mainly because of the technical requirements. Nitration may be accompanied by changes in the physical condition of the fibre. This is more likely in acid mixes where the nitric acid content is greater than 25%. The diagram is split by the areas of swelling and solution which must be avoided if a product of even nitration and high viscosity is required. The nature of the effective nitrating agent in the mixed acid is not firmly established although it was once thought that the NO_2^+ ion becomes important[90] as the water content is reduced and the molecular species change according to the equation:

$$NO_2OH + 2H_2SO_4 \longrightarrow NO_2^+ + 2HSO_4^- + H_3O^+$$

However NO_2^+ is not observed spectroscopically in mixed acids containing less than 80% sulphuric acid, a range far outside those encountered in technical nitrations.

1.9.4 Stabilisation

Nitrocellulose can be an extremely dangerous substance unless it is properly stabilised. It has been suggested that the nitrate group oxidises the cellulose residue liberating nitrous oxides which can autocatalyse degradation.[91] The instability could be due to small amounts of mineral acids and seems more marked for high D.O.S. materials and much less in nitrocelluloses prepared without the use of concentrated sulphuric acid.[92] The stability is generally measured by either the Abel Heat Test[93] or the Bergmann-Junk Test.[94]

Stabilisation takes many forms but usually involves steaming or boiling with many changes of water over a specified period. Although a period of several days is sometimes recommended for blasting explosive nitrocelluloses, several hours is probably sufficient to render the material safe for handling in a dry state.

The formation of sulphate esters during nitration in mixed acid is well substantiated[41] and boiling has the effect of removing such esters although some authors[95] believe that free acid is trapped in the fibrillar structure and is difficult to remove. However it is not possible to assign instability purely to sulphuric acid or its ester since those materials prepared by nitric acid water mixes are also known to be unstable unless washed thoroughly and boiled. Hence it was suggested[96] that an oxidation product of cellulose was formed in nitration which would initiate degradation and could be removed by boiling. Gagnon and co-workers[97] have examined the relationship between sulphate and nitrogen content of unstabilised cellulose nitrates and

found that in general the sulphate content decreased steadily with increasing nitrogen content. This was found also to be true of nitrated wood cellulose. The causes of instability have been further discussed in several publications[41] but it is sufficient to state here that under the moderate boiling procedures outlined in Chapter Three the sulphate ester content is reduced to a negligible level certainly as far as the surface is concerned (from E.S.C.A. data)[98] and probably for the bulk also.

1.10 STRUCTURAL STUDIES

1.10.1 X-Ray Diffraction

The change in the molecular structure of nitrocellulose as the hydroxyl groups of the cellulose chains are progressively replaced by nitrate groups has been well studied and it is now established that the conversion coincides with a massive change in the dimensions of the unit cell.[99] Changes in the spiral angle and nature of the helix[100] have also been recorded and will be dealt with in more detail at the end of this section. However it is believed[101] that the anti-parallel arrangement of chain molecules prevalent in cellulose itself persists in the nitrocellulose structure except perhaps for those nitrated in acids close to the swelling and solution areas of the Miles[41] diagram. In the past fifty years, since the discovery of the diffraction of X-rays by crystalline materials,[102] the method has been applied to cellulosic materials. A great deal of the work was carried out by the French school[103] who claimed to distinguish three distinct X-ray diagrams for the trinitrate,

dinitrate and cellulose structures, the trinitrate being an extremely sharp and clear diagram. However an assignment for a pure dinitrate is untenable especially since the publication of recent ^{13}Cnmr distribution data[104] and the reality is probably a slow transition from the well characterised cellulose diagram to the sharply defined trinitrate structure. Mathieu[103] was perhaps the first to observe a linear relationship between the d(101) interchain spacing and the nitrogen content of the nitrocellulose and much of the early work is reviewed by Miles.[41] Trommel[83] has perhaps done most work on both cell indexing and measurement of the interchain spacing and his work will be reviewed in more detail in the following section, but it is sufficient to note here that the d(101) plane is extremely sensitive to changes in D.O.S. Manley[106], for example, while studying the hydroxyethyl celluloses noted a steady rise in the spacings (7.2^{o}A to 10^{o}A) as the D.O.S. increased. Frey Wyssling[107] has suggested that morphologically the plane is more important than the (002) and according to X-ray evidence[108] for plant cell walls the submicroscopic crystallites have the plane oriented parallel to the surface of the cytoplasm by which they are produced and in some cases the microfibrils show aggregation in that plane. It is assumed that the (101) plane is the principal plane of growth in the cellulose crystallites and that the hydrogen bonds are more active in that plane than in any other. The inference of the work of Trommel[83] on the cell indexing was that in the trinitrate and to some extent also in the intermediate structures the glucose rings were tilted out of the (0 0 2) plane as in cellulose and into the (0 1 2) plane. However the literature

is extremely vague on this matter and even in recent work published by Atkins[100] it is accepted that a true definition of the unit cell has yet to be arrived at. What has been established however is that the spiral angle in cellulose II and probably cellulose I also is 180° coinciding with an axial advance of 0.519 nm. A flat ribbon shaped helix has also been identified defined crystallographically as 2_1. In cellulose trinitrate thehelix is 5_2 i.e. five monomers in two turns resulting in an axial advance of 0.508nm. The rotation between nomomers is now 144° and hence there is a relaxation within the cellulose helix of 36° per monomer. It is likely in this arrangement that both left and right hand chiralities occur so an accumulation of twist is unlikely. Atkins[100] has recently presented data relating to the three possible conformations of the primary nitrate groups and these are reproduced by computer drawings in Figure 4. Lewis[109] has used this data and come to the conclusion that conformation gg is incompatible with birefringence data.

Summarising then, it would appear that very little is known about the relationship between microstructure and distribution of nitrate groups in relation to interchain d(101) spacing. This interesting point forms the basis of the work discussed in Chapter Six which analyses distribution data from ^{13}Cnmr and compares it to the X-ray diffraction data.

1.10.2 Nuclear Magnetic Resonance (N.M.R.)

Due to the viscosity of normal nitrocellulose solutions attempts to record high resolution proton n.m.r. spectra of such materials have met with failure. Stephan

CELLULOSE TRINITRATE TS VIEW XROT 50 YROT 10

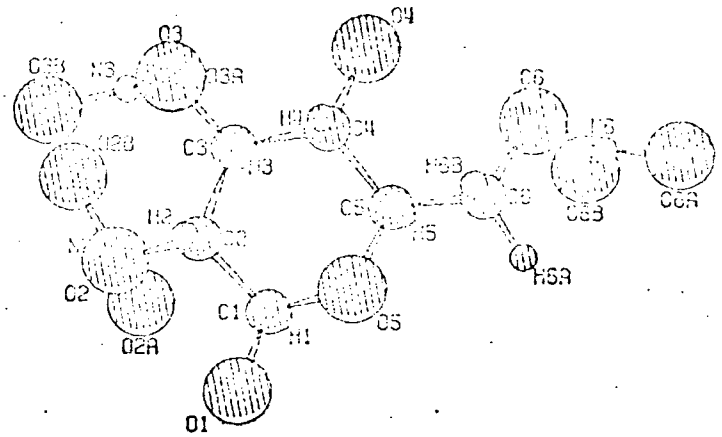

CELLULOSE TRINITRATE GT VIEW XROT 50 YROT 10

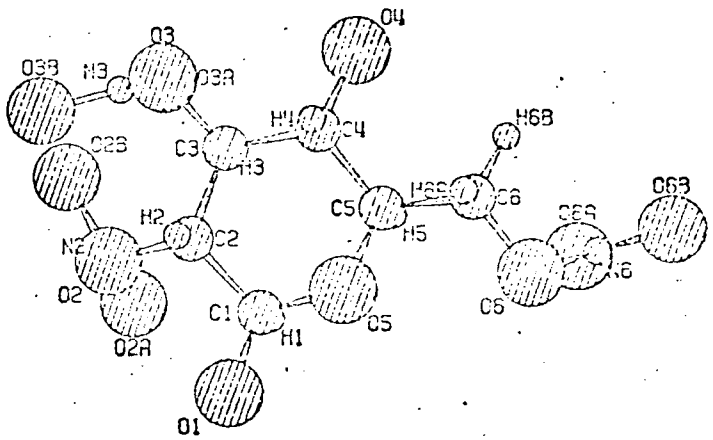

CELLULOSE TRINITRATE GG VIEW XROT 50 YROT 10

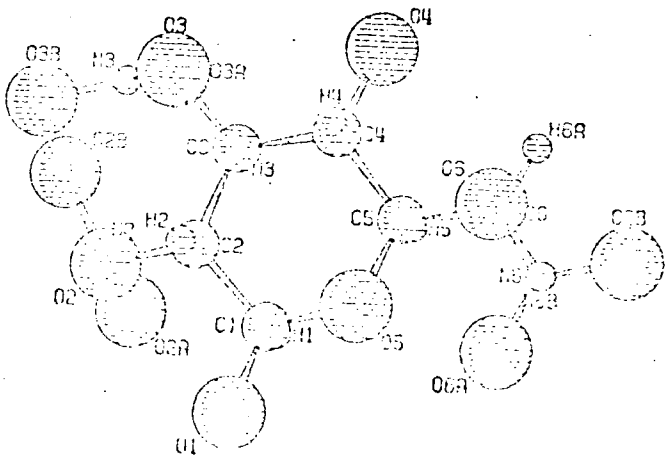

Figure 4

and Lemanceau[121] have recently applied the method by first reducing the degree of polymerisation of the nitrocellulose by hydrolysis or electron beam degradation. The resultant spectra however are still too poorly resolved to be fully assigned and although other attempts have been made the most important advance in this area was recently made by Wu[133] who obtained high resolution, ^{13}C n.m.r., proton decoupled spectra for a series of nitrocelluloses. The information obtained and the consequences of this investigation are more fully discussed in Chapter Four of this thesis.

1.11 THE NITRATION EQUILIBRIUM OF CELLULOSE

Since cellulose nitrate is an ester of cellulose one would expect that the composition of the nitrating mix would determine the degree of esterification. This suggests that when a cellulose nitrate of high D.O.S. is brought into contact with an acid mix which would normally nitrate cellulose to a low level, (or is a spent acid of such a nitration), denitration or saponification should occur. Berl and Klaye[110] were the first to check this experimentally and came to the conclusion that although cellulose nitrate would denitrate under these conditions the D.O.S. attained was higher than would be expected if cellulose was nitrated in the same mix. In their opinion, the equilibrium was not reached. Later Fabel,[111] Demougin[112] and Bonnet[113] came to the same conclusion. These experiments were reviewed by Miles[41] and were repeated and expanded by Trommel[33], in a series of papers dealing with this complex problem. It is largely as a result of such experiments that some authors still prefer to explain these phenomena in terms of an accessibility argument although it

is now generally accepted in the literature that the nitration of cellulose is an equilibrium reaction. It is hoped that the work described in this thesis will cast some light on these conflicting opinions. It would now be appropriate to consider in some detail the apparently anomalous behaviour of cellulose nitrate outlined particularly in the work of Miles[41] and Trommel[83] since this is particularly relevant to the conclusions arrived at in Chapters Three, Four and Seven of this thesis. Miles[41] has reported that cellulose nitrate prepared by nitration has a lower lattice d(101) spacing, as measured by X-ray diffractometry, than a cellulose nitrate of the same D.O.S. prepared by the denitration methods described earlier. Trommel[83] has also investigated this problem over a range of D.O.S. and his results can be summarised in Figure 5. It is clear from this that the lattice spacings

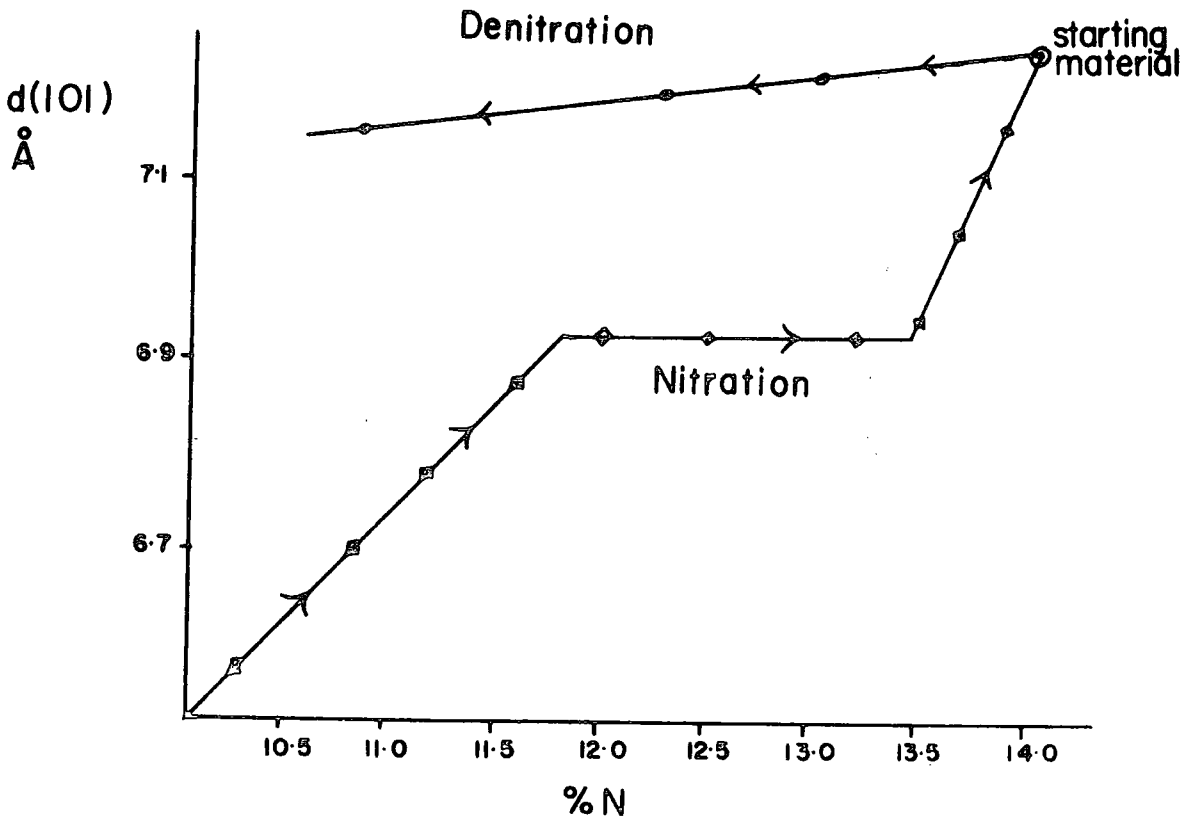

Figure Five Graph of mean X-ray spacings (101) against D.O.S. for nitration and denitration[83]

of denitrated materials are maintained despite the loss of a number of nitrate ester groups, in fact it has been reported that denitrated materials of 12.2% have the same lattice spacing as those with the trinitrate structure ≈ 13.8%. It would seem that, once formed, the conformation adopted in the unit cell of cellulose trinitrate is particularly stable and resistant in some way, perhaps because of a change in H-bonding systems, to normal hydrolysis. Trommel[83] rationalised this data in terms of an accessibility argument in which he postulated areas of very high D.O.S. cellulose nitrate where the fibre is so well crystallised that the acid mix cannot penetrate and bring about denitration. Several lengths of such material along a chain would have the effect of holding the chains apart although other parts of the chain may be either totally cellulosic or relatively unsubstituted. A similar argument was adopted[83] to explain anomalous solubility data for such materials in which it was reported that in general denitrated materials are less soluble in mixtures of alcohol and ether (2:1) than their nitrated counterparts. This information coupled with the inference that nitration and denitration proceed at different speeds leaves this area open to considerable confusion. Trommel[83] has also suggested that the lower the nitrogen content of the starting product, the more closely the equilibrium situation is reached. From an analysis of a series of nitrated and denitrated materials he was also able to predict that the higher the nitrogen content of the starting product above that of the equilibrium condition the faster the initial denitration rate would be. Although some of the conclusions reached are of interest others which are based on experiments involving reprecipitation of NC from acetone and denitration for periods of up

to one year are of less value. Obviously the application of new techniques in this important area could be of immense value in the solving of some of the questions raised from the data reviewed above. In the following chapter the kinetics of the nitration-denitration reactions are investigated at the very surface of cellulosic fibrils by means of E.S.C.A. and the literature is again reviewed in the light of the new concepts arising from the collected data.

1.12 DOUBLE AND TRIPLE BASED PROPELLANTS

1.12.1 Nitrocellulose Pastes

A paste is considered to be the material obtained when certain plasticisers are sorbed into nitrocelluloses to an extent where the fibrous appearance of the nitrocellulose is maintained despite the swelling which takes place. Most typical of these is the nitrocellulose/nitroglycerine system prepared by the 'Wet Mix' process[114,117] in which a fine spray of nitroglycerin is added to the aqueous slurry of nitrocellulose. The structure of this paste is of great importance and the reactions occurring during the process are of especial interest. Lewis[115] has reviewed the relevant literature most of it accumulated at Leeds University during the war. It appears that in the presence of nitroglycerin and water the nitrocellulose is initially wetted preferentially by the water, however, the sorption of nitroglycerin then rapidly takes place and wetting improves until the surface becomes preferentially wetted by nitroglycerin. It is clear that for most of the time the nitrocellulose/nitroglycerin slurry is in the Wet Mix tank

the important process is a diffusion of nitroglycerin from a liquid surface layer into the interior of the fibre. This has stimulated a great deal of work[116] on the sorbtion of organic nitrate esters from the vapour phase into nitrocellulose with the aim of gathering information concerning the rate and mechanism of the diffusion of nitroglycerin into nitrocellulose. The effect of water content on sorption has been found to be considerable in the studies on sorption of isopropyl nitrate.[115]

Certain other propellant ingredients are added to the aqueous slurry in the mix tank. Generally the coolant plasticiser dibutyl phthalate is added and must behave similarly to nitroglycerine, i.e. forming small droplets which wet the fibre and are then absorbed from the liquid phase. Carbamite (diethyl- diphenyl- urea), is sometimes added at this stage unless the propellant is meant for incorporation with picrite. The carbamite is soluble in the nitroglycerin and some may be absorbed into it while it remains as a separate liquid phase. However it is believed that the carbamite will aggregate as unchanged crystalline carbamite. The possibility that some carbamite may dissolve in the liquid nitroglycerin and the general uncertainty of the nature and quantity of free and combined nitroglycerin in such pastes is a topic studied in Chapter Five of this thesis which deals with the characterisation of double based propellants by E.S.C.A. After formation of the paste further additives such as lead salt ballistic modifiers 2-nitrodiphenylamine and triacetin are incorporated. It is known that certain additives for example, lead ß-resorcylate[118] and basic copper salicylate[119] interact in the presence of water to give a double salt in

which the lead and copper are present in equimolar quantities and that this compound is essential for full ballistic development of the propellant. Hence in solventless incorporation one would expect better ballistic properties than in solvent incorporation. After incorporation the paste is dried for 24 hours at 45°C in trays in a stream of air. The differences between solvent and solventless incorporated propellants have been well studied and again reviewed by Miles.[41] In the solvent incorporation process Ayerst[120] lists three processes occurring in the incorporator. These he calls blending, dispersion and gelation. All three are probably occurring together. Blending is obviously a mixing to a level of homogeneity desired whereas dispersion is the breaking up of aggregates such as ballistic modifiers. What Ayerst[120] has called gelation is generally thought to include both swelling, which involves the sorption of solvents into the nitrocellulose lattice and gelatinisation which involves the break up of the individual fibres already swollen into small units by the application of work. The main physical changes known as bind-up* occurring during solvent incorporation has only vague explanations in the literature. It is thought that this is a result of the formation of a sticky cement at the surface of fibres which binds the smaller particles together. A great deal of work needs to be done in this area and a full discussion of the problems involved is beyond the scope of this brief survey.

* Bind up is a dramatic change of the propellant dough from a friable to a plastic state which requires an extra power input to the incorporator.

1.12.2 Triple Based Propellants

Although the work in this thesis deals only with the double based materials for the sake of completeness a summary of the preparation of triple based material will now be given.

The NC/NG paste is made from 13.1% N nitrocellulose and contains about 50% by weight of nitroglycerine this is added to 1½ times its own weight of picrite and solvent (90% acetone, 10% water) is added at the level of 20% of the total weight of solids. After 1½ hours of mixing in the incorporator carbamite is added. Bind up generally takes several hours.

1.12.3 Hot Rolling

The process of rolling between hot rollers is an important one to consider since all materials used in Chapter Five were subjected to this technique.
Rolling is generally restricted to the compacting of solventless pastes and it is generally thought that the rolling breaks up the nitrocellulose matrix to a lower state of aggregation. Due to the probability of high levels of hydrocarbon transferred from rollers to the surface of propellants the materials used for E.S.C.A. analysis (Chapter Five) were prepared using specially cleaned rollers allowing direct analysis.

1.13 Summary of the Areas of Interest

Against the necessarily brief survey of the literature here presented one is left with a number of important questions in all three sections. The interaction of cellulose fibres

with reagents for example is of immense importance in relation to a number of important reactions and ideas about the possible morphology and fibrillar structure of the fibres. How reagents diffuse into fibrils and the extent of their reaction is a process not yet fully understood. Much of this ignorance arises from the lack of a technique to examine the very surface of the fibres compared to the many methods for the investigation of bulk properties. A similar problem is probably also responsible for the gap in knowledge in the absorbtion of plasticisers into nitrocellulose and also the sorption of other liquids which are known not to enter the crystalline regions of the fibre. The general dimensions of the ultimate fibril in celluloses and particularly in nitrocellulose remains a mystery and it is only recently that it has been realised that the dimensions may change according to the maturity and source of the fibre. The problem in past years appears to be concerned with the erroneous belief that cellulose is a chemical which can be bottled and categorised hence authors have neglected to quote the source of their linters or cottons rendering much of their work unrepeatable. The whole question of cellulose morphology remains open and the various models proposed rarely fit all the data but are modelled on a particular set of experiments. For example the complex question of accessibility to various reagents has never been fully explained and again requires a technique such as X-ray electron spectroscopy (E.S.C.A.) to delineate between bulk and surface properties. The application of E.S.C.A. to analysis of cellulosic materials promises a great deal and in the particular area of U.V. degradation of such materials it has obvious advantages.

The initial attack of any reagent or type of radiation is at the surface and only E.S.C.A., (and related techniques), can offer any realistic means of monitoring changes at the surface ($\simeq 50A^{o}$) induced by, in particular, U.V. exposure.

In addition to the almost complete lack of information pertaining to the surface characteristics, both physical and chemical, of fibres, surprisingly little is known about how substituents are distributed within a residue, (between the C_2, C_3 and C_6 hydroxyls), and also along a chain (i.e. sequence distribution). In the case of cellulose acetates where fully acetylated material is more common the problem need not be addressed but when considering the nitrate ester these questions assume greater importance. Such information may well help to resolve the anomalies encountered in nitration/denitration equilibrium. Are nitrate groups in particular positions resistant to denitration for example and does denitration take place preferentially alongside a residue already partly denitrated? Clearly these questions require a technique capable of analysing the bulk and although proton n.m.r.[121] has been shown to have limited application to cellulosic systems the advent of high resolution, proton decoupled, ^{13}C n.m.r. may well yield the desired information. A detailed knowledge of the distribution characteristics over a variety of nitrogen contents may allow for the first time the calculation of expected birefringence values and the advancement of this classical technique from a purely qualitative procedure to a semi-quantitative method backed by theoretical calculations. The importance of birefringence[109] as an analytical tool would thus be enhanced and may then be used to study in depth

the orientation of nitrate ester groups within the fibrillar structure. In combination with X-ray diffraction (which because of the fibrous nature of the samples gives data which is difficult to interpret), significant advances could be made in structural determinations. In addition to this the comparison of X-ray diffraction data and in particular the d(101) interchain spacing with distribution data may shed light on the complex changes in microstructure which occur in nitrated and denitrated materials and yield an explanation of the differences in d(101) spacings encountered in materials of the same D.O.S. prepared by different means.

Hence it is clear that the application of modern spectroscopic techniques to a polymeric system whose potential was realised in the 19th century may well allow a much fuller understanding of the bulk and surface chemistries involved. It is the purpose of this thesis therefore to examine many of the questions raised above by the use and application of several analytical techniques.

CHAPTER TWO

THE BASIC PRINCIPLES AND USES OF E.S.C.A. (X-RAY PHOTOELECTRON SPECTROSCOPY), ^{13}C NUCLEAR MAGNETIC RESONANCE AND OPTICAL MICROSCOPY

PART I

ELECTRON SPECTROSCOPY FOR CHEMICAL ANALYSIS (E.S.C.A.)

2.1 INTRODUCTION

As early as 1888 Hallwachs[139] working in Germany observed and recorded the effect of ultra violet light on electrically charged sheers of zinc and this was followed in 1905 by the publication of Einstein's work on the photoelectric effect.[196] However it was not until much later that De Broglie[140] and Robinson[141] studied the emission of electrons by X-rays and attempted to analyse the energies of the photoelectrons with a magnetic analyser. Although the resolution was too poor to reveal any fine structure correlations were made between energy levels of electron orbitals and increases in emission of photoelectrons with kinetic energy. It was not until the 1950's, however, that Siegbahn[142] and co-workers revived the principle of X-ray photoelectron spectroscopy and developed an iron-free magnetic double focussing electron spectrometer with high resolution properties. In 1954 attempts were made to record high resolution photoelectron spectra excited by soft X-rays. The observation of sharp lines which could be distinguished from the background electron veil can be said to have materially changed the course and future of the technique, since the photoelectrons to which such lines could be attributed did not appear to suffer energy loss and therefore indicated the binding energy of the atomic level from which they were ejected. A great step forward was the realisation, from work on copper and its oxides,[143] that chemical shifts observed in the spectra were related to the environment of the core levels involved. The general utility of the

technique was not fully realised until as late as 1964 however. Siegbahn has reviewed much of his early work in 1968 in 'E.S.C.A., Atomic Molecular and Solid State structure studied by means of Electron Spectroscopy'.[144] Later work was published in 1969 in the standard text 'E.S.C.A. Applied to Free Molecules'.[145] Since the early 1970's an enormous research effort has been directed at all aspects of instrumentation and the application of E.S.C.A. to a variety of industrial and academic problems has made the technique the most important and adaptable means of analysing surface characteristics. Since much of the work described in this thesis is directly or indirectly related to measurements made by E.S.C.A. a brief explanation of the principles involved and application of X-ray photoelectron spectroscopy will now be given.

2.2 THE E.S.C.A. EXPERIMENT

The interaction of a monoenergetic beam of X-rays with an atom in a molecule results in the emission of an electron whose kinetic energy is related to the nature of the atom.[144] $MgK\alpha_{1,2}$ and $AlK\alpha_{1,2}$ are the most commonly employed soft X-ray sources with photon energies of 1253.7 ev and 1486.6 ev respectively although the advent of electronically operated dual anodes in modern spectrometers had led to an increased use of harder sources such as Ti, (photon energy 4510 ev), for analytical depth profiling purposes. The lifetimes of the core hole states are typically 10^{-13} - 10^{-15} seconds[146] emphasising the extremely short time intervals encountered in E.S.C.A. experiments compared to most other spectroscopic techniques. The total kinetic energy (K.E.) of an emitted photoelectron including contributions from the vibrational

rotational and translational motions as well as electronic is given by

$$K.E. = h\nu - B.E. - Er \qquad \text{(Eq. 2.1}$$

where $h\nu$ is the energy of the incident photon; (ν is the frequency of the X-ray radiation h is Plancks constant); B.E. is the binding energy of the photoejected electron and Er is the recoil energy of the atom, a quantity which decreases with increased atomic number and in fact it is only for the first few members of the periodic table that a recoil energy greater than 0.1 ev has been computed.[144] With the present resolution of typical E.S.C.A. spectra of solid systems contributions from translational, vibrational and rotational motions are seldom observed and assuming a negligible contribution from Er the general equation reduces to:

$$KE = h\nu - B.E. \qquad \text{(Eq. 2.2)}$$

The most convenient reference level for a conducting sample is the Fermi level or electron chemical potential which is generally defined as the highest occupied level whereas the work function ϕs for a solid is given by the energy difference between the free electron (vacuum) level and the Fermi level in a solid. The vacuum levels for the solid sample and the spectrometer may however be different and an emitted electron will experience either a retarding or accelerating potential equal to $\phi s - \phi$ spectrometer (work function of the spectrometer). In E.S.C.A. it is the kinetic energy of the electron as it enters the analyser that is measured and taking zero binding energy to be the Fermi level of the sample the following equation results:

$$B.E. = h\nu - KE - \phi spec. \qquad \text{(Eq. 2.3)}$$

The binding energy, referred to the Fermi level does not depend upon the work function of the sample but on that of

the spectrometer and this represents a constant correction to all binding energies. It is clear that for conducting samples in electrical contact with the spectrometer the Fermi level serves as a useful reference level. For insulating samples however the Fermi level is not well characterised analytically and lies between the filled valence levels and the empty conduction band. Sample charging in such materials is an important and much studied phenomenon and is caused by the generation of large currents at the surface of the samples. These currents consist of 'clouds' of secondary electrons produced by the interaction of the primary photoelectrons with matter and play an important role in establishing an electrical equilibrium at the surface of the sample.

Although, in some cases sample charging in insulating samples can be considered a major problem it has been shown in this laboratory that the measurement of charge built up on a sample and its time dependence can be extremely useful in the investigation of the electrical and chemical characteristics of the material. In the study of the surface modification of an ethylene-tetrafluoroethylene copolymer system, for example, it has been shown that the rate of decrease of sample charging in a range of these materials reflects the decreasing fluorine content in the surface regions.[170]

In an insulating sample the secondary electrons constitute 99% of the total flux whereas in a conducting material the figure is closer to 20%. This is not a large problem since standards are used to calibrate the binding energy scale and this will be discussed in a later section. Several processes accompany photoionisation; Auger and X-ray fluorescence for example are relatively slow processes and hence have

a negligible effect on the K.E. of the photoejected electron. Electronic relaxation processes, on the other hand, such as shake up and shake off are rapid processes resulting in a measurable change in K.E. of the emitted electron. Since the work in this thesis does not utilise either the Auger or the X-ray fluorescence techniques neither will be considered in detail here although excellent reviews are available elsewhere.[170] The basic processes involved in Auger and X-ray fluorescence however are outlined in Figure 6 and

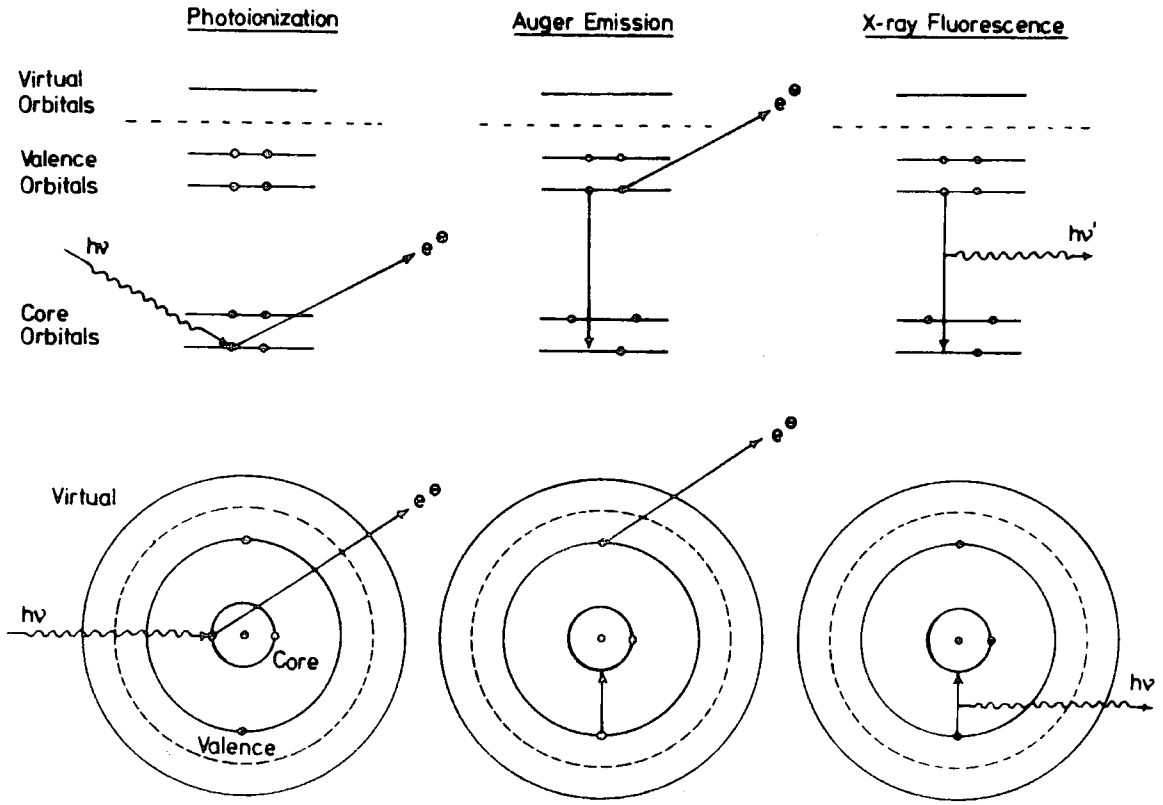

Figure Six Schematic of direct photoionisation, Auger and X-ray fluorescence processes

It is evident from Figure 7 that the efficiency of the Auger process decreases with increasing atomic number whereas the X-ray fluorescence yield increases along the periodic table. The development of the so-called Auger parameter by Wagner[147]

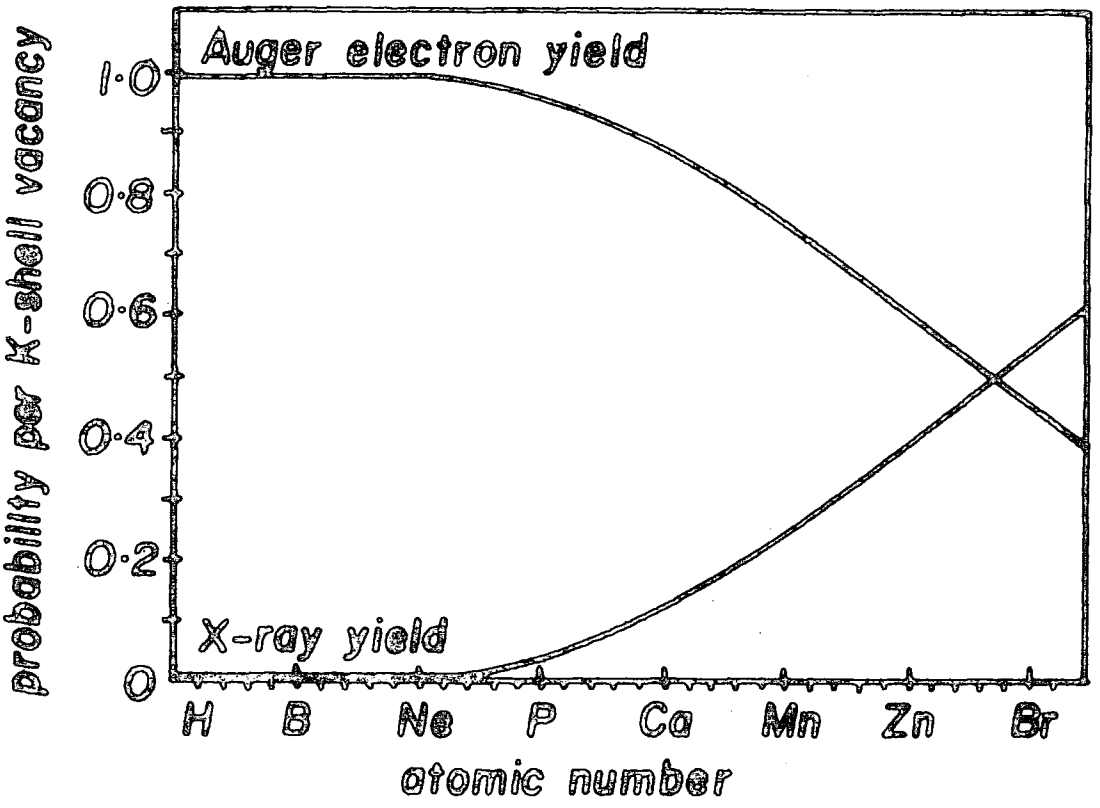

Figure Seven Yields of the Auger and X-ray fluorescence processes as a function of atomic number

in recent years has enhanced the importance of the technique although the parameter, (defined as the difference in kinetic energy between the photoelectron line and the intense core-type Auger line from the same element), has yet to be applied successfully to polymeric systems. The main advantages of the parameter are that charging and work function corrections are not needed and vacuum level data can be compared directly to Fermi level data.

2.3 ELECTRONIC RELAXATION

Following the photoionisation of core electrons a substantial rearrangement of electron levels takes place in a process referred to as relaxation.[148-150] Two such processes known as shake up and shake off are shown in Figure 8.

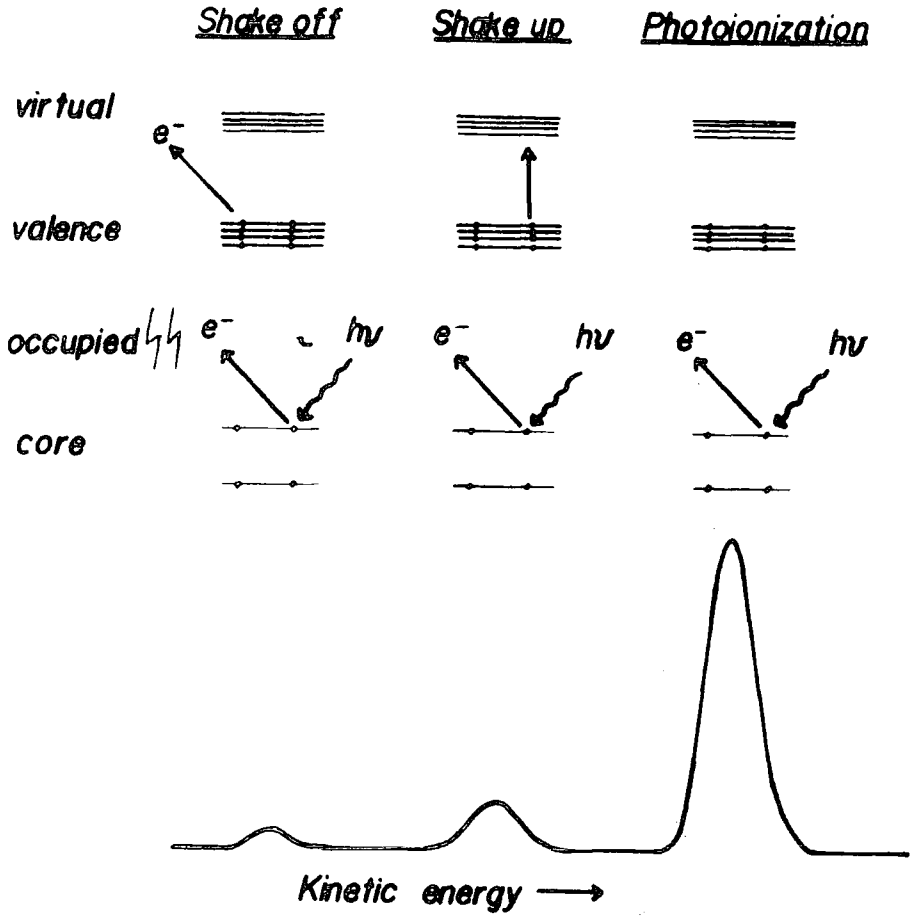

Figure Eight Schematic of Shake-up and Shake-off Processes

Shake up involves the simultaneous excitation of a valence electron from an occupied to an unoccupied level whereas shake off is an ionisation of a valence electron. Both these events result in excited states of the core ionized species with a lowered K.E. of the primary photoelectron hence since the energy for both these processes comes from the original photo-ionisation there is a need to adjust equation (2.2) to account for these multielectron processes

$$KE = h\nu - BE - \bar{E} \qquad \text{(Eq. 2.4)}$$

where $\bar{E}$ is the total energy of the multi electron processes. These excitations largely follow monopole selection rules, and the relative intensities of the shake up, shake off and photoionisation peaks are related to the relaxation energies.[151-155] This relationship was first established theoretically by Manne and Åberg.[192] They showed that the weighted average over

the direct photoionization and shake up and shake off peaks corresponds to the binding energy of the unrelaxed systems. This is shown diagrammatically in Figure 9. The transition

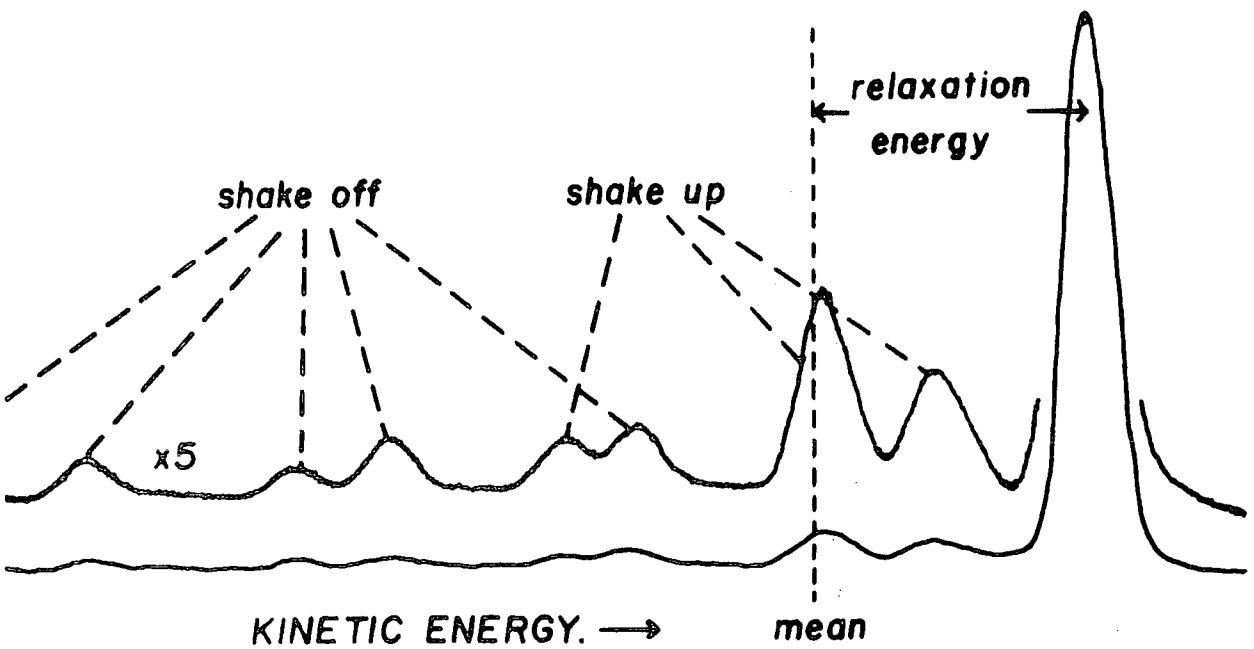

Figure 9 Relationship between relaxation energy and relative intensities of photoionisation, shake-up and shake-off peaks

probabilities for high energy shake off processes are relatively small compared to the shake up processes (which are of lower energy) and these transitions of higher probability fall close to the weighted mean. It might be expected that the relaxation energy should be available from experimental measurements but this is not generally the case since the smaller shake off peaks are often obscured by the so-called inelastic tail. (This tail is caused by the direct photoelectrons losing energy due to inelastic collisions and may extend to as far as 20 ev below the direct ionisation peak.

2.4 CHEMICAL SHIFTS

The energies of core levels are characteristic of a given atom and are sensitive to the electronic environment of that atom.[154] Small changes in environment of an atom give rise to measurable changes or 'shifts' in binding energies of photoemitted electrons. The experimental chemical shifts can be calculated using several theoretical approaches:

(1) Quantum mechanical models[155-157] (potential at an atom model)

(2) Madelung charge potential model[144]

(3) Equivalent cores model[158]

(4) Koopmans Theorem[160].

A full explanation of these methods is outside the scope of this introduction to E.S.C.A. but the importance of such calculations in confirming experimental shifts is demonstrated in Chapter Three.

The range in shift for individual core levels can in some cases be very large indeed (≈ 10 ev for the C_{1s} in fluorinated carbon species) and in others where the E.S.C.A. shift is small the utilisation of the Wagner Auger parameter[147] (see earlier section) has allowed further delineation of chemical environments.

2.5 ENERGY REFERENCING

Three basic situations may arise for solid samples in the spectrometer. They may be either in electrical contact with the spectrometer as is the case where thin films are deposited *in situ* on a conducting substrate in the spectrometer source; they may be thick insulating samples mounted on Scotch tape and not in contact with the machine, or they

may be polymer films deposited on a conducting substrate in which case they may act abnormally and exhibit time dependent charging. In the first case it is possible to mount the specimens on a gold substrate and monitor the Au $4f_{7/2}$ core level[146] to provide a reliable reference point (84 ev). The second case applies to most polymeric materials and the most convenient reference is the hydrocarbon contamination at 285 ev (B.E.). In most samples studied in this thesis the binding energies are quoted with reference to the hydrocarbon peak. The third case is unusual and requires the application of bias potentials to determine the corrected binding energies.[161]

2.6 FIXED ANGLE STUDIES

For a homogeneous thick sample the total intensity I of the elastic peak for photoemission from a core level, i, is given by

$$dIi = F\alpha i\ Ni\ Ki\ e^{-x/\lambda i}\ dx \qquad [162\ 163] \qquad \text{(eq. 2.5)}$$

where F is the X-ray flux and is determined by the power and efficiency of the X-ray gun.

αi is the cross section of photoionisation of the core level i and is essentially a measure of the probability that a certain core level will be ionised by the radiation.[164] (This quantity is in principle calculable from fundamental properties of the atom[165] or can be measured by gas phase E.S.C.A. experiments). It is well established that the cross section in the dipole approximation, for randomly oriented polyatomic molecules and unpolarised light is of the form

$$\alpha i = \alpha i^{TOT}/_{4\pi}\ \left[1-\tfrac{1}{4}\beta i(3\ Cos^2\phi-1)\right] \qquad \text{(eq. 2.6)}$$

where βi is the assymetry parameter[195] of the core level and αTOT_i is the total cross section of the level.

Ki is the spectrometer factor which is dependent on the detector efficiency, the transmission qualities of the analyser and the geometric arrangement of the sample chamber to the analyser.

λi is the electron mean free path, (the distance in the solid through which the photoemitted electrons will travel before 1/e of them have not suffered energy loss through inelastic collision.

Electron mean free paths may be calculated theoretically[209] or determined experimentally.[210] The mean free path is a function of kinetic energy of the photoionised electrons and ranges from $\sim 4\text{A}^{\circ}$ for electrons of about 80ev kinetic energy to $\approx 30\text{A}^{\circ}$ for electrons of above 1500ev.

The sampling depth on the other hand is defined as the depth from which 95% of the signal from a given core level arises. In general the sampling depth is equal to three times the mean free path.

Ni is the number of atoms per unit volume on which the core level is localised. The most significant property of Ni is that the relative signal intensities for the core levels of different atoms in a homogeneous sample are directly related to the overall stoichiometry of the atoms in the sample. This is due to the fact that the peak intensity from a given core level is directly proportional to the number per unit volume of the atom in the sample

$$\frac{Ii}{Ij} = \frac{F\ \alpha i\ Ni\ ki\ \lambda i}{F\ \alpha j\ Nj\ kj\ \lambda j} \qquad \text{(Eq. 2.7)}$$

where Ii and Ij are core level intensities. If i and j are core levels of the same atom then $\frac{Ii}{Ij} = \frac{Ni}{Nj}$. If i and j are different core levels then ki αi λi ≠ kj αj λj and

$$\frac{Ni}{Nj} = \frac{Ii\ kj\ \alpha j\ \lambda j}{Ij\ ki\ \alpha i\ \lambda i} \qquad \text{(Eq. 2.8)}$$

The ratio $\frac{kj\ \alpha j\ \lambda j}{ki\ \alpha i\ \lambda i}$ is known as the sensitivity factor which can be determined from known samples of simple stoichiometry. These ratios depend on the individual spectrometer and should not be quoted here.

The use of angular studies to delineate surface and subsurface is a well established technique used extensively in this laboratory.[193] However as has been previously explained, (c.f. Chapter One), the physical nature of cellulose fibres which subtend a variety of angles of acceptance to the analyser precludes the use of this technique for these studies.

2.7 LINE SHAPE ANALYSIS

The large inherent width of core level signals from E.S.C.A. measurements has led to the need for accurate line shape analysis, for delineation of core environments within a given envelope.[146] The major contribution to broad linewidths comes from the polychromatic X-ray photon source although with efficient monochromatisation of the photon source the need for such analysis may well disappear. However with present instrumentation a precise method of analysis remains a necessity to make full use of the available information levels from E.S.C.A.

The measured linewidths for core levels may be expressed as

$$(\Delta EF.W.H.M.)^2 = (\Delta E_x)^2 + (\Delta E_{spec})^2 + (\Delta Ecl)^2 \qquad (Eq.2.9)$$

where ΔE F.W.H.M. is the measured width at half of the height of the peak (known as the full width half maximum F.W.H.M.)

ΔE_x is the inherent F.W.H.M. of the X-ray source.

E_{spec} is the contribution to the total F.W.H.M. from the spectrometer, (particularly from the analyser) and Ecl is the natural width of the core level under investigation. It is well substantiated that the contributions to ΔE F.W.H.M. from ΔE_x for the more popular sources is essentially Lorentzian line shapes whereas the contribution from ΔE_{spec} are known to be Gaussian and are primarily due to the analyser, focussing and detector imperfections. The nature of the lineshape from Ecl is dependent on the Auger and X-ray fluorescence processes and is essentially Gaussian. The convolution of these shapes produces a general lineshape with Gaussian characteristics,[145] the Lorentzian contributions showing in the tails although it is believed that the use of pure Gaussian shapes introduces only small errors and this therefore forms the basis of most analogue techniques.

The resolution of complex line shapes in the E.S.C.A. spectrum can be approached mathematically in the form of mathematical enhancement, (derivative spectroscopy),[166-168] or by curve fitting either digitally or by analogue means. Since both methods have been adopted for analysis in this thesis both will be considered here.

(a) Derivative Spectroscopy

This is a technique for obtaining first and, more generally, second derivatives of an E.S.C.A. signal with respect to kinetic energies, thus enabling a more complete resolution

of overlapping signals. For an overlap of two equal bands (separated by one half width or more). Smith[169] has shown that second order derivative is sufficient although fourth order derivatives have been obtained. Although an increase in resolution of ≈1.8 times the original has been obtained from second derivative spectroscopy the S/N ratio is reduced and the relative intensities of individual components cannot be extracted. It would seem that the major advantages are that the number and kinetic energy of the components of a given envelope can be fairly accurately determined. The application of this technique is demonstrated in Chapter Three where the unusual binding energies of carbons bonded to nitrate ester groups is shown for propyl and isopropyl nitrate as well as for nitrocellulose itself.

(b) Curve Fitting Procedures

Digital techniques of curve fitting have developed rapidly with the advent of microprocessors interfaced with larger computers and with increased automation of data accumulation it is no longer true to say that such methods are less convenient than analogue methods. The advantages of analogue methods, however, are evident in analysis of non routine samples where 'hands on' experience of an analogue curve resolver is extremely useful. To have both methods at one's disposal would therefore represent the ideal situation.

The principles of curve fitting are well established[144.170] and will not be considered here but it is often the case that without a high level of theoretical competence and a knowledge of model systems complex line shapes cannot be satisfactorily fitted.

2.8 INSTRUMENTATION

Since the early work of Siegbahn[144,145] many commercial spectrometers have appeared on the market. The work outlined in the coming chapters was carried out on an A.E.I. (Kratos) ES 200 A/B spectrometer[172] and on the E.S. 300 model fitted with a Mg/Ti dual anode. It is appropriate here to describe the equipment in some detail.

(a) X-ray Equipment

In the E.S. 200 instrument a Marconi-Elliot type GXS high voltage generator is used with variable voltage and current output. Whereas the E.S. 300 is fitted with a smaller solid state system. X-ray photon sources of the Henke[191] design (Ti Mg or Al) are used and for the softer sources the flux is in the order of 0.1 rad/sec[171] which is essentially, non destructive, for most polymeric systems.

The work in this thesis utilises Mg and Ti anodes although the use of monochromatised Al kα radiation can improve resolution. Mention should also be made here of a possible problem with the use of polychromatic radiation. In the case of the magnesium anode the $k\alpha_{3,4}$ satellite of an N_{1s} level corresponding to a nitrate ester group is coincident in binding energy with the main photoionisation peaks for several nitrogen containing systems (e.g. amines). This is further discussed in Chapter Five.

Al kα radiation can be monochromatised by a crystal (quartz) diffraction technique,[144] to eliminate the satellites and the continuum to produce pure $k\alpha_{1,2}$ radiation.

Difficulties in locating a suitable crystal with the appropriate lattice for monochromatising Mg kα radiation

have prevented a more widespread use of monochromatised X-ray radiation.

Figure 10, however, illustrates the three basic systems for Al kα monochromatisation; these are (a) slit filtering; (b) dispersion compensation, and (c) fine focussing. Method (a) is employed in the A.E.I. system which can, in principle, produce linewidths of 0.2 ev.

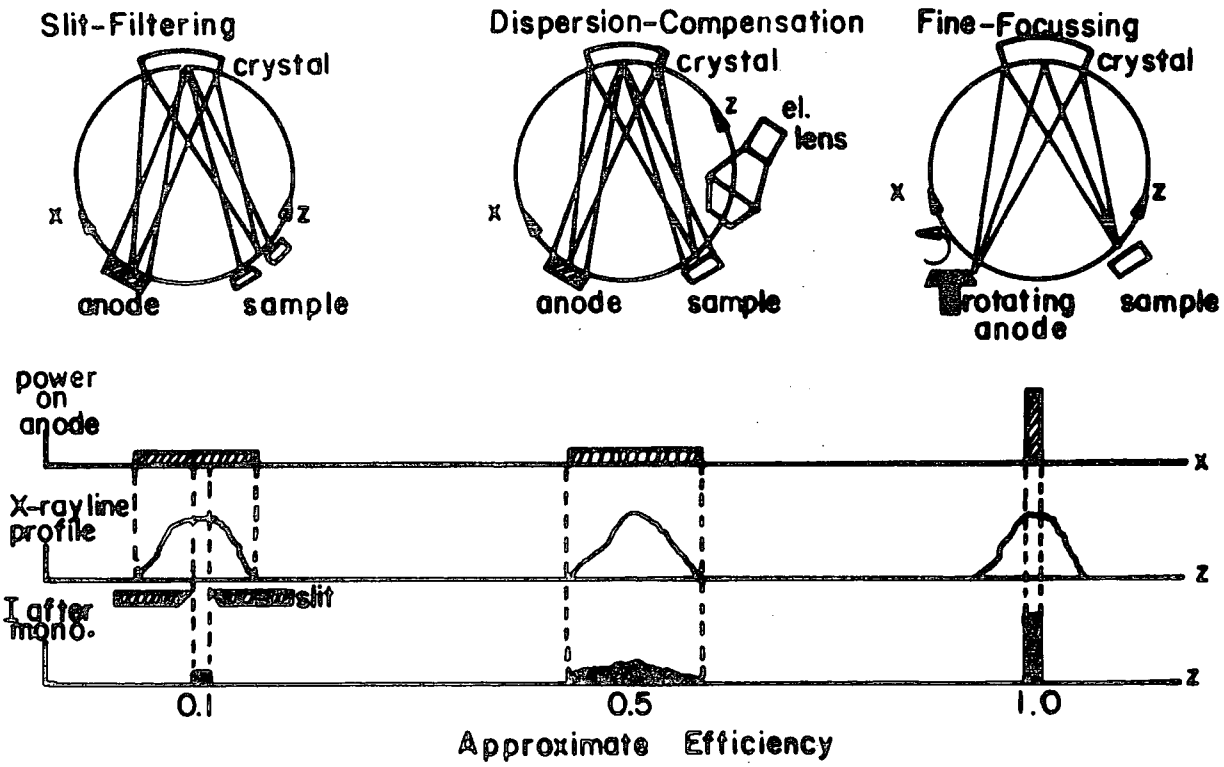

Figure Ten Diagram of alternative monochromation systems employed for Alkα monochromatisation

(b) Sample Chamber

The general format of an A.E.I. E.S. 300 electron spectrometer sample chamber is shown in Figure 11. The window separating the X-ray source from the sample ensures that scattered electrons from the filament do not enter the chamber and is generally made of aluminium or beryllium.

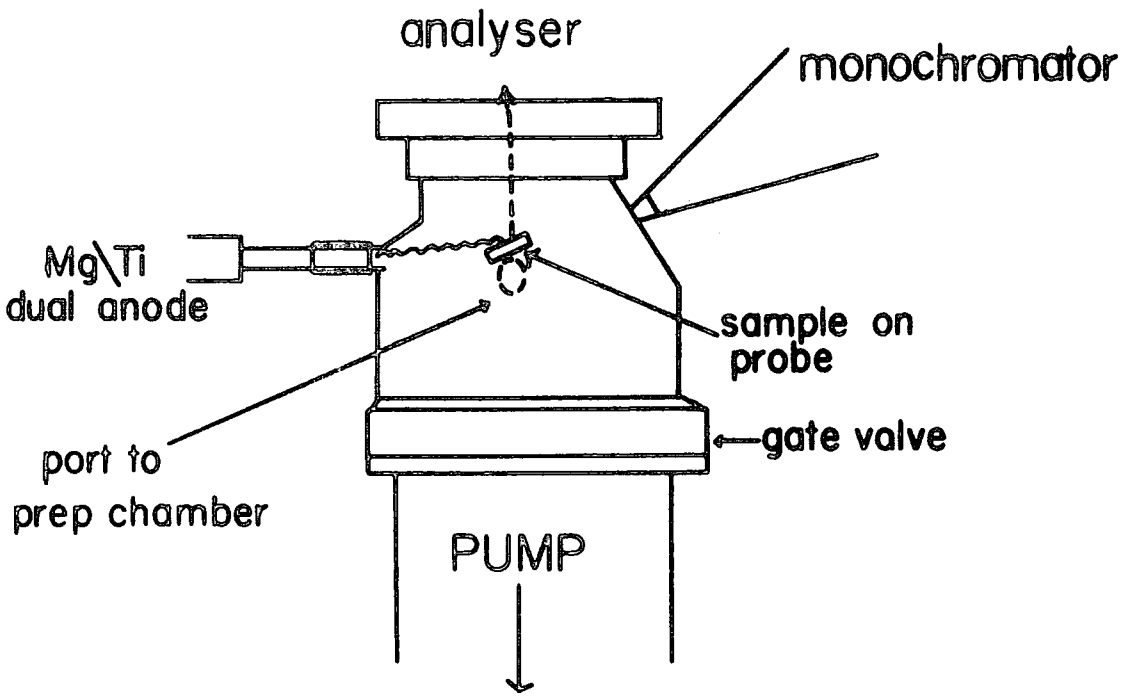

Figure 11 Schematic of the sample chamber in the E.S.300 (see text)

The chamber in both the E.S. 200 A/B and the E.S. 300 is accessed by many sample ports and in the case of the E.S. 300 by a pre-chamber in which a sample may be pretreated before analysis. The sample is mounted on a probe tip, (typically 18mm x 5mm), using double sided Scotch tape and is pushed through the insertion lock to the high vacuum chamber for analysis. The temperature of the sample tip is variable and may be rotated for angular studies. For polymer films and smooth metal surfaces such measurements are an important facet of X-ray analysis since they yield depth profile information, (thus the depth sample is dependent on the angle subtended to the X-ray beam). For fibrous samples, however

it has been shown that the fibres may lie with their axes at all angles to the beam and this precludes the use of angular studies of cellulose and its fibrous derivatives. For this reason this important topic will not be further discussed here.

(c) Analyser

The analyser in an A.E.I. spectrometer is a hemispherical double focussing electrostatic analyser which was originally described by Purcell[173] but is now enclosed within two mu-metal shields for protection from stray magnetic influence. The resolution of the instrument is dependent on the mean radius of the hemispheres, R, the width of the entrance slit and the width of the exit slit. The resolution $\Delta E/E$, where E is the energy of the electrons, is $\Delta E/E = \frac{R}{W}$ where W is the combined widths of the slits. The resolution can be enhanced by retarding the electrons before they enter the analyser so as to reduce their kinetic energy. Hence the electrons pass through a lens system before entering the analyser which (a) focusses the electrons and (b) applies a retarding potential for resolution control.[174] Focussing is achieved in the E.S. 200 A/B and the E.S. 300 by simultaneously scanning the retarding potential applied to the lens and the hemi-spherical potential while keeping a constant ratio between the two.

This is known as the fixed retardation ratio (F.R.R.). Both spectrometers are also capable of being run in the fixed analyser transmission (F.A.T.) mode in which the potential applied to the lens system is scanned while the potential between the hemispheres is held constant. This mode tends to discriminate in favour of low kinetic energy electrons and

in studies of high binding energy systems it is particularly useful. However in these studies the F.R.R. mode was always used. The absolute resolution also depends upon the natural width of the X-ray line $\Delta E_{X\text{-}ray}$; the width of core level studied. ΔCl; the line broadening due to solid state effects in the sample ΔESS and the broadening due to spectrometer irregularities. ΔES.

Hence for a solid sample,

$$(\Delta Em)^2 = (\Delta Ex)^2 + (\Delta ECl)^2 + (\Delta ESS)^2 + (\Delta ES)^2$$

(d) Detector

The electrons of a given K.E. pass through the exit slit of the analyser into an electron multiplier. The output pulses are amplified and processed in a data handling system. The data is recorded as either electron counts per second vs. kinetic energy of the electron or in a step scan where the field is increased by preset increments and the electrons are counted for a fixed length of time or as, in some cases, a certain number of counts are timed. The step scan may be used in conjunction with a multi-channel analyser to accumulate data over a period of time. The signal/noise ratio increases as the square root of the number of scans.

2.9 CHEMICAL TAGGING

When a particular functional group is at a particularly low level in a given sample or when the binding energy of a core level in such a group is very close to that in a different environment it may be advantageous to 'tag' the group with an atom, (or group containing an atom), with a high cross section for photoionisation. Thus it is possible to monitor

changes in the numbers of such groups after certain chemical or physical treatments using E.S.C.A. The use of trifluoroethanol and trifluoroacetic acid as tagging reagents is well known[175]. However a complete study has never been made on samples of known composition and molecular weight. In equilibrium exchanges the problem lies in forcing the reaction to completion but in general a reagent must -

(a) not dissolve the polymer

(b) react uniquely with the functional group.

The application of such techniques to cellulose and nitrocellulose are readily apparent. In cellulose itself it would be interesting to know the level of carboxyl groups at the surface and also if they survive the nitration process. A unique tag on such groups could yield significant information in a number of important areas which at present is precluded by the low level of carboxyl groups in natural cellulose. It may also be possible to tag free hydroxyls in partially nitrated materials and hence obtain information about the reactions occurring at the surface. during nitration in mixed acids. In Chapter Four of this thesis the value of chemical tagging is shown in relation to the iodination of primary nitrate groups in cellulose nitrate.

PART II

NUCLEAR MAGNETIC RESONANCE (N.M.R)

2.10 INTRODUCTION

In 1924 Pauli[194] suggested that certain nuclei possess angular momentum p and hence a magnetic moment μ. This was later confirmed by spectroscopic work which enabled values of the angular momentum and magnetic moment to be determined for many nuclei. In the presence of an applied magnetic field such magnetic moments take up specific orientations and it is possible to observe transitions occurring between the nuclear energy levels associated with these orientations by irradiating with energy of a suitable frequency. This forms the basis of nuclear magnetic resonance spectroscopy[175-178] (N.M.R.) and in the following pages a brief review of the principles and applications of the technique is presented.

2.11 NUCLEAR SPIN AND MAGNETIC MOMENT

All nuclei carry a charge and in certain cases this charge 'spins' on the nuclear axis generating a magnetic dipole along this axis. The angular momentum of the spinning charge can be described in terms of spin numbers I which may take values of 0, $\frac{1}{2}$, 1, 3/2 and so forth (I = 0 denotes no spin). The intrinsic magnitude of the generated dipole is expressed in terms of nuclear magnetic moment μ. Several nuclei (^{1}H ^{19}F ^{13}C ^{31}P) have a spin number I of $\frac{1}{2}$ and a uniform spherical charge distribution whereas nuclei with I > 1 have a non spherical distribution of charge giving rise to an electric quadropole moment which, as will be described

later , affects the relaxation times (see Section 2.15). The spin number I determines the number of orientations a nucleus may assume in an external magnetic field in accordance with the formula 2I + 1. This introduction to n.m.r. is primarily concerned with protons whose spin is $\frac{1}{2}$,(i.e.^{13}C), in which the proton may assume two orientations in the magnetic field.

2.12 NUCLEAR PRECESSION

A nucleus spinning in a static magnetic field behaves somewhat like a gyroscope in a gravitational field. As shown in Figure 12, the spin axis (which coincides with the magnetic moment vector μ) precesses about Ho. The frequency of this precession is known as the Larmor frequency of the observed nucleus, νo. The magnetic moments of spinning nuclei do not align along the direction of Ho but in fact the Larmor precession is accelerated by increasing the strength Ho of the field vector Ho_1. Therefore $\nu o \propto Ho$.

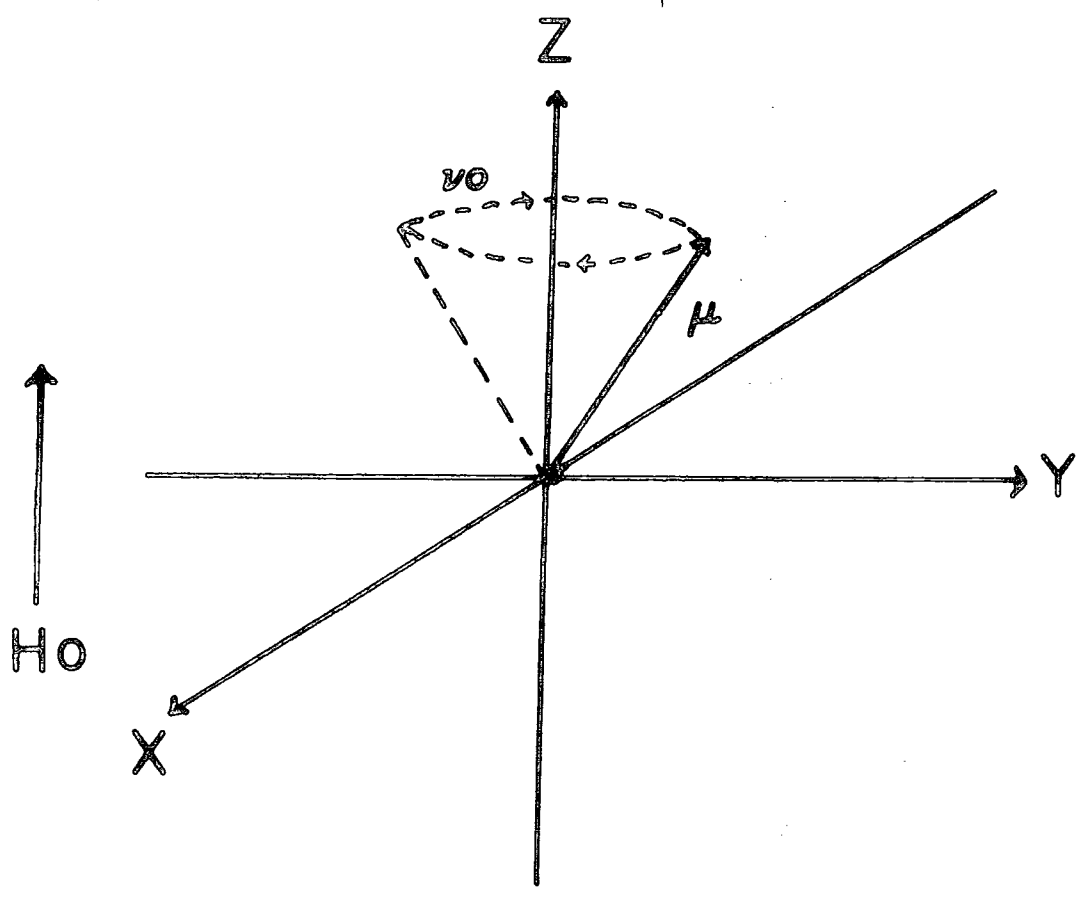

2.13 ENERGY LEVELS

The energy of the magnetic moment μ in a given field Ho is given by the product of the two

$$E = - \mu o . Ho = - \gamma \frac{h}{2\pi} I Ho. \qquad \text{(Eq. 2.12)}$$

A nucleus with total spin quantum number I may occupy (2I + 1) different energy levels in a magnetic field. For nuclei with $I = \frac{1}{2}$ (e.g. ^{1}H, ^{13}C, ^{15}N, ^{19}F, ^{31}P), two spin alignments relative to Ho arise, these are denoted $+\frac{1}{2}$ and $-\frac{1}{2}$.

The energies $E + \frac{1}{2}$ and $E - \frac{1}{2}$ and the energy difference ΔE between the two levels are shown in the following equation.

$$E + \tfrac{1}{2} = -\mu o . Ho = -\gamma \frac{h}{4\pi} . Ho$$

$$E - \tfrac{1}{2} = \mu o . Ho = \gamma \frac{h}{4\pi} . Ho$$

$$\Delta E = E-\tfrac{1}{2} - E+\tfrac{1}{2} = 2\mu oHo = \gamma \frac{h}{2\pi} Ho. \qquad \text{(Eq. 2.13)}$$

2.14 NUCLEAR MAGNETIC RESONANCE

ΔE above is the difference between the energies of precession along and opposite to Ho. The Larmor precession frequency νo of nuclei with $I = \frac{1}{2}$ can be calculated since

$E = h\nu o$.

Hence $\nu o = \frac{\gamma}{2\pi} . Ho$ (Eq. 2.14)

An alternating magnetic field Hl with frequency ν irradiating a multitude of nuclear spins precessing in the static field Ho may overcome ΔE if it meets the following requirement. The vector of the alternating field Hl must rotate in the plane of precession with Larmor frequency νo of the nuclei

to be observed.

$$\nu 1 = \nu o.$$

This results in the spins originally precessing with Ho flip over and now precess against the field. Absorbtion of energy ΔE from Hl then occurs and this is known as nuclear magnetic resonance.[175-178] In order to observe this phenomena a sample with the relevant nuclear spins is placed in a static field Ho. An alternating field Hi with radio-frequency $\nu 1$ is applied perpendicularly to Ho. Usually $\nu 1$ is increased or decreased slowly and continuously during observation. This is known as frequency sweep. When $\nu 1$ matches the Larmor frequency of the nucleus an absorbtion signal is recorded in the receiver of the N.M.R. spectrometer.

Obviously if the process continued one might expect all the nuclei to precess against the field very quickly and no signal was observed. Fortunately however an equilibrium is generally established between precession and relaxation effects and the latter will now be considered.

2.15 RELAXATION EFFECTS

(a) The Equilibrium of Nuclear Spins in the Ho Field

At equilibrium the nuclear magnetic energy levels are populated according to a Boltxmann distribution which favours the lowest energy state. The for two orientations relative to Ho of nuclei with $I=\frac{1}{2}$, the spin populations are symbolised by N+ and N-. The distribution N+/N- can be expressed by the Boltzmann factor

$$\frac{N^+}{N^-} = e^{\frac{\Delta E}{kT}} \simeq 1 + \frac{\Delta E}{kT} = 1 + \frac{2\mu_o Ho}{kT} \qquad \text{(Eq. 2.15)}$$

From the equation above it is readily apparent that the magnetic field Ho should be as large as possible because not only are the energy levels more widely spaced but also the sensitivity is increased.

(b) Spin Lattice Relaxation

At resonance the rf field Hl causes a spin transfer from the lower to the upper level. The equilibrium of the system is disturbed and the nucleus spins relax in a first order rate process with a rate constant $\frac{1}{T1}$ characterising each kind of nuclei. Tl is called the spin-lattice relaxation time. It covers a range of about 10^{-4} to 10^{4}s. In liquids Tl is a measure of the life time of the nucleus and is related to the half maximum intensity of an N.M.R. signal

$$\Delta V_{\frac{1}{2}} > \frac{1}{T1} \qquad \text{(Eq. 2.16)}$$

(c) Spin-Spin Relaxation

In solids and liquids with molecules with 'slow tumbling' dipole-dipole interactions between nuclei become important.

There is also an exchange of energy between the molecules and these tend to shorten the lifetimes of the spin states contributing to line broadening. This is also a first order process called spin-spin relaxation with a time constant $\frac{1}{T2}$. T2 is known as the spin-spin relaxation time. Also $\Delta V_{\frac{1}{2}} = \text{const.} \frac{1}{T2}$. The observed linewidth of the signal also depends upon the field inhomogeneity. Spin-lattice relaxation of a nuclei may be accelerated

(i) by interaction with adjacent nuclei having $I \geq 1$

e.g. (^{2}H, ^{14}N), the electric quadrupole moments of

such nuclei result in additional magnetic fields in the tumbling molecule;

(ii) by interaction with unpaired electrons in paramagnetic compounds (radicals, some metal chelates).

Spin-spin relaxation of nuclei is accelerated when they participate in a dipolar bond ($O-^{1}H$, $N-^{1}H$, $^{13}C-H$). In summary, therefore, all these interactions cause considerable line broadening but T1 also affects the energy level population.

2.16 THE MAGNETISATION VECTORS

For many identical nuclei of $I=\frac{1}{2}$ two orientations are possible for each nucleus. Due to the favouring of the lower spin state (nearly parallel to Ho) more nuclei precess about the direction Ho. The magnetisation vector along this path is denoted by Mo. On disturbance of the equilibrium by an rf field Hl with the frequency νl the magnetic moments μ are forced to precess in phase and the resultant magnetisation vector M is no longer parallel to Ho and has three components along the x y and z axes.

$$M = Mxi + Myi + Mzk \qquad \text{(Eq. 2.17)}$$

Mzk is the longitudinal magnetisation along the z axis, the other two are transverse components. It is possible to describe relaxation in terms of the magnetisation vectors but this is fully presented elsewhere[179] along with a full explanation of the Bloch equations which are beyond the scope of this brief introduction.

2.17 CHEMICAL SHIFT

In an atom or molecule a nucleus a is shielded from the static field Ho by its electrons. The field it actually experiences is Ha a combination of Ho and an additional field H,ind.a induced by the shielding electrons.

$$Ha = Ho - H,ind,a. \qquad \text{(Eq.2.18)}$$

This induced field has a strength proportional to the strength of the applied field Ho so that

$$H,ind,a = \sigma aHo \qquad \text{(Eq.2.19)}$$

where σa is the magnetic shielding constant[180] which characterises the magnetic environment of that nucleus. Since the effective field Ha experienced by the nucleus a is given by $Ha = Ho\ (1 - \sigma 1)$ then the nucleus a will precess at the Larmor frequency $\nu oa = \gamma/2\pi\ Ho\ (1 - \sigma 1)$ in the field Ho. This equation means that nuclei in different environments precess at different frequencies which give rise to the so called chemical shift. An absorbtion signal will be observed for each chemically, non-equivalent nuclei in the system.

2.18 CALIBRATION OF THE N.M.R. SIGNAL

Generally the absorbtion signal of a reference compound such as T.M.S. (trimethylsilane) is assigned a zero shift and all signals are measured from this point and their positions characterised by a frequency difference in Hertz (Hz). In order to get shift values which are independent of the frequency or field strength used the S scale is employed where δS the chemical shift is given by

$$\delta S = \frac{\nu s - \nu R}{Vl} \cdot 10^{-6} \qquad \text{(Eq. 2.20)}$$

where $\nu S - \nu R$ is the difference in frequency between the absorbing nuclei and the position of the reference compound and Vl is the radiofrequency used. The 10^{-6} term is used because the frequency differences are often very small indeed. Signals with small δS relative to T.M.S. are said to appear at high field and the nuclei are strongly shielded whereas the signal with large δS values are said to be at low field due to deshielding where $\sigma 1$ is particularly large.

2.19 SPIN-SPIN COUPLING

If a ^{13}C n.m.r. spectrum is not proton decoupled a complex proton coupled set of signals is obtained so that in a system AmXn (where Am is the number of equivalent nuclei A having a total spin quantum number Ia and Xn is the number of equivalent nuclei X having spin a quantum number Ix), the number of lines in the spectra will be equal to 2nIx + 1 for nucleus A and 2mIa + 1 for nucleus X.

This is true for so called first order systems only. Hence for example the ^{13}C n.m.r. spectra of a methyl group is a quartet according to the above equation, (since $I\alpha = \frac{1}{2}$ and n = 3).

2.20 SENSITIVITY OF ^{13}C N.M.R.

The main problem in observing ^{13}C n.m.r. is concerned with the low natural abundance of this nucleus and its low gyromagnetic ratio γ which yields a much smaller Boltzmann exponent $2\gamma poHo/kT$ than that of protons and give rise to low

sensitivity.[179]

It is possible to artificially enhance the ^{13}C abundance in selected samples or to use concentrated samples if solubility allows. In keeping with the Boltzmann equation it is theoretically possible to enhance the sensitivity by decreasing the temperature. Similarly the Boltzmann exponent can be increased by increasing the magnetic field strength or raising the ratio frequency power if relaxation is sufficiently quick to prevent saturation. Fortunately the accumulation of spectra is feasible by computer which averages the noise, (Computer averaged transients, C.A.T.). The signal/noise ratio increases with the number of scans n.

$$S:N \quad (S:N)_1 \sqrt{n}$$

The most efficient method of sensitivity enhancement in ^{13}C n.m.r. of organic molecules is Pulse Fourier Transform (P.F.T.) in combination with the various decoupling methods.

2.21 CONTINUOUS WAVE N.M.R. SPECTROSCOPY AND PULSED N.M.R.

Generally a continuous radiofrequency field is applied to a sample in a magnetic field, (continuous wave n.m.r.),[176] and the Larmor frequency of the nucleus is matched with that of the field to give the signal. In pulsed n.m.r. the sample is irradiated by short intense r.f. pulses which rotates the vector of magnetisation so that a transverse magnetisation vector results. This vector decays exponentially following the pulse due to spin-spin relaxation. If the r.f. differs from the Larmor frequency of the nuclei to be investigated (off resonance) the interference of the rotating transverse component with the r.f. field gives rise to the effect shown in Figure 13e. The spacing between two beats is the reciprocal

of the difference between the frequency of the pulse and the Larmor frequency $\frac{1}{(\nu_1 - \nu_0)}$. This is known as a Free Induction Decay (F.I.D.) signal and is due to freely relaxing spins after an r.f. pulse.

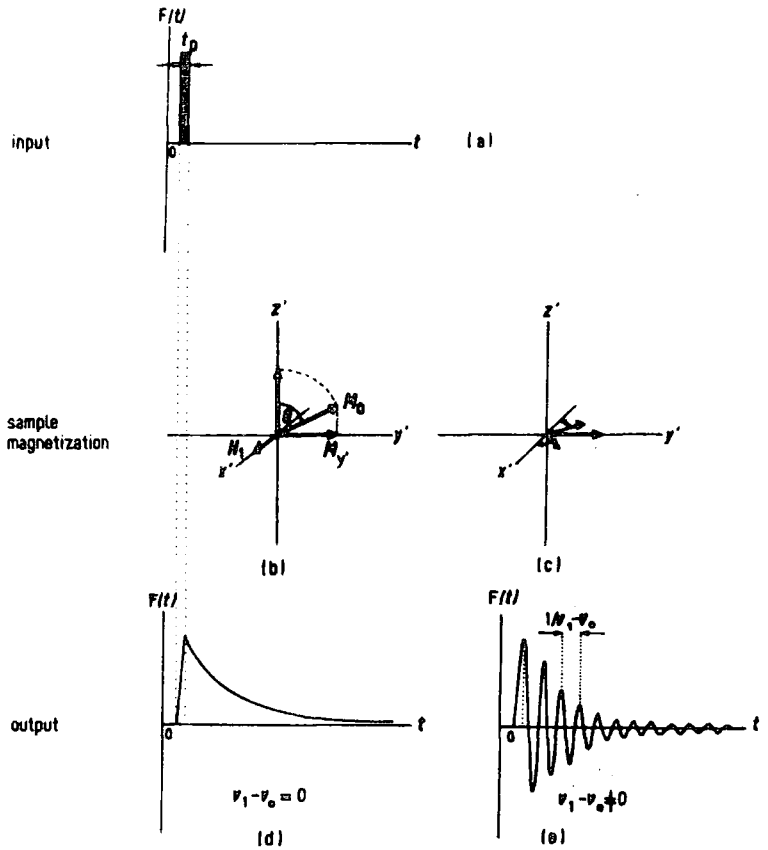

Free induction decay.
(a) rf pulse as input signal; (b) sample magnetization during the rf pulse; (c) free induction decay following the rf pulse; (d) output signal for rf at resonance; (e) output signal for rf off resonance.

Figure Thirteen

2.22 PULSE FOURIER TRANSFORM (P.F.T.) N.M.R. SPECTROSCOPY

F.I.D. signals are converted from analogue to digital form for Fourier transformation[181] in a computer with a memory size of 4-20K. The details of the transformation have been presented elsewhere but using the Fast Fourier Transform (F.F.T.) the computation can take as little as 1 minute for transforming an interferogram. P.F.T. techniques generally require less measuring time and are more sensitive than C.W. n.m.r.

2.23 SPIN DECOUPLING IN ^{13}C N.M.R.

^{13}C C-^{1}H spin coupling effects will vanish when proton broad band decoupling is applied which simplifies the ^{13}C-^{1}H multiplet system. Spin decoupling is achieved by irradiating nuclei not only with a radiofrequency field H1 at resonance with the nuclei to be observed but also with a second alternating field H2 at resonance with those nuclei to be decoupled (e.g. ^{1}H).

2.24 PROTON BROAD BAND DECOUPLING

In a ^{13}C experiment ^{13}C-^{1}H multiplets can be selectively decoupled although in most experiments all ^{13}C-^{1}H multiplets are decoupled for sensitivity and simplicity reasons. This is achieved when the decoupling field H2 covers a range of all proton Larmor frequencies and this is known as broad band decoupling. Decoupling fields are generally modulated using an audiofrequency to give the large range of frequencies required.

2.25 THE NUCLEAR OVERHAUSER EFFECT IN ^{13}C-^{1}H N.M.R.

The increase in sensitivity of N.M.R. experiments involving decoupling is due to the Nuclear Overhauser Effect.[182] Multiplet signals are accumulated into single lines and this can be traced back to an intramolecular dipole-dipole relaxation mechanism. The signal enhancement depends upon the gyro-magnetic ratio of the two atoms concerned (i.e. the observed nucleus and the decoupled nucleus). Quaternary carbons can often be recognised in decoupled spectra since they lack Overhauser effects but primary secondary and tertiary carbons are sometimes indistinguishable. Proton off resonance

decoupling can restore the multiplicity to some extent and allow identification of such carbon species. The Overhauser effect can be quenched by the addition of paramagnetic substances such as tert-butyl nitroxide or cobalt II acetate. These accelerate relaxation by way of dipole-dipole interaction between unpaired electrons and magnetic nuclei reducing the Overhauser effect and allowing integration of peaks due to carbons in different environments.

2.26 THE MAGNET

Commercially available instruments include magnets of about 10 kilogauss to 100 kilogauss. The stronger the magnetic field Ho the better the line separation of chemically shifted nuclei in the frequency scale and the higher is the sensitivity because of increased population of the lower spin levels. High field N.M.R. is achieved using superconducting solenoids giving rise to magnetic fields of 50-100 kilogauss.

2.27 THE SAMPLE

The sample solution is generally placed in a glass tube of diameter 5, 10 or 15mm which is rotated perpendicularly to the magnetic field Ho.[183] In ^{13}C experiments the sample is usually prepared by dissolving in the compound a deuterated solvent used for field/frequency stabilisation. For reference a small amount of a reference compound is added to the sample. A full account of N.M.R. instrumentation can be found elsewhere but it is appropriate at this point to consider the application of the technique in areas related to nitrocellulose and cellulose materials in general.

2.28 ^{13}C N.M.R. OF CARBOHYDRATES

N.M.R. is particularly useful for configurational and conformational investigations in carbohydrate chemistry.[179] Primary, secondary and tertiary carbons in carbohydrate systems can be distinguished by proton off resonance decoupling and a number of rules have been developed for the assignment of peaks in carbohydrate spectra. One of the interesting points to arise from these is that ring carbons with equatorially oriented hydroxyl groups on a saturated six membered ring absorb at lower field than corresponding carbons with equatorially oriented hydroxyl groups. The identification of anomers and mixtures of anomers is therefore possible.[184]

A recent review by Perlin[197] has outlined the use of ^{13}C n.m.r. in the identification and characterisation of carbohydrate polymers. The application of ^{13}C techniques to polysaccharides is remarkably limited although glycogen and cellulose acetate have been studied.[185] Wu[133] has recently published ^{13}C n.m.r. spectra of cellulose nitrates which, although poorly resolved allow the estimation of degree of substitution. Potential information on distribution of nitrate groups in nitrated and denitrated materials should also be available and this is more fully discussed in Chapter Four.

2.29 SOLID STATE MAGIC ANGLE SPINNING N.M.R.

In the last few years the study of polymeric materials in the solid state by n.m.r. has become feasible. Fyfe and Marchessault[198] have used solid state cross polarisation

magic angle n.m.r. to distinguish between the various forms of cellulose, i.e. crystalline and amorphous and it may be that significant information may be available from similar studies of cellulose nitrates.

PART III

OPTICAL MICROSCOPY

2.30 INTRODUCTION

Optical microscopy as a classical technique for the determination of microscopic features and elucidation of crystal structure had its origins long before the development of X-ray diffraction by Bragg[186] in the early part of this century. The application of the method in chemistry, however, was largely confined to the study of inorganic crystals and metallic salts and for this reason was largely superseded as a structural technique by the advent of X-ray analysis which was able to determine with considerable accuracy the positions of atoms within the unit cell. Although still widely used in the geological sciences[187] for the 'fingerprint' identification of minerals its application in chemistry is now largely limited to substances which, because of their physical nature have not been fully investigated by X-ray methods. One area where the use of polarisable microscopes has been very productive is that of fibre chemistry[188] and in particular the study of cellulose and its nitrated derivatives.[82,189] A full discussion of this work will be presented in a later section but it is first necessary to explain the principles and discuss the complex optics involved in the use of polarisable microscopes for analytical purposes.

2.31 POLARISATION OF LIGHT

If we consider light as a wave motion then, in general, it is true to say that vibrations will take place in all directions around the lines of transmission of that light. In many cases, however, the tendency to vibrate in all directions is modified and the waves become restricted for the most part to a single plane of vibration. This is known as polarisation. The production of polarised light can take place through several causes; (1) by reflection from polished surfaces (2) by repeated refraction at an angle through several plates of thin glass, (3) by absorbtion by certain crystals such as tourmaline, (4) by cleavages or prisms of optical calcite. Polarisation by absorbtion is the process most widely used in microscopy and will be further considered here. When light strikes a crystalline material such as tourmaline the vibrations in every plane except one are strongly absorbed giving rise to polarised light. The crystallographic axis c (often the long direction of the crystal) lies parallel to the plane of the vibration.

2.32 DOUBLE REFRACTION

When light passes through a large number of transparent materials it is often doubly refracted into two beams vibrating at right angles to one another.[199] One vibrates at right angles to the optic axis and is called the ordinary ray and the other vibrates parallel to the same axis and is known as the extraordinary ray. The ordinary ray has an index of refraction w and has a velocity $\alpha \frac{1}{w}$ and the extraordinary ray has an index ε and a velocity proportional to $\frac{1}{\varepsilon}$.

2.33 THE NICOL PRISMS

Many polarising microscopes operate using the crossed nicol system which utilise the principle of double refraction to produce plane polarised light. Optically clear calcite is used in nicols and the prism is constructed from two halves cemented together using Canada Balsam. Light entering the base of the prism is split into the ordinary and extraordinary rays. The extraordinary ray has a refractive index n=1.516 at the angle of incidence of the prism whereas the ordinary ray has a refractive index n=1.658. The index of the extra-ordinary ray is close to that of the cementing balsam n=1.537 but that of the ordinary ray is substantially larger. Hence at the balsam boundary the ordinary ray exeeeds the critical angle between itself and the balsam and is consequently re-flected to the side of the prism (Figure 14). The extra-

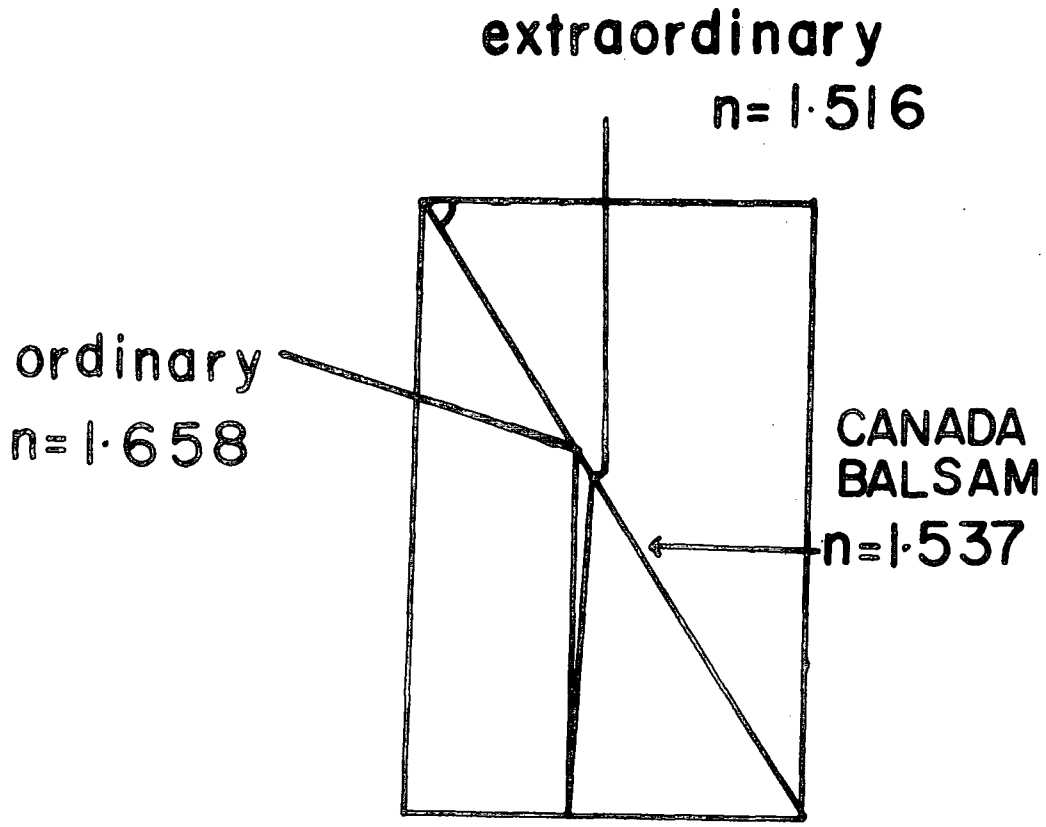

Figure Fourteen Diagram of a nicol prism showing refractive indices at phase boundaries

ordinary ray however does not exceed the critical angle and is hence transmitted without further deviation. Hence the light passing through the lower nicol in a microscope is plane polarised and entirely composed of the extra-ordinary ray. When two nicols are superimposed with their planes of vibration at right angles the nicols are said to be 'crossed'. In a polarisable microscope the lower nicol known as the polariser is fixed whereas the upper nicol can be moved in and out of the crossed position and is known as the analyser. Crossed nicols will produce darkness on the stage if it is unoccupied or if it holds optically anisotropic materials such as glass. Although calcite nicols are still to be found in many of the older microscopes it should be noted that the modern nicols are generally constructed from polaroid.

2.34 OBSERVATION OF SAMPLES BETWEEN CROSSED NICOLS

The polarised light from the lower nicol strikes the anisotropic sample vibrating in one plane. On entering the sample it is split into ordinary and extraordinary rays. Both sets are polarised but at right angles and the light is travelling at different velocities in each plane. As a result when the light emerges one set has travelled further through the material than the other but they continue in a straight line to the analyser continuing to vibrate at right angles. In the upper nicol the rays are resolved to vibrate in a single plane but the initial phase difference is retained. As a result they are in a position to interfere and colours are observed in the microscope image. The colour depends upon the nature of the light and the amount of retardation

of one set to another. The retardation (γ) is given by $\gamma = d(n_2-n_1)$ where d is the thickness of the sample, n_2 is the greater index of refraction and n_1 the lesser. The difference is in fact the effective birefringence for a particular orientation. The phase difference is the retardation divided by the wavelength $p_\lambda = \frac{\gamma}{\lambda}$. When the retardation is some whole multiple of a wavelength $n\lambda$ the waves emerging from the upper nicol become equal and opposite in phase. The resultant is then equal to zero and the field produced is dark. Maximum intensity will occur midway between extinction points, here the retardation is $(2n + 1/2)_\lambda$ and the components of the waves in the plane of the upper nicol are equal and on the same side of the line of transmission. The resultant wave is the sum of the two components. If the anisotropic material lies with the plane of vibration parallel and perpendicular to the planes of the polarisable devices no light passes through the analyser and the material is in a position of extinction.

2.35 MECHANISM OF COMPENSATION

Most polarisable microscopes in common use have an accessory slot located below the analyser into which a range of compensators can be fitted, (a full description of the various types is given in the next section). for the purpose of determining the path difference of the ordinary and extraordinary rays as they emerge from the upper nicol.

The general mechanism of compensation is as follows: suppose that a crystal plate is inserted in the accessory slot so that the fast and slow components oppose those of the original sample. The result will be a reduction in the total path differences produced by the plate and the sample.

Depending on the thickness of the plate one can achieve total or partial compensation. This is nicely demonstrated by the use of a quartz wedge (see Section VIb) and the general mechanism is illustrated in Figure 15.

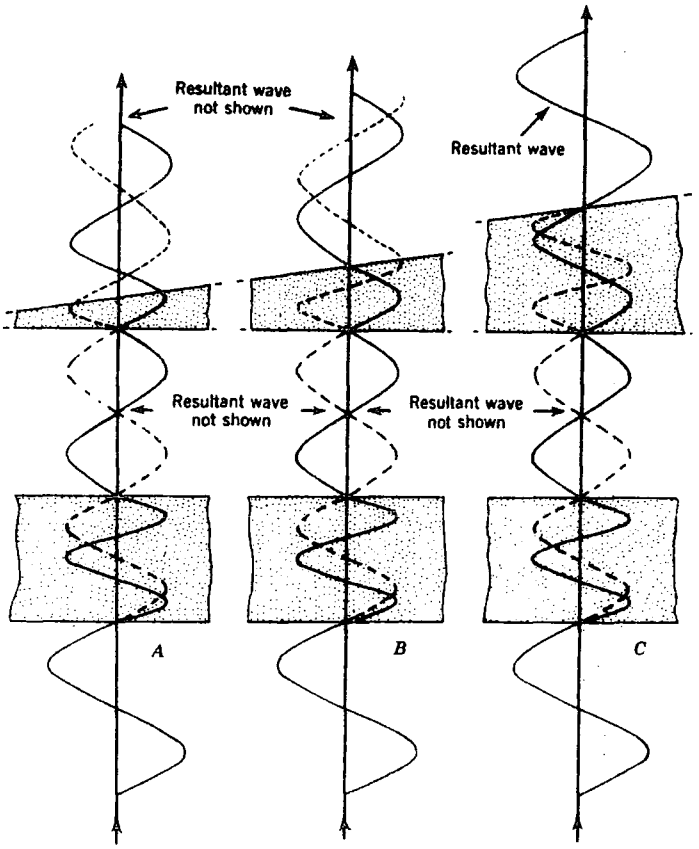

Two-dimensional diagram showing compensation by a quartz wedge. Path difference produced by crystal plate has been nullified by quartz wedge in position *C*.

Figure Fifteen

Monochromatic plane-polarised waves vibrating in a plane 45 degrees from the vibration planes for the crystal are incident on a crystalline sample and are resolved into two sets of waves, one set vibrating in the plane of the diagram, (solid line) and the other vibrating in a plane normal to the first, (dashed line). The crystalline sample illustrated has an orientation, birefringence and thickness such that a path difference of one-half wavelength is produced

between the emergent waves. The waves resulting from the combination of the emergent waves are not shown for the sake of clarity. Compensation of the waves results when the thickness of the wedge is such that the path difference produced by the crystalline sample is nullified as in Figure 15c. The resultant wave, (indicated as a solid line in Figure 15c), vibrates in the same plane as the wave incident on the crystalline sample and in a plane normal to the plane of vibration of the light waves transmitted by the upper polar.

A number of compensators are available which will measure a certain range of path differences and these will be discussed in the following section.

2.36 OPTICAL ACCESSORIES

(A) Quarter Wave Plate

The quarter wave, $(\frac{\lambda}{4})$, plate is made of colourless mica or birefringent plastic mounted in a metal holder suitable for insertion in the accessory slot of the microscope. Usually the direction of the fast component is oriented parallel to the long direction of the holder. If mica is used it is prepared by cleaving it into a sheet of a thickness that produces a path difference of a quarter wavelength. The quarter wave plate is used to determine optical sign from interference figures and to identify fast and slow directions in birefringent plates or fragments.

(B) Graduated Quartz Compensator

This compensator has an etched scale graduated in path difference, millimetres or arbitary units. Graduation therefore generally requires calibration. Compensation

produces a dark line across the wedge and the position of this line gives the path difference directly or by calculation. The theory behind such determinations has been presented in the previous section.

(C) Tilting Compensators

These are inserted in the accessory slot above the objective lens and below the upper polar (analyser) and contain birefringent plates that can be rotated about a horizontal axis so as to vary the effective birefringence between the two components of transmitted light. The Berek compensator, used in much of the work described in Chapter Seven, is particularly popular. It contains a piece of calcite that at the zero position produces no path difference. Rotation will increase the path difference in a controlled manner. To obtain compensation it is first necessary to rotate the stage 45 degrees, (or 135^{o}), from the position of extinction. This is to ensure the fast direction of the vibration of the sample is opposed to the slow direction of the compensator. The compensator is then rotated to produce extinction in the birefringent sample, that is, until the compensator cancels out the path difference produced by the sample. The path difference is read directly from a scale or is calculated by multiplication of angular scale readings by instrumental constants.

(D) Senarmont[200] Method of Measurement of Path Difference

The Senarmont method is widely used for highly accurate measurement of path differences less than a wavelength and requires a specially constructed quarter-wave plate and an upper nicol which can be rotated with precise measurement of the angle of rotation. A birefringent disc

in the quarter wave plate is designed to produce a quarter wavelength path difference for monochromatic light of 540 or 589 Mμ wavelength. The quarter wave plate is placed in the accessory slot of the microscope and in such a position is designed so that its slow direction of vibration is parallel to the vibration direction of the polariser. (It is possible to obtain rotating quarter wave plates which can be set in the required position). The analyser is rotated until it is crossed with respect to the polariser and the sample is rotated to the 45° position. The light from the polariser, (ideally monochromatic light should be used), is resolved into the two components, (slow and fast), by the sample and these combine to give an eliptical vibration. On entering the $\lambda/4$ plate this vibration is resolved along the vibration directions of the plate. If the phase difference between the components on entry is 90° then passage through the plate increases the difference by a further 90°, a total of $\lambda/2$, and they will interfere to give linearly polarised light. If the analyser is then turned to produce extinction the required phase difference can be shown to be equal to twice the angle of rotation of the analyser.

(E) The Elliptical Compensator[201]

This compensator is used in cases where the path difference is less than $\lambda/10$. It consists of a rotatable piece of mica (whose position in relation to the polariser and analyser can be accurately measured) which produces a known path difference. The polariser and analyser are crossed, the compensator is set at extinction and the sample is turned into either of its 45° positions. The compensator is then

rotated until extinction is obtained and if ψ is the angle of rotation it can be shown that

$R = Ro \sin 2\psi$ where R is the relative retardation for the crystal and Ro that for the compensator.

The theory behind this compensator is complex but is a general case of two crystal plates superimposed upon each other (a condition we shall meet in a later section relating to fibres). The intensity of the light transmitted by the analyser is given by the complex equation:

$$I = \sin 2(\psi_2-\psi_1).\ \sin 2\psi_1 \cos 2\psi_2 \sin^2 \frac{\pi}{\lambda} R_1$$
$$+\ \sin 2(\psi_2-\psi_1) \cos 2\psi_1 \sin 2\psi_2 \sin^2 \frac{\pi}{\lambda} R_2$$
$$+\ \cos^2(\psi_2-\psi_1) \sin 2\psi_1 \sin 2\psi_2 \sin^2 \frac{\pi}{\lambda} (R_1 + R_2)$$
$$-\ \sin^2(\psi_2-\psi_1) \sin 2\psi_1 \sin 2\psi_2 \sin^2 \frac{\pi}{\lambda} (R_1 - R_2).$$

where ψ_2 and ψ_1 are the angles made by the slow directions of the sample and compensator plates respectively with the slow direction of the polarised and R_2 and R_1 are their relative retardations.

Fortunately the $\sin^2 \frac{\pi}{\lambda}(x)$ terms where $x = R_1, R_2, R_1-R_2$ or R_1+R_2 can be simplified if R_1 and R_2 are small since the sine of a small angle is almost equal to the value of the angle expressed in radians. Thus for $\sin^2 \frac{\pi}{\lambda} R_1$ we can substitute $(\frac{\pi}{\lambda})^2 (R_1)^2$ and so on. The equation then simplifies to

$$I = (\tfrac{\pi}{\lambda})^2 (R_1 \sin 2\psi_1 + R_2 \sin 2\psi_2)^2 \ldots\ldots$$

In the extinct position $I = 0$ and

$$R_1 \sin 2\psi_1 + R_2 \sin 2\psi_2 = 0$$

In the situation where $2\psi_2 = 90^\circ$ the equation becomes

$$R_2 = -R_1 \sin 2\psi_1$$

2.37 LOCATION OF EXTINCTION POSITIONS

The location of the exact position of extinction is often a subjective procedure resulting in errors in final determinations. To assist the human eye in such observations a number of devices have been developed. The biquartz wedge, for example, is used with a special ocular and cap analyser and is constructed of two plates over which are placed two wedges. The pieces are cut at right angles to the optic axis and zero rotation of the plane of the vibration of light is produced when each half wedge has the same thickness as the underlying plate. A black band across the wedge marks this condition and when a birefringent substance is on the stage extinction can be determined when the illumination of the two halves of the wedge are equal. More often, however, the Lapinay or the Nakamura half shadow plate is used for this purpose. These plates have two segments which are grey colour at extinction but unequally illuminated to either side of extinction. Thus the ease of use of such devices makes them particularly useful.

2.38 APPLICATION OF OPTICAL MICROSCOPY TO CELLULOSE FIBRES

Most natural and artificial fibres are anisotropic to a greater or lesser degree and this arises from the fact that they consist of long chain molecules which tend to be arranged more or less parallel to the fibre axis.[201] This arrangement labels cellulose as a positive uniaxial medium, in other words it has a maximum refractive index for light vibrating parallel to the length of the fibre and a minimum for directions normal to the length. This gives rise to a positive birefringence however for highly acetylated cellulose the

birefringence is negative and this presumably is because the highly polarisable substituents greatly increase the vibrations or polarisability normal to the length.

Cellulose fibres, however, are intricate structures built up in the maturing plant with a spiral wall structure outlined in Chapter One. Depending on the pretreatment and drying procedures the fibre may also have a hollow circular lumen which must affect how we consider a fibre in the path of polarisable light. One could argue for instance, that every individual fibril will act as a tiny crystalline plate but taking the fibre as a whole we can see from Figure 16 that we have a system where the front and back walls of the fibre will act as individual crystal plates separated by the

$n\gamma = n_2$

$n\alpha = n_1$ (see text)

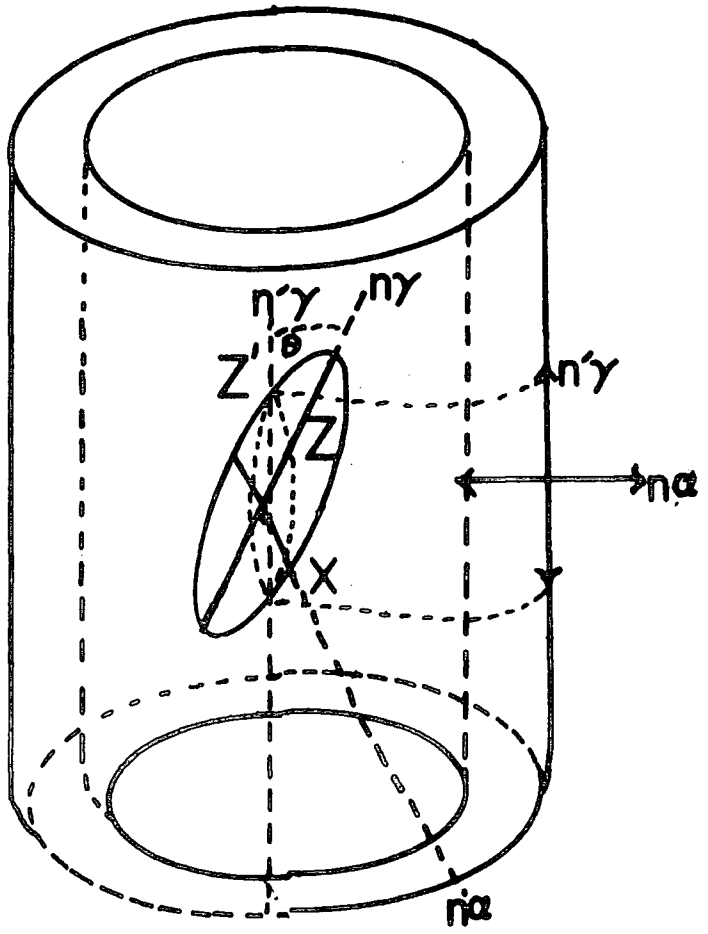

Figure 16 Drawing of a cellulose fibre with a hollow lumen showing front and back walls acting as separate birefringent plates

lumen.[201] It has also been shown that the refractive index along the length of cotton differs from that of ramie and flax,[188] and this can be explained by the relative positions of the spiral structures relative to the fibre axis. In ramie and flax the molecules are wound in a very steep spiral almost parallel to the fibre axis whereas in cotton the spiral is much shallower making an angle of $\approx 30^{\circ}$ with the axis. Hence when a cotton fibre is examined under crossed nicols it does not extinguish completely in any position but the light transmitted has a minimum intensity when the fibre is in certain positions. This is thought to result from the spiral arrangement. Consider Figure 16, the light passes through the front and back walls of the fibre and the vibration directions for these two walls are at an angle which, for a perfectly cylindrical fibre, reaches a maximum of 2θ between the slow directions. It can be further demonstrated using similar arguments to those presented in Sect.2.36 (E) that the intensity of light transmitted is a function of θ and also that the phase difference may also be a function of θ. Hence the actual physical state of the fibre may contribute to the birefringence. The work of Meredith,[188] (using the Becke Line method for determination of refractive indices in cellulose fibres), suggests that the nature of the convolutions is indeed related to the birefringence and this aspect is further discussed in Chapter Six. In Figure 16 n_2 - the index is that corresponding to the major axis OZ of the section XOZ'. n_1 is not affected by the inclination of this indicatrix. Thus this index is the same in cotton ramie and flux whereas the index n_2 changes with the spiral angle.

2.39 GLOSSARY OF TERMS

BIAXIAL CRYSTAL - Crystals of the orthorhombic monoclinic and triclinic systems are biaxial. When light passes through such crystals it is split into two rays neither of which obey the laws of refraction, i.e. two extraordinary rays.

BIREFRINGENCE - The difference between the maximum and minimum refractive indices in an anisotropic substance. (n_2-n_1).

CIRCULAR POLARISATION - The light emerging from anisotropic media is generally elliptically polarised except where the phase difference is equal to 90° or 270° and the amplitudes of the component vibrations are equal; in such cases the light is circularly polarised.

COMPENSATION - Compensation is the equalisation of paths of the ordinary and extraordinary rays to produce darkness or a specific colour in the field of view.

COMPENSATORS - Plastic or mineral discs with specifically known optical properties to produce compensation of the rays emerging from the sample.

DOUBLE REFRACTION - The splitting of plane polarised light into ordinary and extraordinary rays.

ELLIPTICAL POLARISATION - Polarised light which is the resultant of the rays emerging from an anisotropic medium.

EXTRAORDINARY RAY (AND ORDINARY) - This ray is that which does not obey the laws of refraction and its velocity will depend on whether the crystal is positively or negatively birefringent. Ordinary rays are those that follow the standard laws of refraction.

FAST DIRECTIONS (AND SLOW) - This refers to the trace of the plane of fibration of the component for which the crystal plate in the accessory has a relatively lower refractive index. The trace of the plane of vibration is the intersection of the plane with a surface such as a crystal plate. Slow directions are the reverse of the above.

On the other hand, the fast component generally refers to the fast ray in a crystalline material and is a measure of the velocity of the ray, generally the fast ray is that with the lowest refractive index and *vice versa*.

ISOTROPIC AND ANISOTROPIC - An isotropic material (e.g. glasses) will not give colours and will remain dark in the polarisable microscope image. Anisotropic materials will extinguish at four angles separated by 90^{o}.

(VECTORS) ELECTRIC - Simple oscillatory wave motion consists of a combination of uniform forward movement and simple harmonic oscillation at right angles to the direction of movement. In some cases it is convenient to refer to this as a forward movement of the electric vector oscillation.

CHAPTER THREE

E.S.C.A. STUDIES OF NITRATED AND DENITRATED CELLULOSIC MATERIALS

3.1 Introduction

Many of the important properties of nitrocellulose based formulations may be expected to depend on surface phenomena and it is perhaps surprising that so little attention has previously been directed at this aspect of the chemistry of nitrocelluloses. Since the initial reaction of any nitrating medium with cellulose fibrils is at the surface and since it is the surface which interfaces with the surroundings, the question of the mechanism of synthesis, of initial burn rate and of denitration are circumscribed by details of structure and bonding in not only the bulk but also in the outermost few tens of Angstroms of the surface. The paucity of data on details of structure and bonding in the surface regions of nitrocelluloses can be traced to a lack of any convenient technique for monitoring surface chemistry and the changes therein consequent upon chemical reactions initiated at the surface.

The advent of E.S.C.A. over the past decade as a powerful tool for elaborating details of structure and bonding in polymeric systems[202] means the direct investigation of surface nitration and denitration of cellulosic materials is a realistic possibility.

In this chapter detailed studies of the kinetics and mechanism of the surface nitration and denitration of celluloses using the wide range of information levels available from E.S.C.A., (which have been outlined in Chapter Three), are presented.

The dual anode capability of the AEI E.S. 300 spectrometer is used for depth profiling and with comparison to bulk data this provides considerable new insight into this important area.

3.2 The Nitration of Cellulose, Background Information

The main point of interest in technical nitration in mixed acid is the question of the degree of substitution and how this relates to the acid mix composition.

In theory it is possible to obtain any degree of substitution from mixed acids by varying the acid-water ratios.[41] However although the theoretical maximum degree of substitution is 3, in practice this is not attained and the maximum degree of substitution is ≈2.8. This is particularly so with respect to the surface D.O.S. (see section 3.4.2.)

A definitive answer as to why this should be has not thus far been given since in a heterogeneous process the delineation between the possible explanations requires a technique which can clearly distinguish surface from bulk phenomena.

The question of limiting degree of substitution (usually established by a micro Kjeldahl bulk determination) in nitrocelluloses could *a priori* be rationalised in terms of two extreme models.

The first can be attributed to the micro and microscopic structure of the cellulose. Thus inhomogeneities in the bulk structure could conceivably give rise to accessible and inaccessible regions. Since nitration must depend on the diffusion of reagent throughout the bulk structure a

further consideration is that there may well be a concentration profile throughout the structure (Figure 17). On

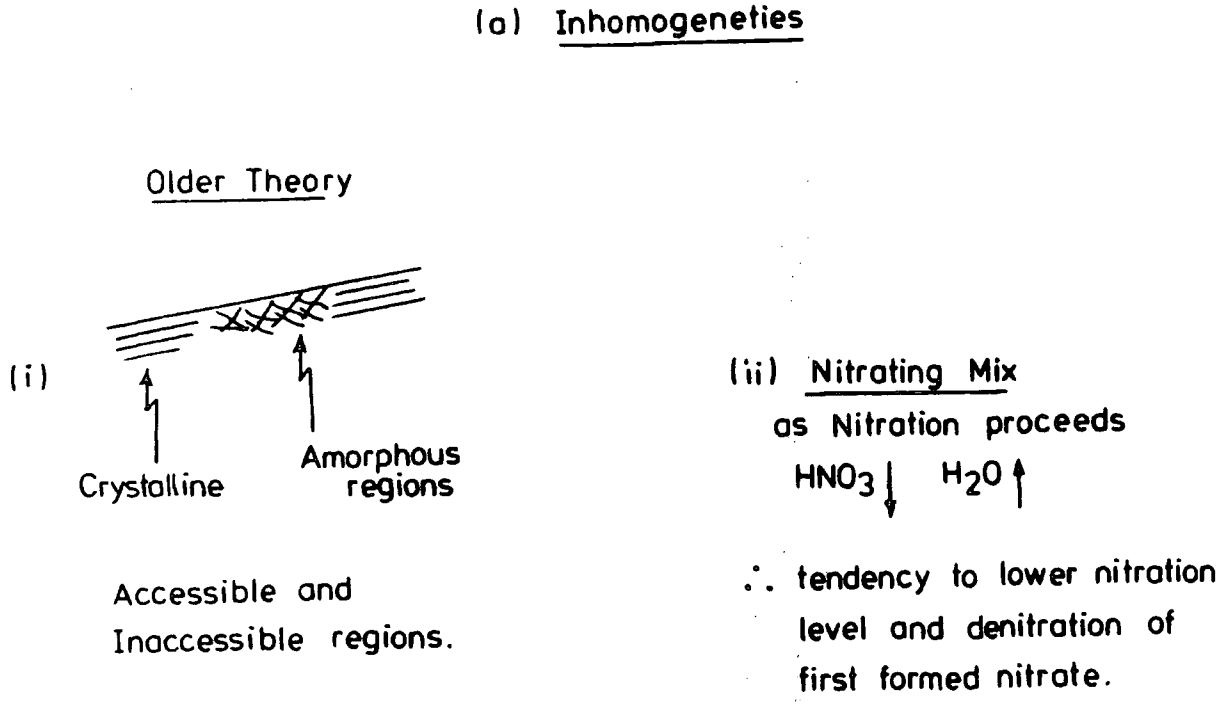

Figure Seventeen Diagram showing (a) possible inhomogeneities in a cellulose fibre and (b) the possibility of a concentration profile throughout the structure

this basis the less than maximum degree of substitution is attributable to an inhomogeneous bulk structure corresponding to regions of completely nitrated regions of material and unreacted inaccessible regions.

There are fundamental objections to this theory however which are described fully in a later chapter.

An alternative and somewhat more plausible explanation is that since nitration is generally considered a reversible esterification process then the ≈ 2.8 degree of substitution typically observed represents an equilibrium situation.

A full discussion of the fringe micellar model of structure and the more recent microfibrillar theory has already been presented in Chapter One and it is plain that an intermediate model would be more realistic.

The main feature of the model being that amorphous regions between crystallites run in continuous veins throughout the polymer and are not randomly distributed as in the fringed micelle theory.

In any heterogeneous process it is the surface which provides a window on the reaction however as has been previously noted the studies to date have been focussed on the bulk chemistry. Therefore presented here is a detailed comparison of the surface and bulk nitration and denitration of cellulosic materials in terms of degree of substitution and relative rates of reactions.

3.3 Experimental

It is important to specify both the source of raw cellulose and the methods used to nitrate since both can be a major source of variability.[41] In this section the basic procedures for preparation of nitrated and denitrated material used throughout the work presented in this thesis are outlined.

The general procedures are indicated schematically in Figure 18. Commercially produced, (Hercules Powder Co.), linters which had been pressed into paper form were used. The original cotton of American origin was dewaxed and depectinised. A Shirley fluidity of 8.8 and approximate degree of polymerisation 1100 was recorded for the linters which were vacuum dried at 60° for 2 hours and stored over

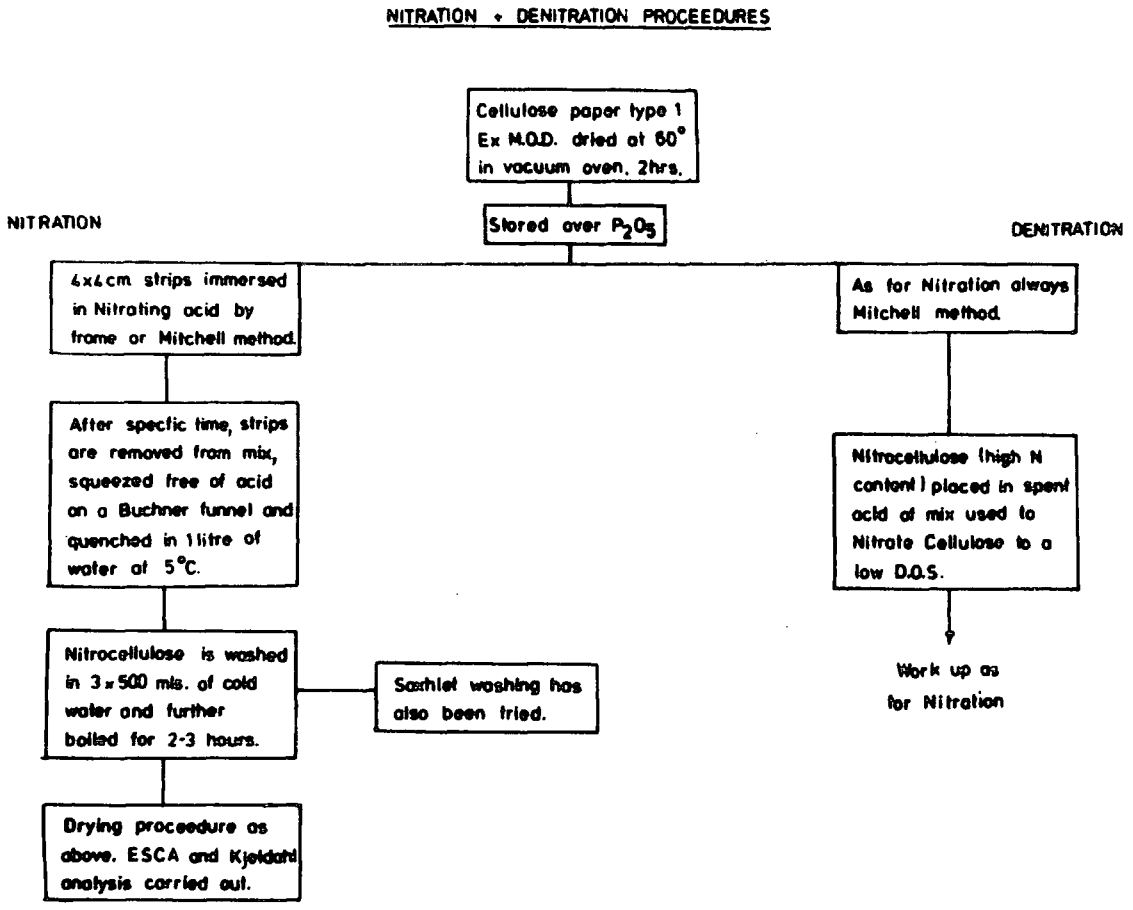

Figure Eighteen Schematic of the preparative methods of nitration and denitration

P_2O_5 for several days before use. This provides a starting cellulose sample with < 2% water content.

Nitrations and denitrations were accomplished by immersion in the appropriate acid mix of sample strips (4cm x 4cm) for a given period of time using an apparatus such as that depicted in Figure 19.

Bulk nitrogen determinations have been carried out using a modified micro-Kjeldahl technique.

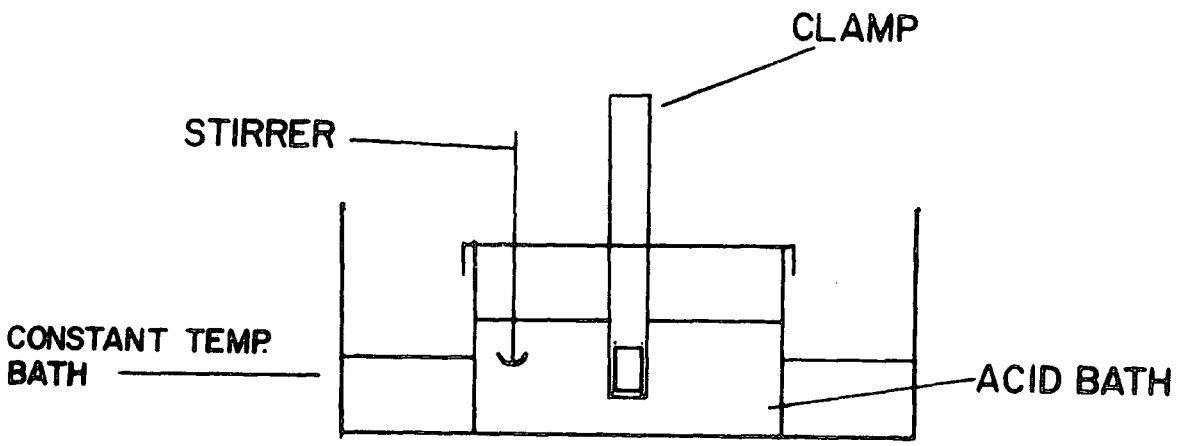

Figure Nineteen Apparatus used for the nitration of cellulose

3.4 Results and Discussion

3.4.1 Preliminary Analysis

In order to carry out a thorough analysis of core level binding energies of characteristic components in nitrocellulose spectra it is first necessary to study a range of model compounds. For this purpose the following samples were studied as thin films deposited *in situ* by a cold probe and reservoir shaft method on a gold substrate: propyl nitrate, N-butyl nitrate, isopropyl nitrate, butyl nitrite and nitromethane. All samples were commercially available and of purity >97%. They were therefore used without further purification. Spectra were recorded on an

A.E.I. E.S.200B spectrometer and deconvoluted using a Du Pont 310 curve resolver. Core level binding energies were referenced to the Fermi level by monitoring the Au $^4F_{7/2}$ signal in the early stages of deposition. The core level binding energies (N_{1s}, C_{1s}, O_{1s}) of the samples are presented in Figure 20, together with binding energies of comparable systems obtained from non empirical L.C.A.O., M.O., S.C.F. calculations.

COMPARISON OF THEORETICAL MODEL COMPOUNDS WITH EXPERIMENT

Molecule	Solid Phase Experimental B.E. (eV)					Theoretical B.E. (eV) (Corrected)				
	C_{1s}		N_{1s}	O_{1s}		C_{1s}		N_{1s}	O_{1s}	
CH_3CN						286.8	287.5	400.4		
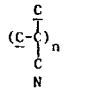	285.0	286.4	399.5							
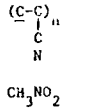	285.0	286.3	399.3							
CH_3NO_2		286.8	406.8	534.3			286.8	406.8	534.1	
CH_3ONO							286.8	404.9	534.9	535.3
$CH_3CH_2CH_2CH_2ONO$	285.0	286.7	405.0	534.2	535.2					
CH_3ONO_2							287.4	407.7	536.2	534.5
$CH_3CH_2ONO_2$	285.0	287.0	408.1	535.0	534.2					
$CH_3CH_2CH_2ONO_2$	285.0	287.1	408.0	535.5	534.1					
$CH_3CH_2(ONO_2)CH_3$	285.0	287.0	408.1	535.3	534.1					
$CH_3CH_2CH_2CH_2ONO_2$	285.0	286.5	408.0	535.5	534.3					
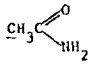						284.8	288.4	399.5	533.1	
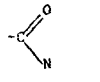		288.1	399.8	532.8						
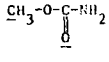						286.8	290.2	400.3	534.4	532.6
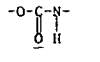		289.8	400.4	534.1	532.5					

Fig. 20 Diagram of theoretical binding energies, (actual and corrected for charging), of selected nitrogen containing species

The N_{1s} core levels show distinct shifts which facilitate identification of nitrate nitrite and nitro functionalities which could conceivably arise in spectra of nitrocelluloses, e.g. a 3ev shift is observed between an aliphatic nitrate and its nitrite. The nitro group has an N_{1s} binding energy at

406.8, equispaced between the nitrate and nitrite.

Of great interest also is the large primary shift on the carbon bonded to the nitrate ester 2.1ev from hydrocarbon referenced to 285ev.

Previous to this work studies of prototype systems for oxidative functionalisation of polymers have revealed that the additivity of oxygen as a substituent effect is typically 1.5 ± 0.4 ev; hence C-C = 285 ev; C-O = 286.5; $C<^{O}_{O}$ = 288 ev; $C<^{O}_{O}_{O}$ = 289.5. However it is evident from both practical determination of C_{1s} binding energies in organic nitrates and from theoretical calculations on the methyl nitrate system[203] that the C_{1s} shift in a C-O-X group where X = NO_2 is about 2.2 ev. This is nicely shown in the double derivative spectra, cf Chapter Two, for propyl and isopropyl nitrate and also of cellulose and cellulose nitrate, (presented in Figure 21).

The data confirms that a nitrate ester functionality has a substantially greater shift than might be anticipated on the basis of a simple additivity model and that this increased shift at a carbon associated with the conversion of an alcohol into its nitrate ester ($>C\text{-}OH \longrightarrow > C\text{-}ONO_2$) endows E.S.C.A. with considerable potential for monitoring changes in surface chemistry associated with nitrate ester formation.

Recent investigations[203] arising from this initial work have confirmed the anomalous effect of the nitrate ester and other nitrogen functionalities in particular with reference to the cyano group on adjacent C_{1s} binding energies.

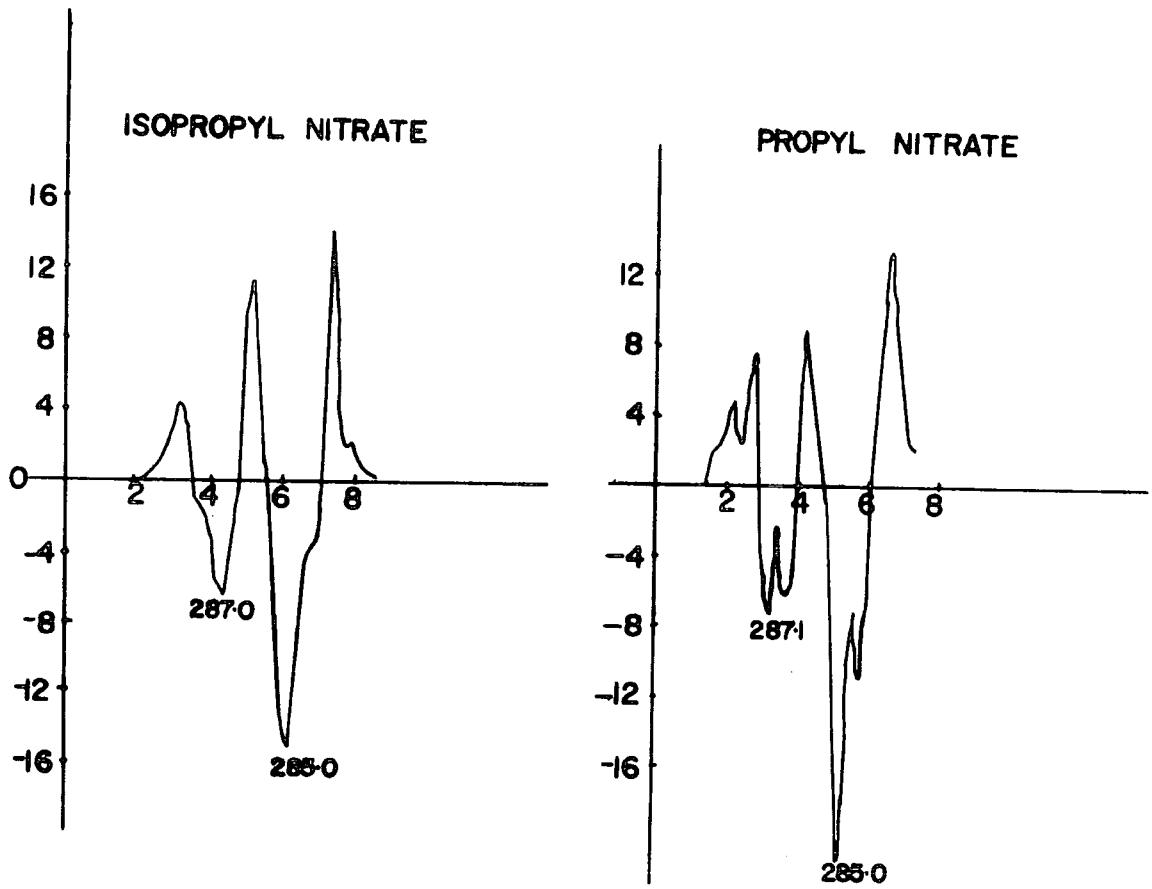

Fig. 21 Double derivative C_{1s} spectra of isopropyl and propyl nitrate and cellulose and cellulose nitrate showing the distinctive C_{1s} shift of the $\underline{C} - O - N\begin{matrix}=O\\ \searrow O\end{matrix}$ group

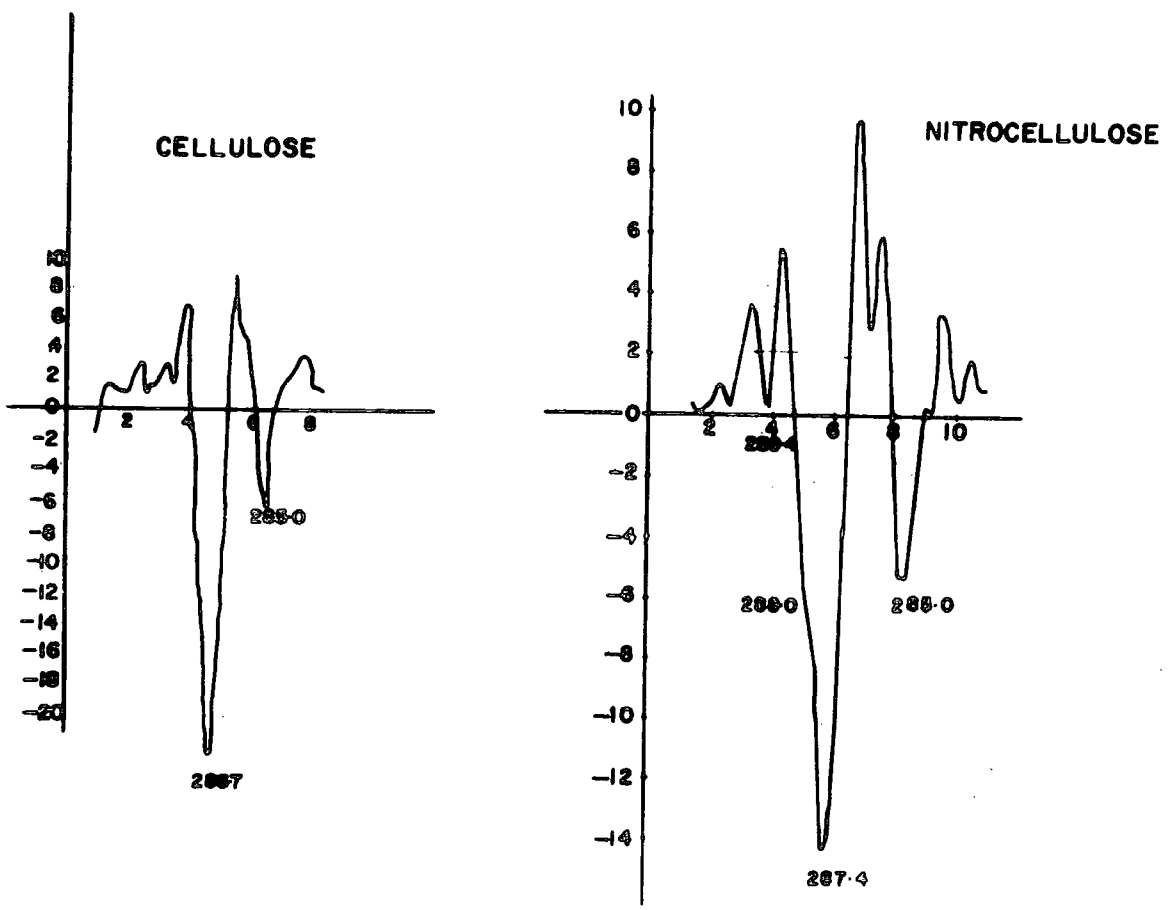

The core level, (C_{1s}, O_{1s}, N_{1s}), spectra for a typical nitrocellulose sample which has been commercially produced is shown in Figure 22. The C_{1s} spectrum shows 3 distinctive

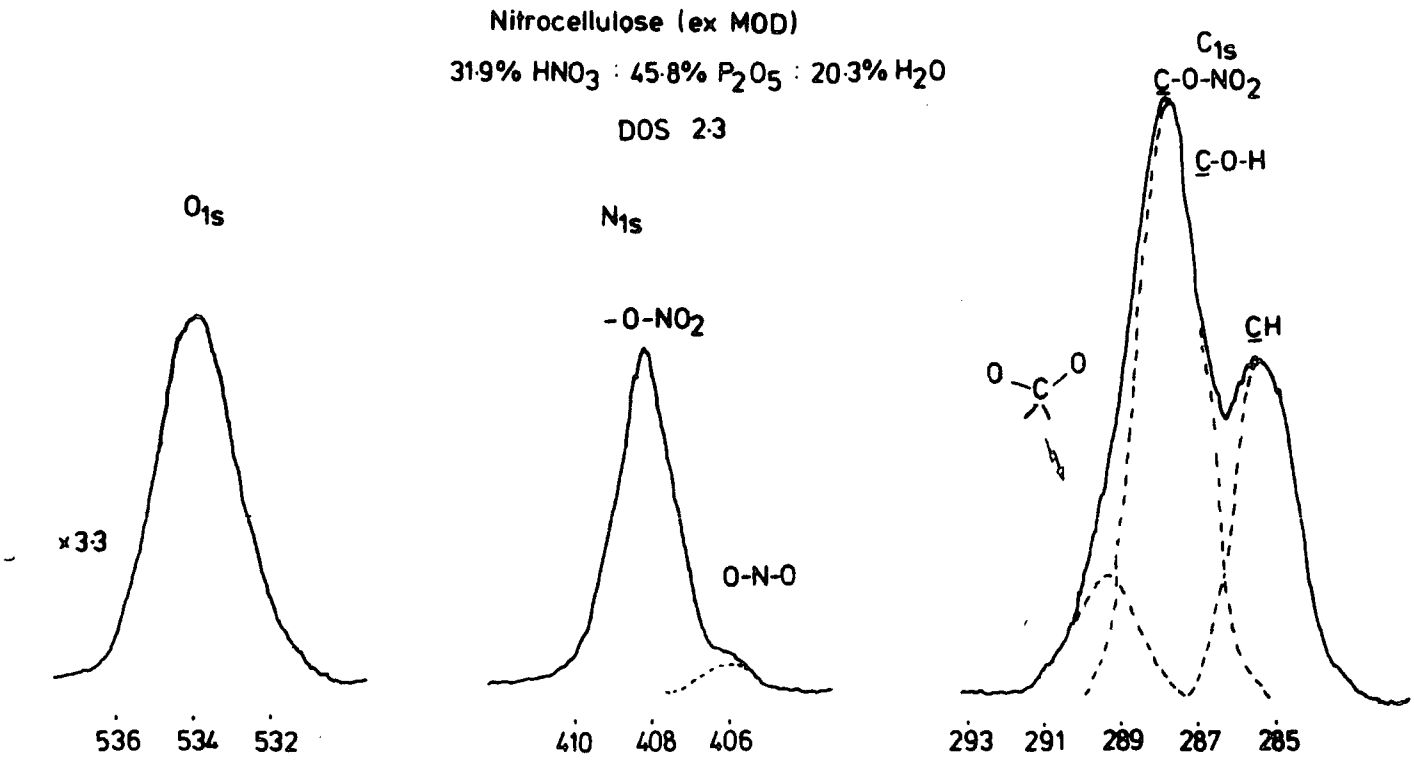

Fig. 22 Typical E.S.C.A. spectrum of a nitrated cellulose

components, (once a standard line shape analysis has been carried out). Thus the central component at 287.4 ev arises predominantly from the carbons C_2, C_3 and C_6 bearing the nitrate ester functionality with contributions from C_4 and C_5. C_1 uniquely attached to 2 oxygens in the cyclic hemiacetal formulation of the ß-D-glucopyranose rings is at the highest binding energy. The component at 285 ev arises from extraneous hydrocarbon which we will show later is confined to the very surface of the sample. In cellulose samples irrespective of source and type (e.g. linters or

paper type) the hydrocarbon signal observed is variable but inevitably present. The N_{1s} signal consists of an intense high binding energy component and (c.f. Figure 20) comparison with model systems unambiguously identifies this as originating from the nitrate ester groups $-O-NO_2$. In industrial scale nitrations a low binding energy component is often observed at ~ 405 ev and thus is associated with nitrite ester groups. In the laboratory scale nitrations where conditions are perhaps more precisely controlled such structural features are at a much lower level. Conventional nitrite traps (urea, ascorbic acid) dissolved in the nitrating mix to obviate the possibility of formation of nitrite esters have no effect(it is also interesting that doseing acid mixes with excess NO_2 does not increase the low levels of such structural features and it could be that they arise as a result of reactions occurring during stabilisation and storage). The effect of such esters on the surface chemistry and other factors concerned with initial burn rate of propellant has still to be investigated.

The O_{1s} levels are essentially composed of three peaks: the first at low binding energy 533.4 ev is comparable to the O_{1s} levels in cellulose itself and due to unitrated C-OH groups, ring and hemiacetal link oxygens. The central peak located at 534.5 ev is assigned to the $-\underset{\underline{O}}{\overset{\underline{O}}{\nearrow\!\!\!\searrow}}$ oxygens while the highest binding energy constituent at 535.5 ev arises from the C-$\underline{O}$-N functionality.

The binding energies are confirmed by theoretical studies on simple model nitrogen compounds[203] (Figure 20).

With a knowledge of sensitivity factors for the various core levels it is possible to straightforwardly work out the degree of substitution D.O.S. (average number of nitro-ester functionalities per glucose residue). Thus the integrated C_{1s}/N_{1s} area ratios (excluding the extraneous hydrocarbon component) yields a D.O.S. of 2.3 for the phosphoric/nitric nitrating mix; identical with that determined from micro-Kjeldahl bulk analysis. The total C_{1s}/O_{1s} ratio indicates that there is little residual water in the nitrated sample.

With fibrillar samples such as linters papers any information on vertical inhomogeneities into the sample may only be inferred by looking at different levels corresponding to different escape depths (c.f. Chapter Two). The use of $\frac{O1s}{O2s}$ core level area ratios, for example, as a means of depth profiling has been fully described elsewhere[170] but essentially utilises the fact that O_{2s} photo emitted electrons originate from much deeper in the sample than O_{1s} electrons. The O1s/O2s area ratio is thus a measure of oxygen content as a function of depth. O1s/O2s area ratios have been measured for a series of cellulose nitrates and Figure 23 illustrates the decrease in $\frac{O1s}{O2s}$ ratios and hence increase in nitration levels with time for a variety of acid mixes. This method however suffers from several inaccuracies and a full depth profile analysis requires a more sensitive method. Such a method is now available with the advent of the dual Mg/Ti anode facility. Consider, for example, the problem of the extraneous hydrocarbon observed in the E.S.C.A. Mg $k\alpha$ spectra of celluloses. Clearly the good agreement between bulk and surface analyses of material nitrated for 2 hours suggests

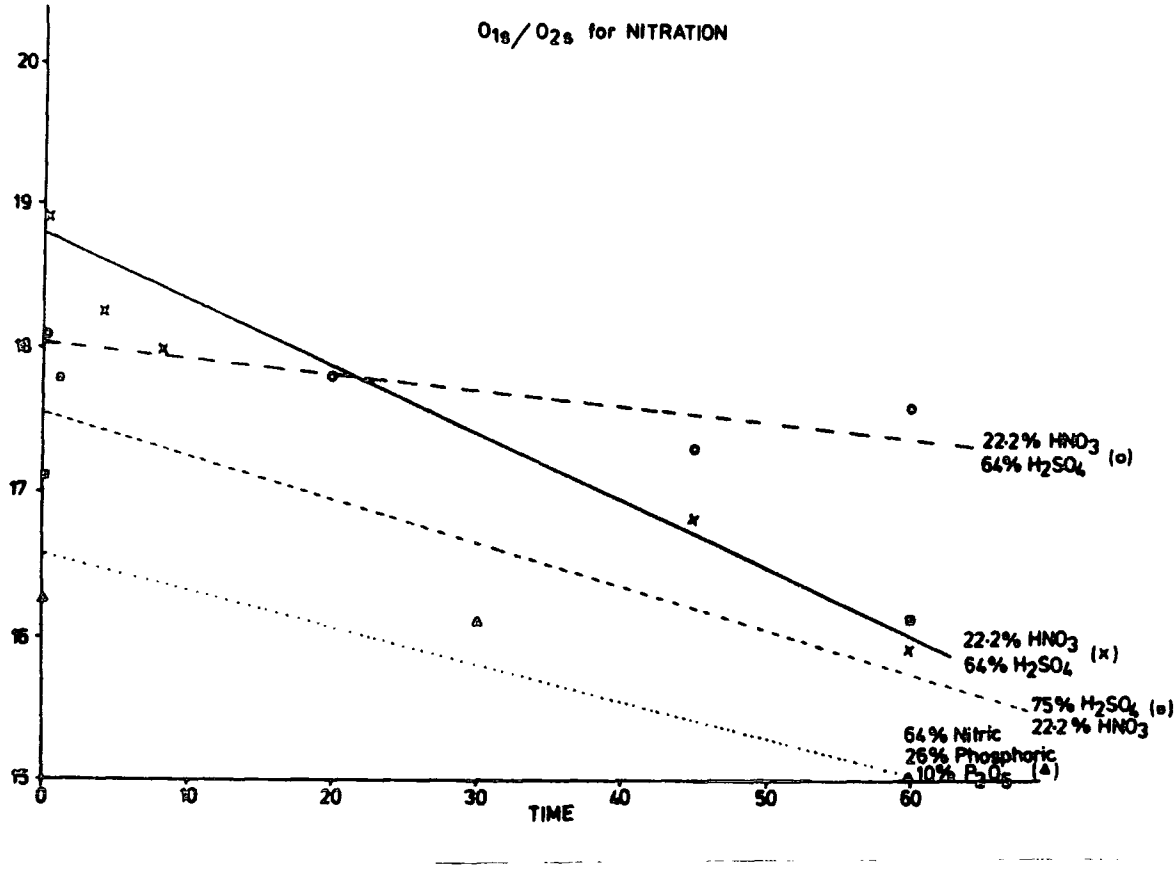

Fig. 23 Graph of O_{1s}/O_{2s} core level area ratios against time for a series of cellulose nitrations

that the sample is uniformally nitrated and the extraneous hydrocarbon must therefore be localised at the surface perhaps in the form of a patched overlayer since in most cases there may well be significantly less than a monolayer present. One way of establishing the purely surface nature of this hydrocarbon, (since the usual angular dependent studies are not feasible, c.f. Chapter One), is to compare D.O.S. averaged over different sampling depths. Whereas for Mgkα the typical sampling depth will be ~50Å for Ti kα with photon energy 4510 ev a figure of ~300Å would be more appropriate. Figure 24 shows N_{1s} and C_{1s} spectra for cellulose linters paper nitrated for 300 seconds in a low nitrating mix. Whereas the Mg kα for the C_{1s} levels show a significant contribution from the extraneous hydrocarbon the corresponding

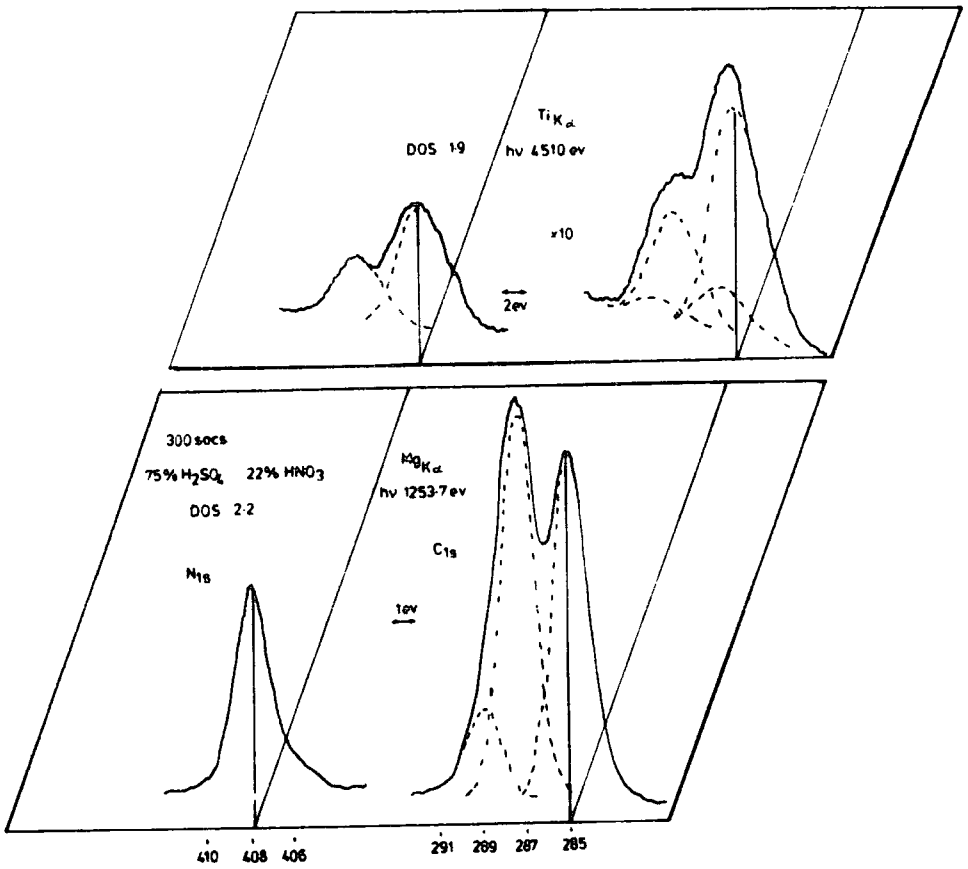

Figure 24

line shape analysis for the Tikα spectra is described with no contribution from hydrocarbon since even monolayer coverage (~5Å) would contribute a negligible contribution to the C_{1s} levels for electrons having a mean free path at least an order of magnitude greater (~90Å). This shows the great value of having a variable photon source routinely available. The use of Mg and Ti anodes for examining depth profiles in nitrocelluloses as a function of time is described later.

The relative sensitivity of nitrocelluloses to photochemical decompositions is known and it is therefore necessary to investigate the sensitivity to interrogation by means of E.S.C.A. of nitrated and denitrated cellulose samples. It may readily be shown that on a typical time scale for the E.S.C.A. investigations photochemical degradation is negligible. At the typical dose rates involved, (typical X-ray power ~150 watts), significant signs of decomposition require irradiation periods of >2 hours. The main reaction appears to be a photoreduction. Thus the high binding energy component in the N_{1s} spectrum appropriate to $-O-NO_2$ structural features is accompanied in the case of material subjected to irradiation for extended periods by a small peak at low binding energy possibly attributable to $-\overset{O}{\overset{\|}{C}}-NH$ functionality (cf. Chapter Five). Figure 25 shows the change in N_{1s} levels with time of irradiation and it can be seen that even after 5 hours the low binding energy functionality still only represents a small fraction of the total N_{1s} spectrum. We may conclude from that that X-ray degradation is negligible during the time scale of a typical E.S.C.A. investigation but that the appearance of a low binding energy component is an

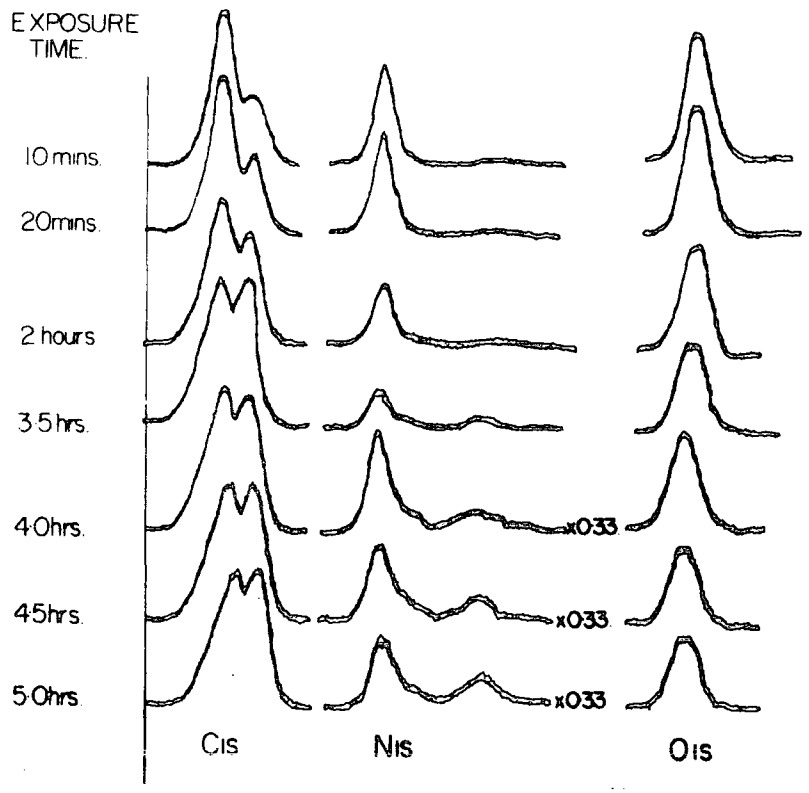

Fig. 25 Diagram showing the N_{1s} core level of a typical nitrocellulose on continuous X-ray irradiation with a Mgkα soft X-ray source

important photochemical feature which will be investigated further in Chapter Five.

3.4.2 Detailed Studies of Nitration and Denitration

For a nitrating mix of a given composition one of the most important features of interest is the question as to how rapidly an equilibrium D.O.S. is established in the surface regions accessible to E.S.C.A. As an example Figure 26 shows core level spectra for samples of the same batch of linters papers nitrated for different periods in a nitrating mix consisting of 75% H_2SO_4; 22.2% HNO_3; 2.8% H_2O.

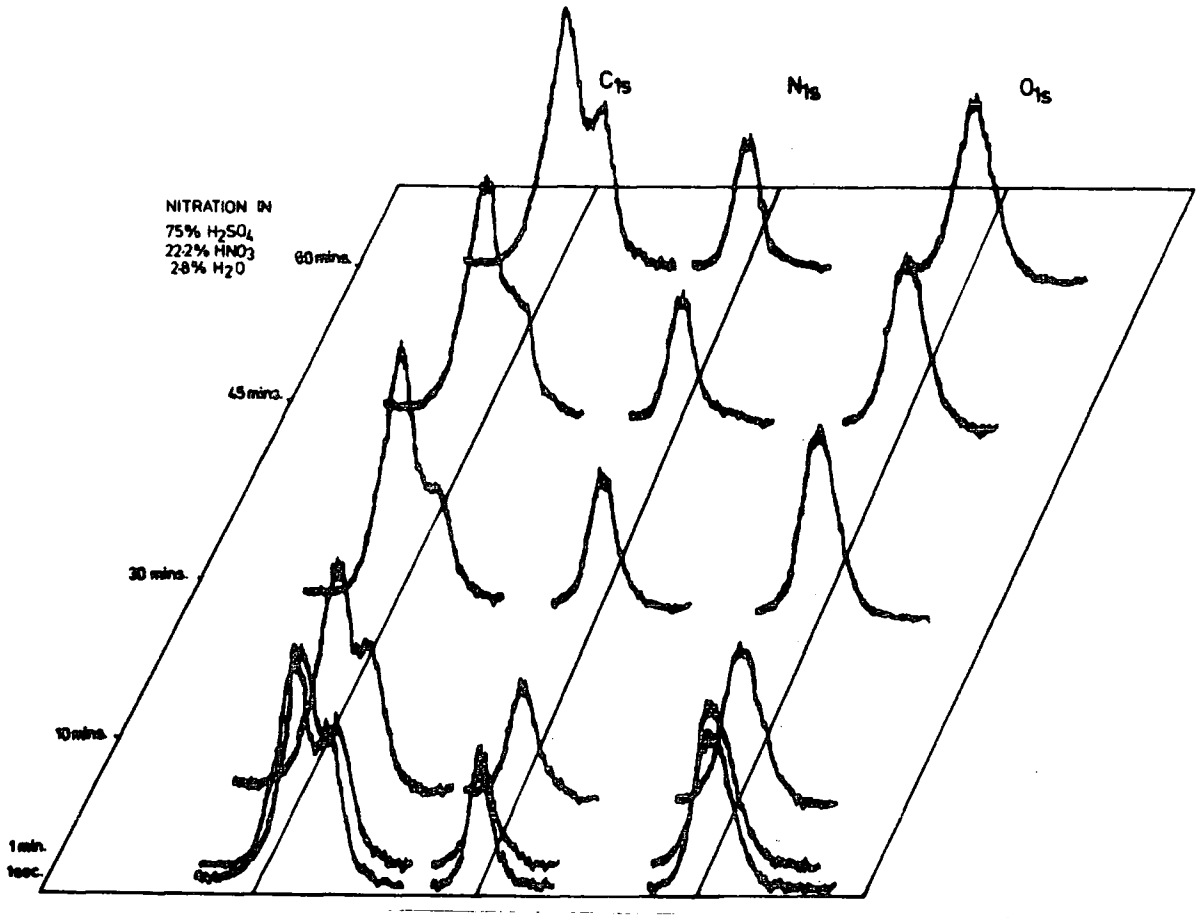

Fig. 26 Diagram showing C_{1s} and N_{1s} core levels as a function of time for nitration in a given acid mix

The N_{1s} levels which provide a ready means of following the nitration remain constant in intensity from reaction times of 1 sec. to 1 hr. This indicates that on the E.S.C.A. depth scale, equilibrium is very rapidly established. This is not entirely unexpected since the diffusion of nitrating mix into the outermost 50Å or so of the cellulose fibrils is expected to occur rapidly. A similar comparison is shown in Figure 27 for samples studied by means of the harder Tikα X-ray source. Here the sampling depth will be several hundred Angstroms yet the spectra recorded after reaction times of 1 sec. and 300 secs. are closely similar. It is clear therefore that the equilibrium D.O.S. is rapidly established in the surface regions.

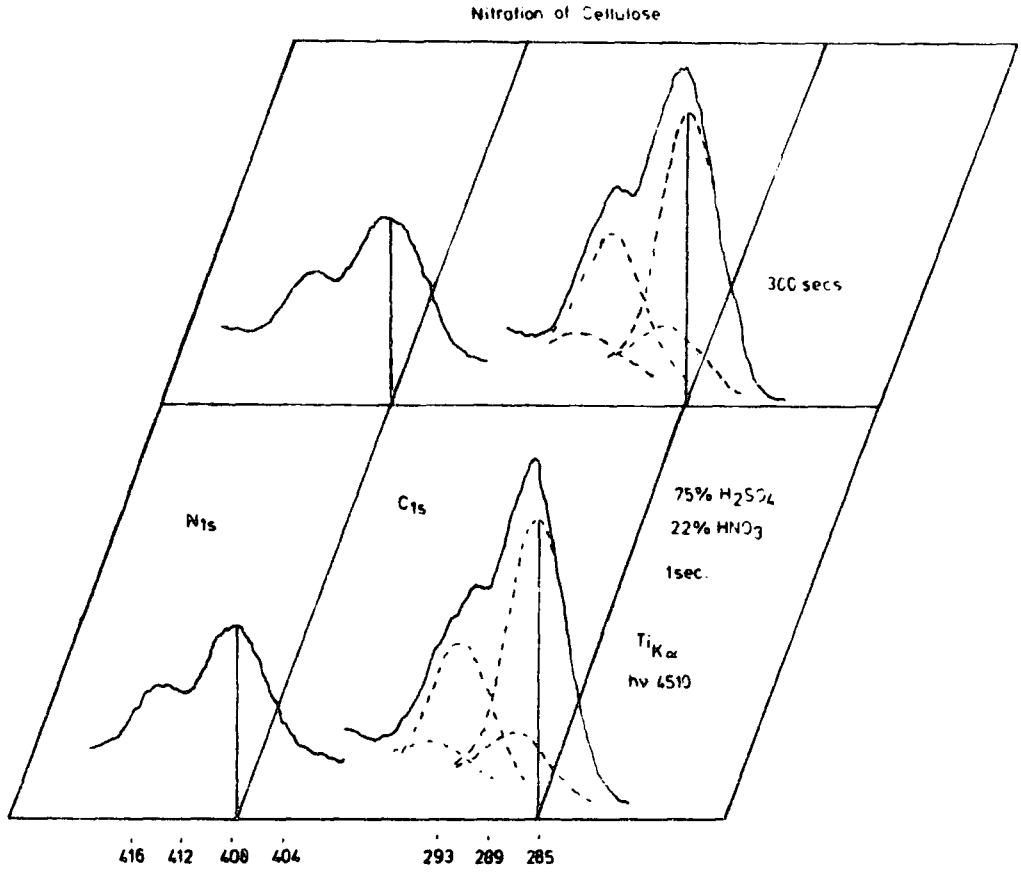

Figure Twenty-Seven

The gross features of the equilibria which are involved in determining the overall D.O.S. in the surface regions of cotton fibrils is outlined schematically in Figure 28. For mixed acid nitrating mixes it has been proposed that the sulphuric acid component does not diffuse into the crystalline microfibrils but acts purely as an intra-fibrillar swelling agent[41,3] and this could obviously lead to differences in D.O.S. for the surface and bulk regions of samples since only in the surface regions is sulphonation truly competitive with nitration. An important question which E.S.C.A. is potentially capable of answering is whether sulphate esters may be detected in the surface regions of nitrated material Mgk$\alpha_{1,2}$ spectra for the N_{1s}. S2p and C_{1s} regions of cotton linters

(i) $\sim O-H + 2HNO_3 \overset{K_1}{\rightleftharpoons} \sim O-NO_2 + HNO_3.H_2O$

$HNO_3.H_2O \overset{K_2}{\rightleftharpoons} HNO_3 + H_2O$

$\sim O-H + HNO_3 \overset{K}{\rightleftharpoons} \sim O-NO_2 + H_2O$

$K = \frac{K_1}{K_2}$ Nitration - denitration equlibrium rapidly established ?

(ii) Competitive sulphonation

$\sim O-H + H_2SO_4 \rightleftharpoons \sim O-SO_3H + H_2O$

(iii) Work up procedure

Hydrolysis

$\sim O-NO_2 + H_2O \rightleftharpoons \sim O-H + HNO_3$

Figure 28 Schematic of nitration-denitration equilibria

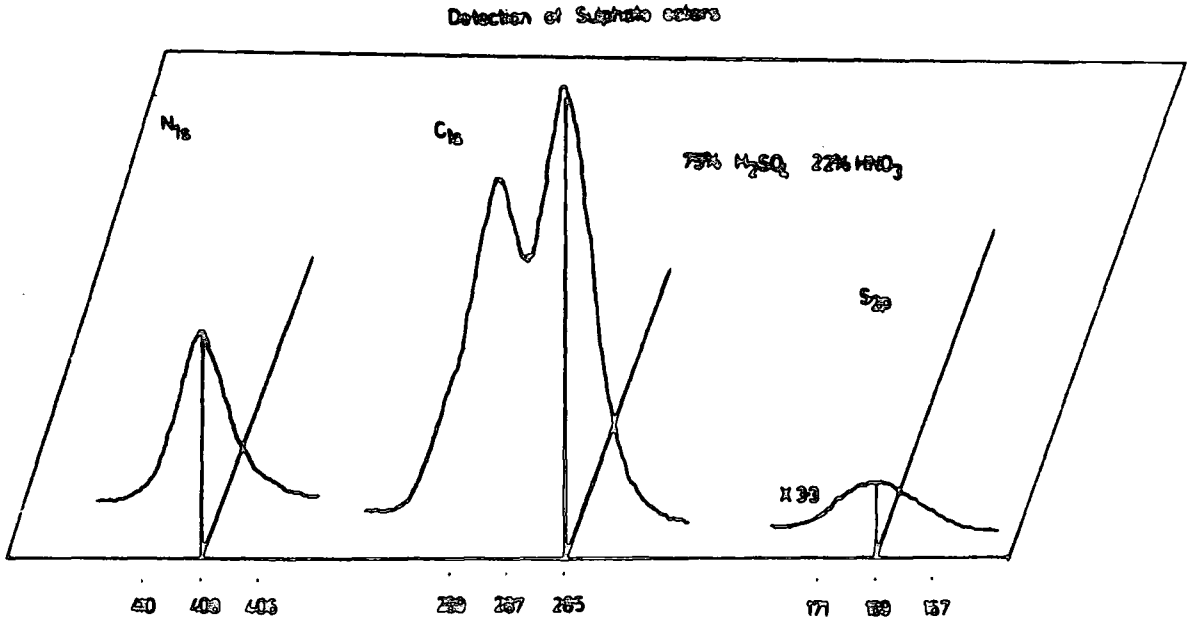

Figure 29

for nitrated material are shown in Figure 29. A low level S2p signal is detected and the high binding energy of ~169ev identifies this as arising from sulphate ester groups. It is clear therefore that sulphate esters are formed in the surface regions.

Comparable studies with the Tikα X-ray source with a larger sampling depth shows virtually no evidence for sulphate esters and E.S.C.A. therefore uniquely demonstrates the surface nature of such groups.

The final D.O.S. for a nitrocellulose. at least as far as the surface is concerned depends on nitration - denitration - sulphonation equilibria. The fact that the D.O.S. is rapidly established suggests that denitration is competitive with nitration whilst the fact that even in high sulphuric mixes the D.O.S. is still appreciable illustrates that nitrate ester formation is morefacile than sulphate ester formation. The rapidity with which the nitration-denitration equilibria are established in the surface regions is nicely illustrated by the data displayed in Figure 30. Thus for starting material, D.O.S. 2.7 denitration of the outermost few tens of Angstroms is rapid and dependent on acid mix. In 79.1% HNO_3 denitration in 1 sec. is to D.O.S. 2.3 since this mix is close to the minimum necessary for nitration to be effected without dissolution in the acid, while for 84.4% HNO_3 denitration is to a D.O.S. of 2.5 in a 1 second time scale. Corresponding Tikα spectra indicate that the degree of denitration is slightly lower than for the Mgkα X-ray source.

The extreme sensitivity of E.S.C.A. in the detection of the initial stages of reactions is nicely displayed by the comparative data given in Figure 31.

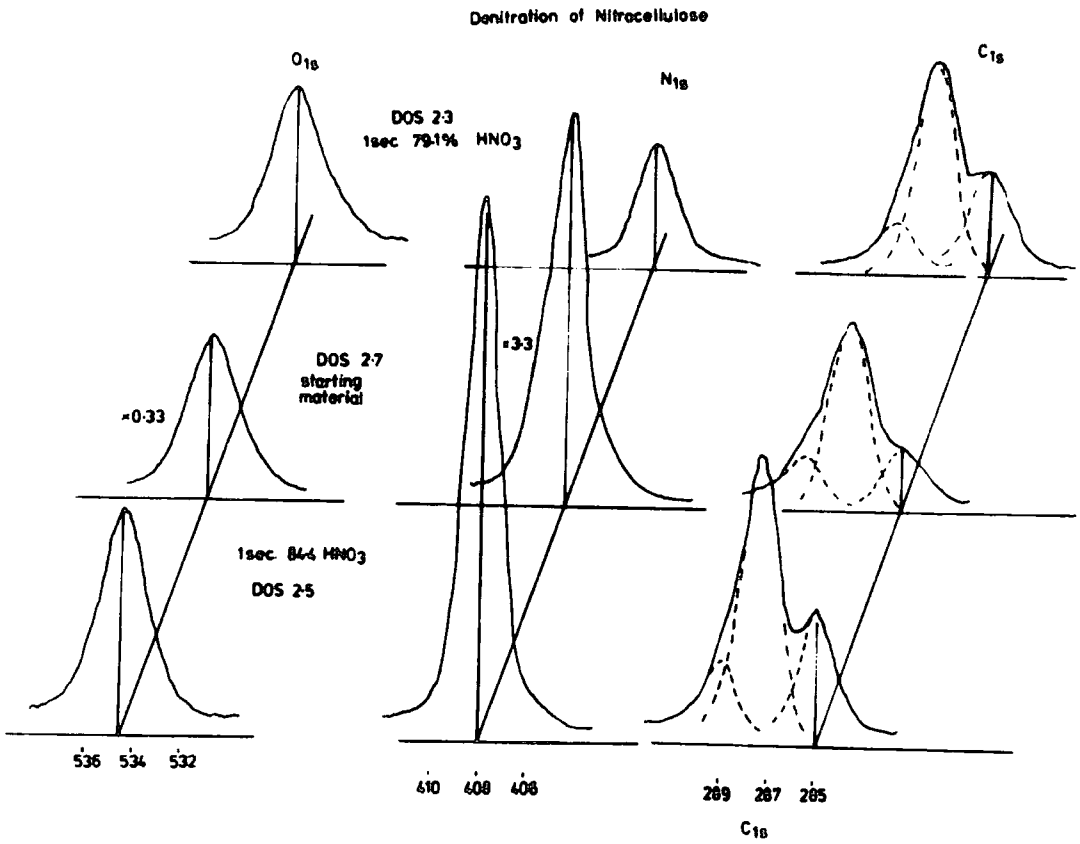

Figure 30

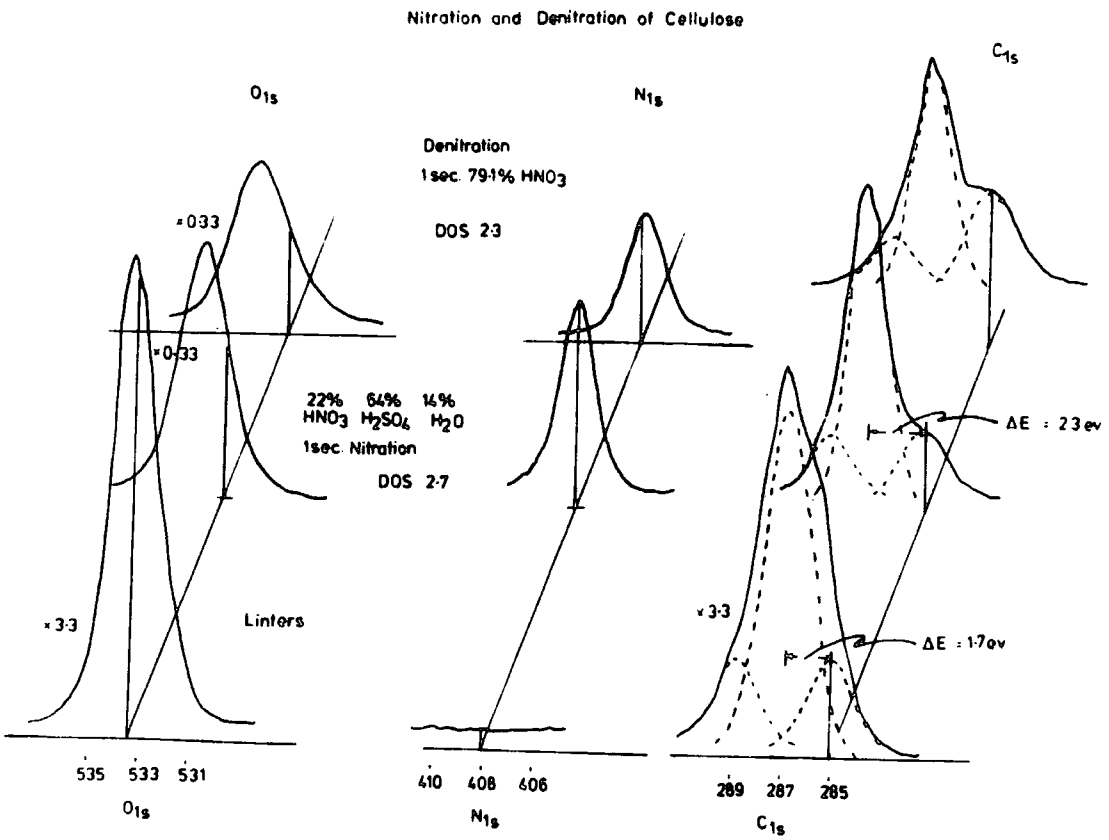

Figure 31

This shows the nitration and denitration of cellulosic samples. The substantial secondary shift of the nitrate ester group (c.f. introduction) is shown by the shift to high binding energy compared with the extraneous hydrocarbon peak. (ΔE 2.3 ev for the $\underline{C}$ - O - NO_2 component compared with ΔE 1.7 ev for cellulose itself).

Systematic studies have been made of nitrations in both nitric-phosphoric and nitric sulphuric mixes, both from a surface and bulk point of view. For nitric-phosphoric mixes the D.O.S. depends on the composition and there is little evidence for formation of phosphate esters.(E.S.C.A studies reveal no trace of phosphate ester groups in washed nitrocelluloses prepared by this method).

The D.O.S. in the surface region therefore represents the equilibrium between nitration and denitration. Since equilibrium in the bulk requires diffusion of reagents then naturally establishment of this equilibrium occurs on a longer time scale plan for the surface. The important feature however is that the D.O.S. obtained from bulk analyses is essentially the same as for the surface regions (Figure 32).

The situation with regard to nitrations in mixed acid is considerably more complex and representative data for bulk and surface nitrations are given in Figure 33.

Considering firstly the data for the 64% sulphuric mix the surface D.O.S. as assessed by E.S.C.A. utilising the Mgkα source is essentially established after 1 second exposure and remains constant thereafter. The diffusion of nitrating mix into the bulk leads to a time dependent D.O.S. which tends to approach that of the surface. As the sulphuric acid

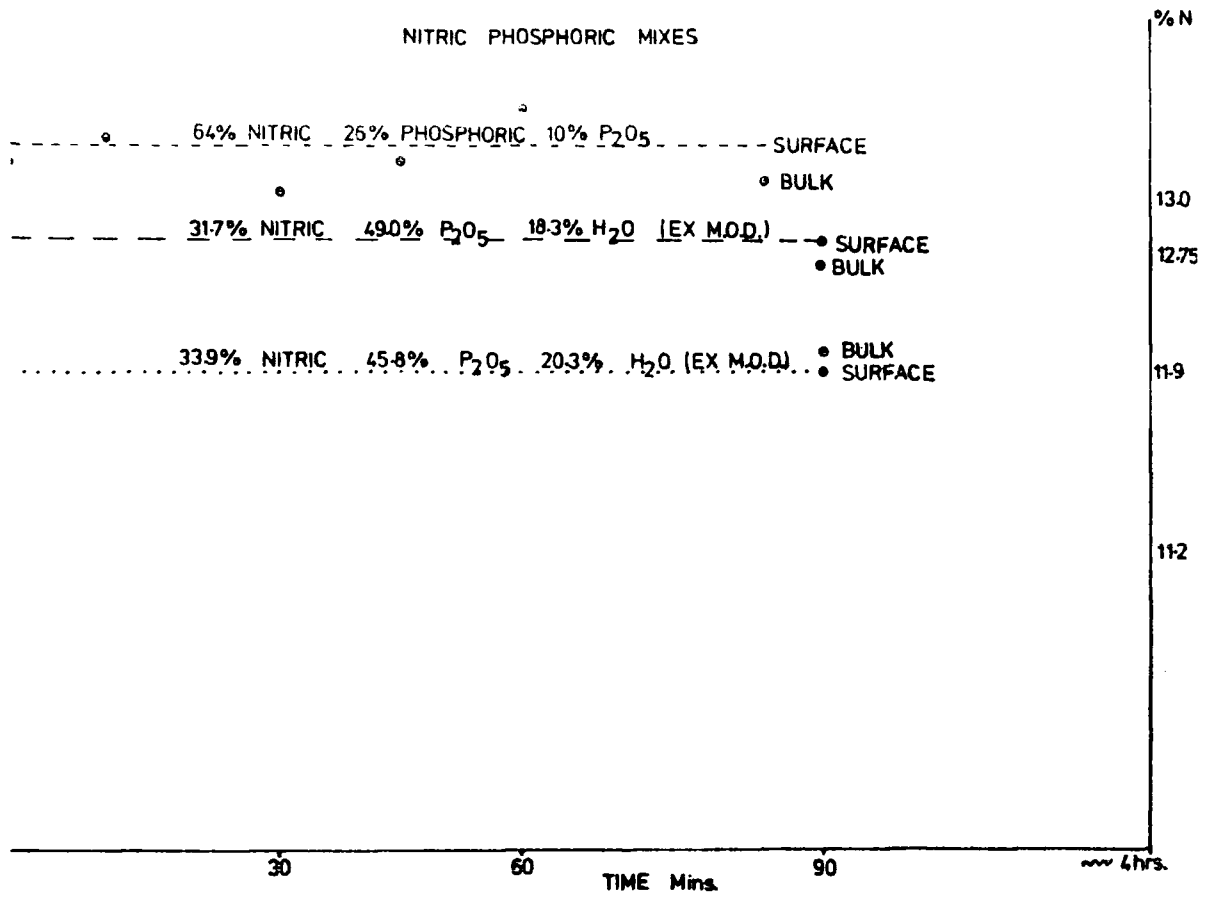

Fig. 32 Graph showing the surface and bulk D.O.S. of cellulose nitrates prepared in nitric-phosphoric mixes

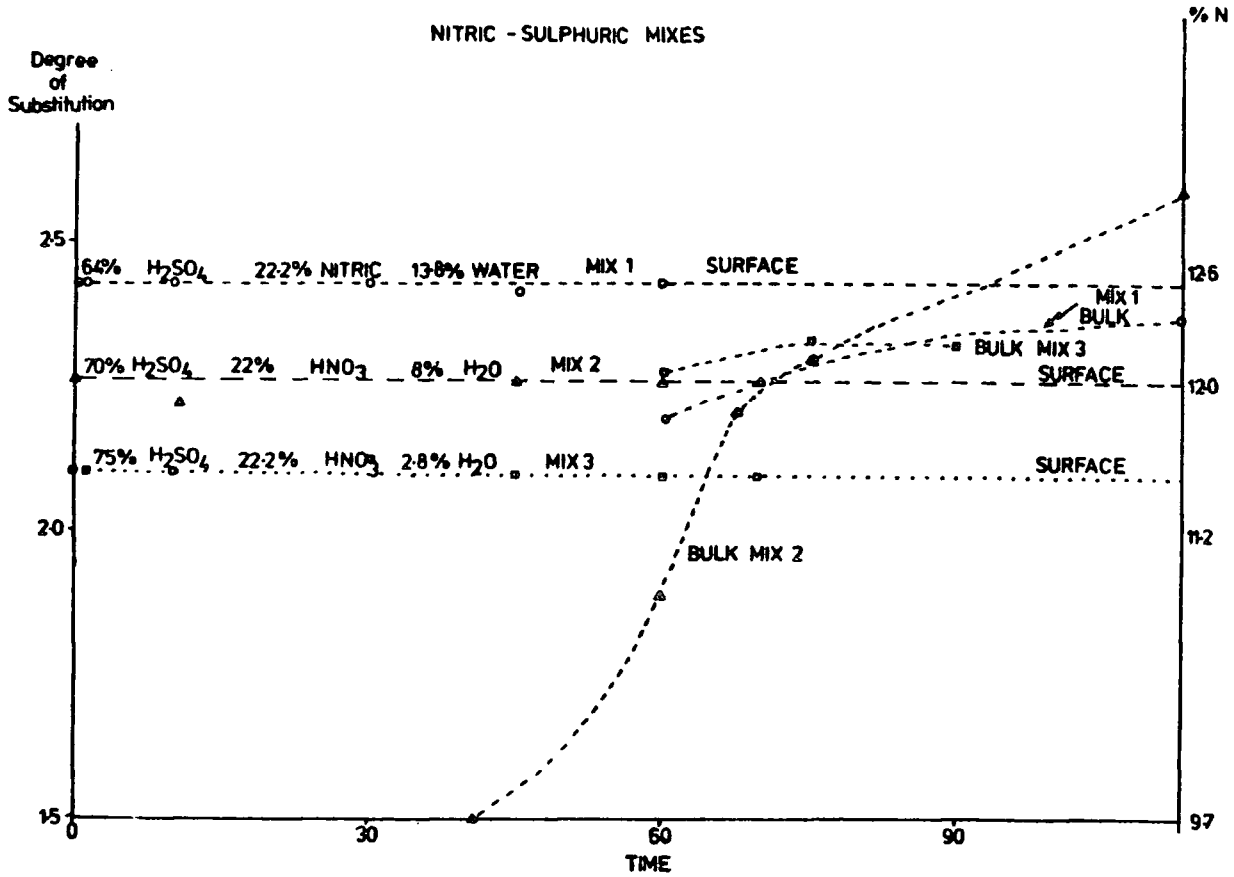

Fig. 33 Graph showing the surface and bulk D.O.S. of cellulose nitrates prepared in mixed acids

content is increased and water content decreased the surface D.O.S. decreases. In terms of competitive equilibria we might anticipate that as the sulphuric acid content increases the formation of sulphate esters becomes more likely. The suggestion has been made that in mixed acid nitrations the sulphuric acid does not penetrate the bulk or that at least the nitric acid precedes the sulphuric acid into the crystalline structure[41,3] and on this basis we might anticipate significant differences in surface and bulk chemistry irrespective of time scale. E.S.C.A. has demonstrated this in detail for the first time. Thus for both the 70% mix and the 75% sulphuric mixes the D.O.S. of the surface is actually lower than for the bulk.

Examination of Tikα spectra of such material however reveals a D.O.S. higher than that recorded using a Mgkα source. The measurement of D.O.S. using Tikα source and using the appropriate line shape analysis appears to reflect much more closely the nitrogen content of the bulk (Figure 33).

The rate of denitration and nitration has been a matter of considerable debate in the past and some workers have recorded that the rate of nitration appears considerably greater than that of denitration.[83,41,205] This has often been ascribed to a difference in the rate of diffusion of acids in and out of the crystalline material. This is an important question which E.S.C.A. is potentially capable of answering. Figure 34 displays time dependent data for a series of denitrations of 2.8 D.O.S. material in nitric acid/water mixes of various strengths. In comparison with the instantaneous nitration studies presented in Figure 31 it is plain that differences do exist in the outermost few tens of

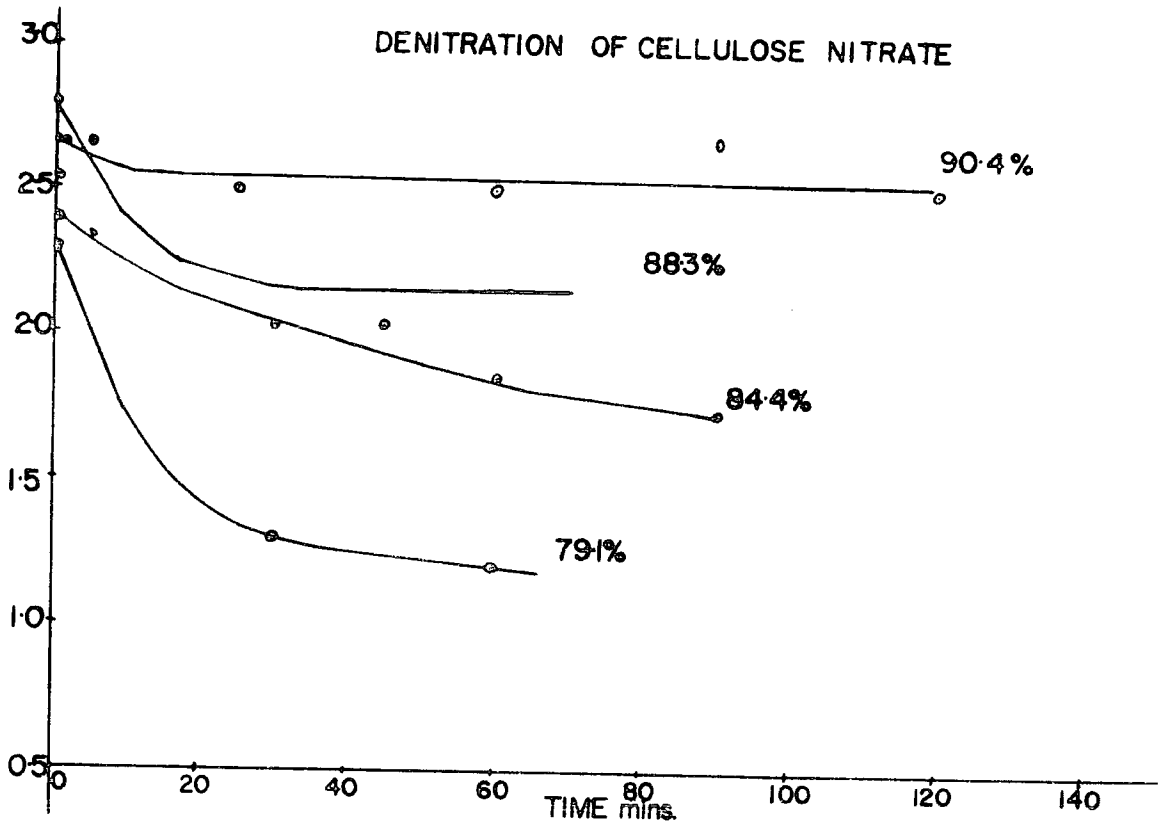

Fig. 34 Diagram showing the D.O.S. of the surface versus time for a series of denitrations in acid-water mixes

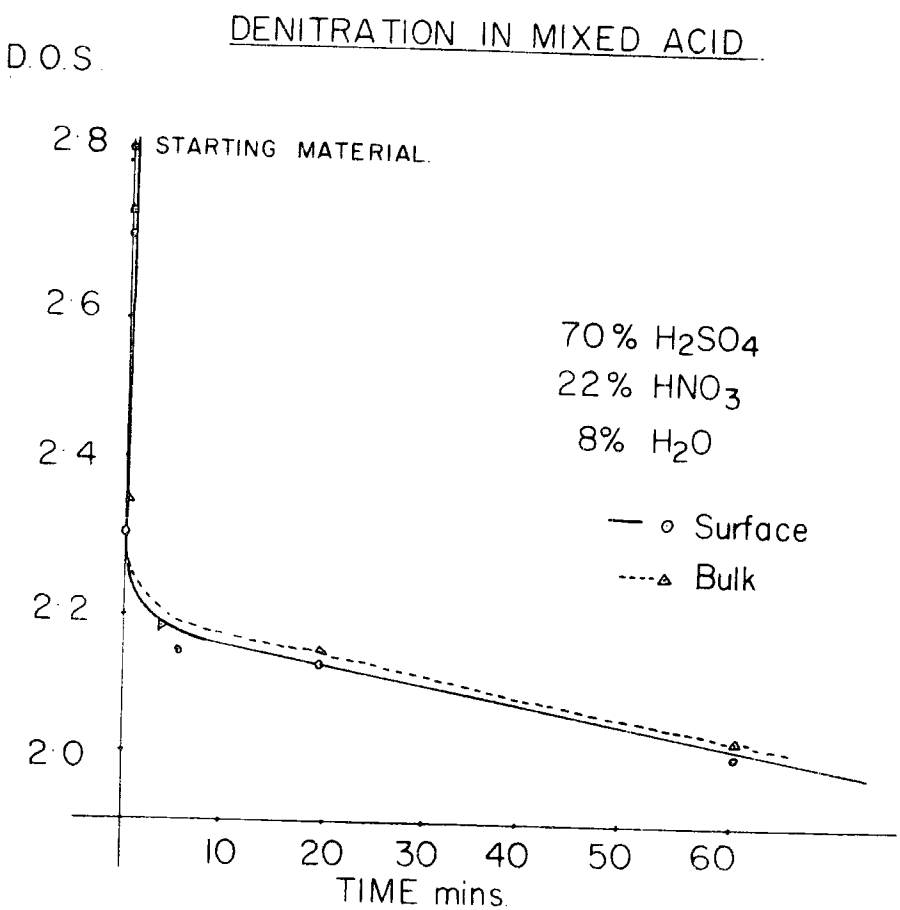

Fig. 35 Mixed acid denitrations

angstroms when considering denitration in this media. The D.O.S. finally attained is dependent on the acid composition and it would appear that the greater the difference in D.O.S. between starting material and final D.O.S. achieved in a given mix the faster the initial rate of denitration (c.f. Chapter One). The denitration of 2.8 D.O.S. material in mixed acids (nitric/sulphuric) is shown in Figure 35 and it can immediately be seen that the initial rate of denitration is very fast indeed and comparable to that in nitration. It may be that the slower second stage of the denitration may be explained in terms of a different reactivity of primary nitrate groups towards denitrating acids. This possibility is further explored in Chapter Four.

Important observations were also made in this study regarding the degradation of nitrocelluloses in the acid mixes over extended periods of time. Trommel[205,83] first observed in a denitration with time experiment in a nitric acid/water mix a continuous drop in nitrogen content over a period of one year. Miles[41] has reported similar behaviour over shorter time periods. It is obvious that both the equilibrium and accessibility schools of thought find this inconsistent with either theory. An equilibrium should be established within minutes and it is unclear how a cellulose will become more accessible to a given mix the longer it is immersed.

However it is clear from examination of carbon-oxygen ratios that denitrations in acid mixes for longer than 12 hours given oxygen levels in excess of that required by the measured nitrogen content. (This has been supported to some extent by ^{13}Cnmr spectra of such material). To conclude this presentation of the application of E.S.C.A. in this important area mention will now be made of experiments carried out to determine

the extent of reaction of various reagents with cellulose itself. It has long been realised that methods of measuring the crystallinity of cellulose by the extent of reaction (c.f. Chapter One) of sodium metaperiodate, for instance, is an inaccurate procedure, the result of which will depend, to a large degree, on the type of cellulose used and the nature of the reagent. Of primary concern is whether the reagent is truly penetrating the so-called amorphous regions leaving the crystalline parts unscathed or whether the reaction is confined to the surface regions of individual fibrils and the degree of crystallinity obtained is in fact only a measure of the available surface area. In this work dry type 1 cellulose was treated with 0.1m sodium periodate for 24 hours in the dark, with sodium hypochlorite for 24 hours or with a combination of both with a washing procedure between the two treatments. The oxidation of cellulose by periodate solutions in the dark is known to proceed, (without side reactions), by the following mechanism:

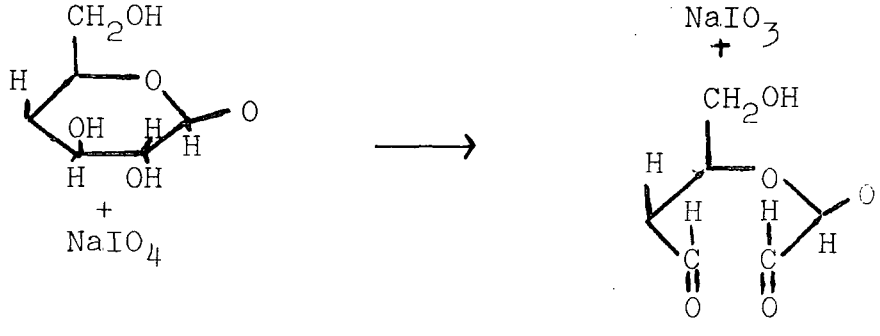

According to this equation the oxygen consumption of a periodate oxycellulose is equal to the percentage of the chain units that have been oxidised. The uptake of oxygen can thus be calculated using the titration methods of Müller and Friedberger[44] and the amount of oxygen consumed per 100 glucose units can be estimated. The oxidation of cellulose

by hypochlorite solutions has been studied by Clibbens[43] and has been shown to depend on the pH of the solution. In this work the oxidation was carried out at pH 7.4 which according to Nevell[44] gives rise to increased aldehydic and carboxyl content. The consumption of oxygen was again calculated by titration methods,[44] and compared to C_{1s}/O_{1s} ratios obtained from E.S.C.A. analysis of the dry oxidised materials. The results of this study are shown in Figure 36 where it is clear that the reaction is confined almost entirely to the surface of fibrils (50Å or less) and must cast further doubts on crystallinity measurements using such reagents.

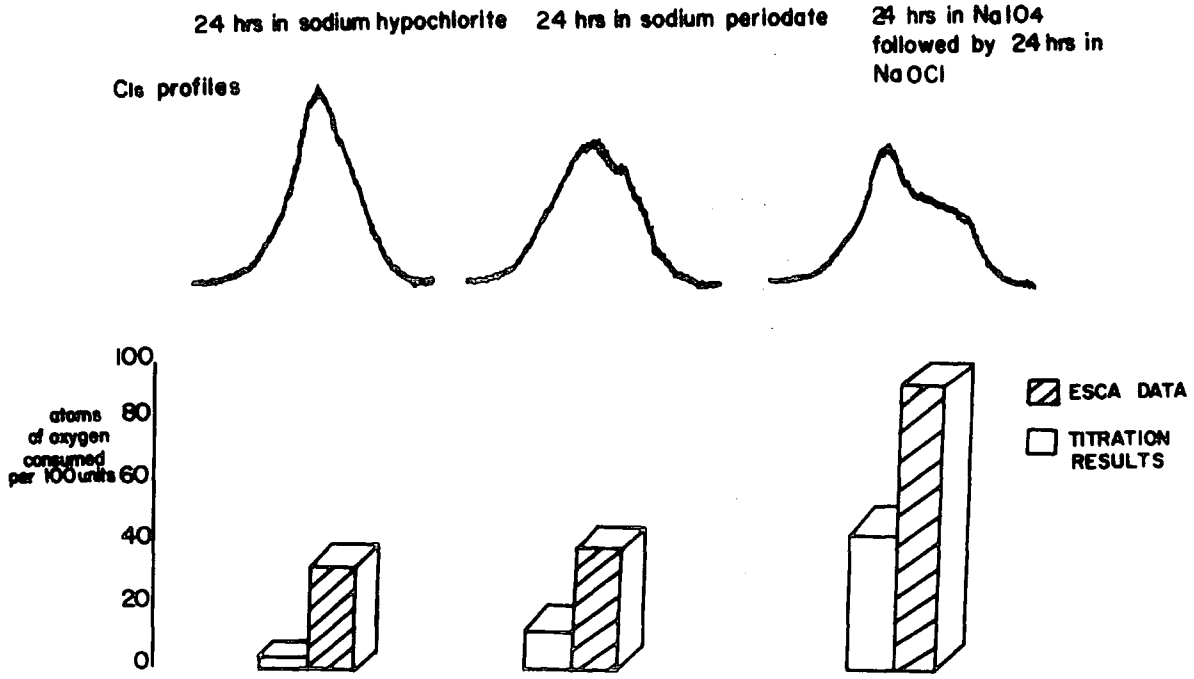

Fig. 36 Graphical representation of the inhomogeneous oxidation of cellulose

It is clear therefore that E.S.C.A. provides a new dimension to this complex problem of the nitration-denitration of cellulosic materials as well as information on cellulose itself and the work described here provides a strong basis for the study of even more complex systems represented by double based propellant formations (c.f. Chapter Five).

CHAPTER FOUR

THE APPLICATION OF CARBON-13 MAGNETIC RESONANCE TO THE DETERMINATION OF PARTIAL DEGREES OF SUBSTITUTION IN CELLULOSE NITRATES

4.1 Introduction

A considerable volume of literature has appeared over the last eighty years concerned with the technical nitration of cellulosic materials.[41] Both the displacement and 'technical' processes have been thoroughly investigated although surprisingly a number of fundamental questions remain unanswered. However although there are still some arguments in favour of the 'accessibility' theory, (see Chapter One), it is now generally accepted that under the conditions and media employed in most technical nitrations the final D.O.S. of the bulk material is under thermodynamic control. In Chapter Three we have shown that this is true in the outermost few tens of Angstroms although the convolution of factors which determine the overall stoichiometry are such that the surface is often distinctively different from the bulk.

Some of the most intriguing aspects of the nitration and denitration of cellulosic materials are related to the anomalous changes in interchain spacing as a function of degree of substitution. These results recorded by Miles[41] and Trommel[83,205,213] are more thoroughly discussed in an earlier chapter. The fact that such spacings differ for materials of the same D.O.S. produced by nitration and denitration and the apparent differences in solubility in alcohol-ether of such samples must reflect the detailed differences in chemical microstructure and substitution patterns in individual and sequences of β-D-glucopyranose residues (c.f. Chapter Six). It is not inconceivable that nitrocelluloses of the same degree of substitution prepared by displacement or technical

processes may be structurally different according to the nitrating and quenching procedures employed. This has, in fact, recently been suggested by results obtained by Lewis from optical path difference measurements.[214]

It is clear however that a knowledge of substitution patterns in materials produced by nitration and denitration is essential for a full understanding of this interesting problem but although extensive investigations have now been made of overall D.O.S. over a variety of nitrating and denitrating conditions very little information has been available on the partial D.O.S. at the C_6 primary and C_2 and C_3 secondary sites in individual glucose residues. The first indication that equilibrium degree of substitution at different sites in the glucose rings were not the same came from the iodination experiments of Murray and Purves.[206] By specifically displacing primary nitrate esters by iodide, (typically NaI in acetylacetone at a temperature of 115°C), it was shown that in partially substituted nitro celluloses the partial D.O.S. for the primary site was always greater than that for the secondary sites. Unfortunately with materials of D.O.S. >2 which includes all those of technical importance considerable degradation occurs during the reaction. This is nicely shown by electron micrographs of material of 2.7 D.O.S. and <2.0 D.O.S. treated for identical time periods, (6 hours), by the reagent. The fibrous structure which is maintained throughout nitration and denitration reactions is completely destroyed by the reaction on 2.7 D.O.S. nitrocellulose whereas the low degree of substitution is structurally unaffected.

Attempts to use E.S.C.A. to follow iodine replacement and hence C_6 substitution patterns have been made but the

results are not conclusive. Figure 37, for example, illustrates the C_{1s} and I3d core levels for a nitrocellulose denitrated for 40 mins. in 79.1% nitric acid and subsequently with the NaI/acetylacetone reagent for a period of 12 hours.

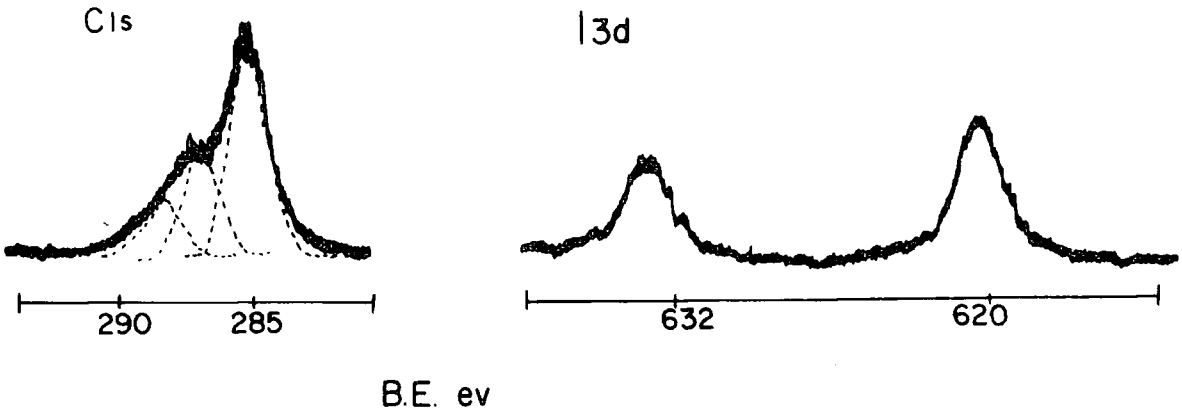

Fig. 37 Core level I_{3d} and C_{1s} spectrum of a denitrated cellulose nitrate treated with NaI in acetyl acetone for 12 hours

This nitrocellulose which is fibrous in character, (re, electron micrograph studies), and apparently unaffected by side reactions gives a total D.O.S. of iodine, (in the form of $-CH_2I$), of ≈0.5. Comparison with Figure 35 in Chapter Three reveals an expected D.O.S. of nitrate ester groups of ~1.1 for such a material denitrated in this mix for 40 mins.

It is readily apparent from this that there is far more iodinated material in the primary position than would be

expected on the basis of three equivalent equilibrium constants for denitration at the C_2 C_3 and C_6 positions and it would appear that the primary position is less susceptible to denitration than nitrate groups at the other positions. However the problems associated with this method are apparent from electron micrographs and it is by no means certain that the almost quantitative conversion of the $-CH_2ONO_2 \longrightarrow -CH_2I$ observed in glucose derivatives applies to high molecular weight celluloses. As we have already observed in certain cases in Chapter Two the surface is not always representative of the bulk and as a window on bulk behaviour and for establishment of rate information this chemical tagging method has limited application. It becomes apparent that a method of determining distribution of nitrate groups and partial degrees of substitution in a range of nitrocelluloses from very low to very high D.O.S. is essential for elucidation of this complex problem. Thus we turn our attention to the data pertaining to n.m.r. studies.

A possible method of obtaining high resolution n.m.r. spectra of cellulosic material has recently arisen following the work of Leader[215] who has used hexafluoroacetone in ethyl acetate solution to react with organic compounds containing active hydrogen groups to form adducts containing the probe group $-C-(CF_3)_2-OH$. ^{19}F n.m.r. spectra can thus be obtained with high sensitivity since six fluorine atoms are placed in close proximity to the functional group tagged. Hydrogen bonding abilities of the unusual $-C(CF_3)_2-OH$ probe group also enable it to interact with the solvent and all groups in the compound which are likely to be involved in hydrogen bonding. For instance when intramolecular H-bonding is possible as in

the adduct of CH_3 O CH_2 CH_2 OH it may exist as a rapidly exchanging mixture of the solvent bonded and intramolecular H-bonded forms as shown below and hence gives an averaged chemical shift for the fluorine-containing species involved.

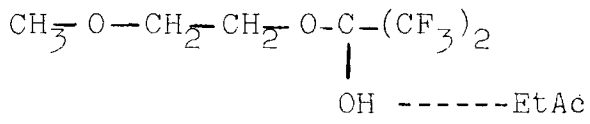

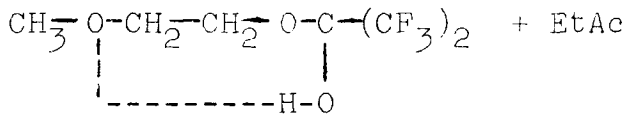

In some cases these equilibria may be shifted far to the right resulting in a stable intramolecularly bonded adduct. In other cases however the solvent bonded and intramolecular H-bonded forms may be of comparable stability and coexist giving an averaged adduct line position. Since the reactions affecting adduct chemical shifts are, (under the conditions normally used), controlled only by temperature and the chemical properties of the solvent and compound tested they result in definite chemical shifts independent of minor variations in concentration. In order to investigate the feasibility of studying polyols and eventually cellulosic materials using this method both d-glucose and β-methyl-D-glucoside have been tagged with the probe group and the ^{19}F n.m.r. spectra obtained are shown in Figure 38. These complex spectra reveal detailed differences presumably due not only to direct chemical shifts but also the change in H-bonding systems brought about by the presence or absence of a methyl group at the C_1 position. The technique clearly shows promise but the applicability of the method to cellulosic materials is likely to be restricted by solubility problems. Hence the problem of obtaining

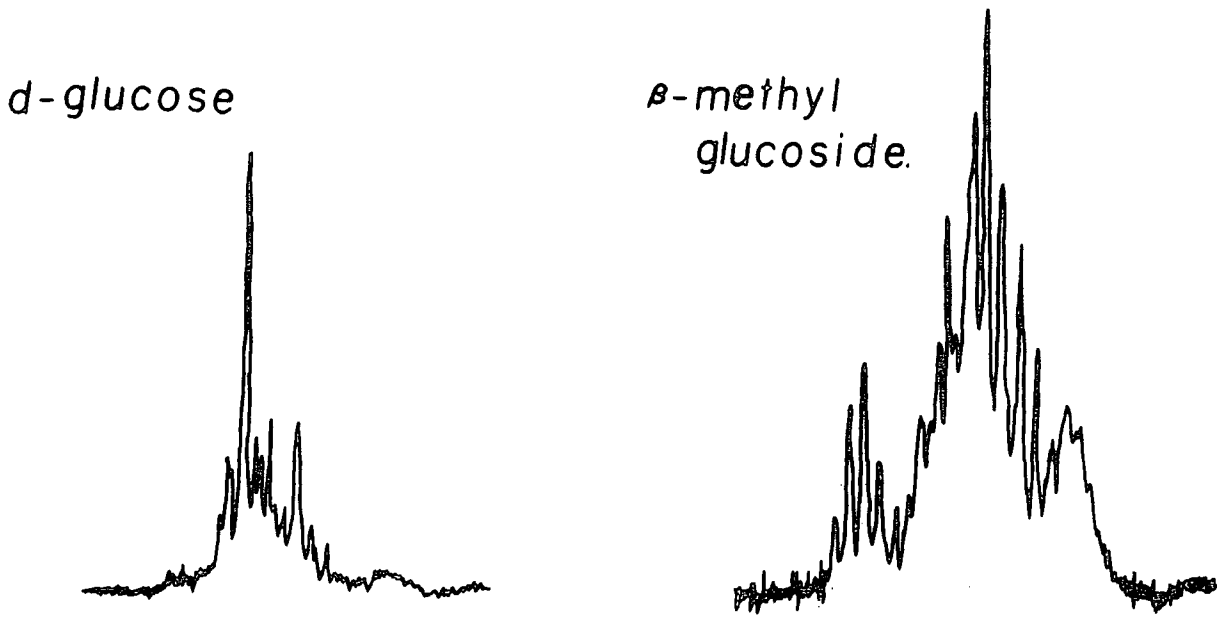

Fig. 38 ^{19}F n.m.r. spectra of glucose and β-methyl glucoside treated with hexafluoroacetone reagent

information on the partial degrees of substitution in cellulose nitrates remains.

An important advance in this area has recently been reported by Wu.[216] By careful examination of the noise decoupled ^{13}C n.m.r. spectra of model systems he has shown that it is possible to assign components in the region ~100 p.p.m. to the low field of T.M.S. to the anomeric (C_1) carbon in the variously substituted glucose residues. This has demonstrated unambiguously that the equilibrium partial D.O.S. is in the order $C_6 > C_2 > C_3$. An analysis based solely on the anomeric C_1 carbon, however, has certain inherent weaknesses which can be largely eliminated by using the remainder of the ^{13}C n.m.r. data from C_2-C_6 once appropriate

assignments have been confirmed. The problems associated with complete analysis of signals arising from anomeric carbons are presented in Section 4.3 but are essentially concerned with signal to noise ratios which are unlikely to be resolved with present instrumentation.

In this chapter therefore a detailed ^{13}C n.m.r. analysis of the substitution patterns in both nitrated and denitrated cellulosic materials is presented. A complete assignment of peaks allows a considerable amount of information to be extracted over a range of degree of substitutions and a survey of anomeric signals in spectra of particularly good signal/noise ratio yields some hitherto unsuspected results pertaining to sequence distribution.

The prime objectives of this study, which refers to the bulk and which complements the work on surface chemistry presented in Chapter Three, may be summarised as follows: to investigate -

(a) nitration in different acid mixes for fixed periods of time;

(b) denitration in different acid mixes for fixed periods of time;

(c) denitration in a given mix as a function of time.

4.2 Experimental

Nitrated material for analysis in this work was prepared by methods described in Chapter Three and from cellulose of identical type and source. Nitrations were carried out for 2 hours - a period which it has been shown gives rise to homogeneous material. 10% by weight solutions of the polymer were made up in dimethylsulphoxide-d_6. The ^{13}C n.m.r. proton

noise decoupled (75.5 MHz.) spectra were recorded on a Varian Associates S.C.300 spectrometer at 75-80°C with typical acquisition times of 12 hours corresponding to the accumulation of ~10^5 transients. The carbon chemical shifts are reported with respect to the internal tetramethylsilane, (Me_4Si) reference. Peak areas were determined by spectral integration. Low temperature (25-29°C) n.m.r. spectra were also recorded but were found to be broad and poorly resolved due to high viscosity whereas high temperature conditions ≈90°C as used by Wu[216] give discoloured solutions and additional small peaks on long acquisition times (c.f. data in ref.216). These phenomena have also been observed in this work but to a lesser extent and the nitrogen content of certain samples have been determined by a modified Kjeldahl method, (c.f. Appendix), and found to be comparable with the D.O.S. calculated from analysis of the n.m.r. data and the percentage nitrogen expected from standard tables for nitration in the particular acid mixes used.

The iodinations described in the introduction were carried out by methods outlined in the work of Murray and Purves.[217] E.S.C.A. analysis was carried out on an E.S.200B spectrometer and C_{1s}/I_{3d} ratios calculated from sensitivity factors obtained from model compound analysis.

4.3 Results and Discussion

4.3.1 Introduction

The analysis of partial D.O.S. based solely on the anomeric region is extremely difficult and this is evident from the spectra in Figure 39. (The spectrum is for a nitrated material D.O.S. initially 2.83 denitrated in 82% HNO_3 for a

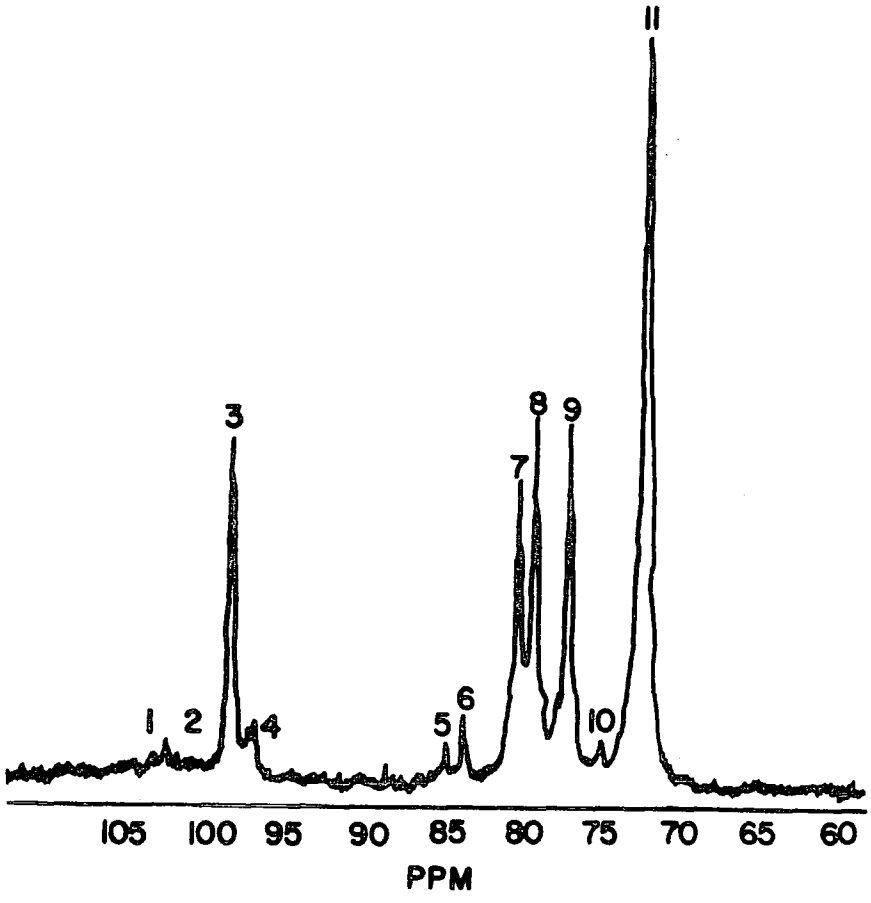

Fig. 39 ^{13}C n.m.r., (75.5 MHz proton decoupled), spectrum of a 2.8 D.O.S. NC denitrated for 20 seconds in 82% HNO_3/18% H_2O

period of 20 seconds). Whilst the components at 99.7 p.p.m. and 98.4 p.p.m. assigned to the anomeric carbon in trisubstituted and 2,6,-disubstituted are well resolved the higher field region arising from 3,6 disubstituted and 6-monosubstituted glucose residues is largely unresolved. Comparison of the whole series of spectra for nitrated and denitrated materials does allow however an unambiguous assignment of the lower region of the ^{13}C n.m.r. spectra arising from C_2-C_6. Thus the component at 83.2 p.p.m. corresponds to C_2 in 2,6 disubstituted glucose residues and that at 85.2 p.p.m. arises from C_3 in 3,6-disubstituted glucose residues. Since the Nuclear Overhauser enhancements, (N.O.E.), cf. Chapter Two, for C_1-C_5

are essentially the same (see later) a direct ratio of peak areas allows an accurate ratio of the disubstituted products. This, taken in conjunction with a total integral for the highest field region for the anomeric carbons and the area ratios for the two lower field components allows a partitioning of substitution patterns into tri, di and mono-substituted glucose residues. (A full assignment of peaks is given in Table 4.1).

Table 4.1

Peak No.	Assignment	
1	C1 in	3,6-disubstituted
2	C1 in	6-monosubstituted
3	C1 in	trisubstituted
4	C1 in	2,6-disubstituted
5	C3 in	3,6-disubstituted
6	C2 in	2,6-disubstituted
7	C3 in	trisubstituted
8	C4 in	trisubstituted (remains constant)
9	C2 in	trisubstituted
10	C2 in	3,6-disubstituted
11	C6 and C5	(coincident in frequency and shift insensitive to remaining substitution pattern)

It can be seen that the minor component at 74.5 p.p.m. arising from C_2 in the 3,6-disubstituted residues has the same intensity as that of the component at 85.2 p.p.m. due to C_3 in the 3,6-disubstituted residue as required by the assignment. It should also be noted that the intensity of the component at

83.2 p.p.m., (C_2 in the 2,6-disubstituted residues), is again equal to that of the lowest field component in the anomeric region as required once more by this assignment. The intense components at 80.2 p.p.m., 79.1 p.p.m. and 76.9 p.p.m. are assigned to C_3, C_4 and C_2 respectively in the tri-substituted residues while the largest peak at 71.6 p.p.m. corresponds to C_6 nitrated material, (shift insensitive to remaining substitution patterns), and also to C_5 which is fortuitously coincident in frequency.

Since we would anticipate that C_5 would have a comparable N.O.E. to C_2-C_4 we may subtract the ratioed intensity for the component at C_5 from the total integrated intensity for the component at 81.6 p.p.m. and thus provide an estimate of the correcting factor to account for differences in N.O.E. for the methylene group at C_6.

The factor of 1.5, (accounting for decoupling effects in the ^{13}C experiment), derived from this analysis has then been used to estimate the extent of unnitrated material in appropriate cases from an analysis of the component at 60.5 p.p.m. assigned to C_6, (CH_2-OH).

With respect to the problem of anomalous lattice spacings it may be interesting to examine the available data for information pertaining to sequence distribution before considering in detail our limited objective of determining partial degrees of substitution. Trommel[83,213] has suggested that material prepared by denitration of high D.O.S. material is likely to consist of large chain sections of fully nitrated material adjacent to segments of unnitrated glucose residues. This, it is postulated, is due to the fact that denitration is more likely in residues adjacent to those already of low

D.O.S. Sequence information is therefore of great interest and it is evident from the spectrum in Figure 40 that such data is potentially available especially from the high field anomeric carbon region which is particularly susceptible to subtle changes in magnetic environment. The spectrum which

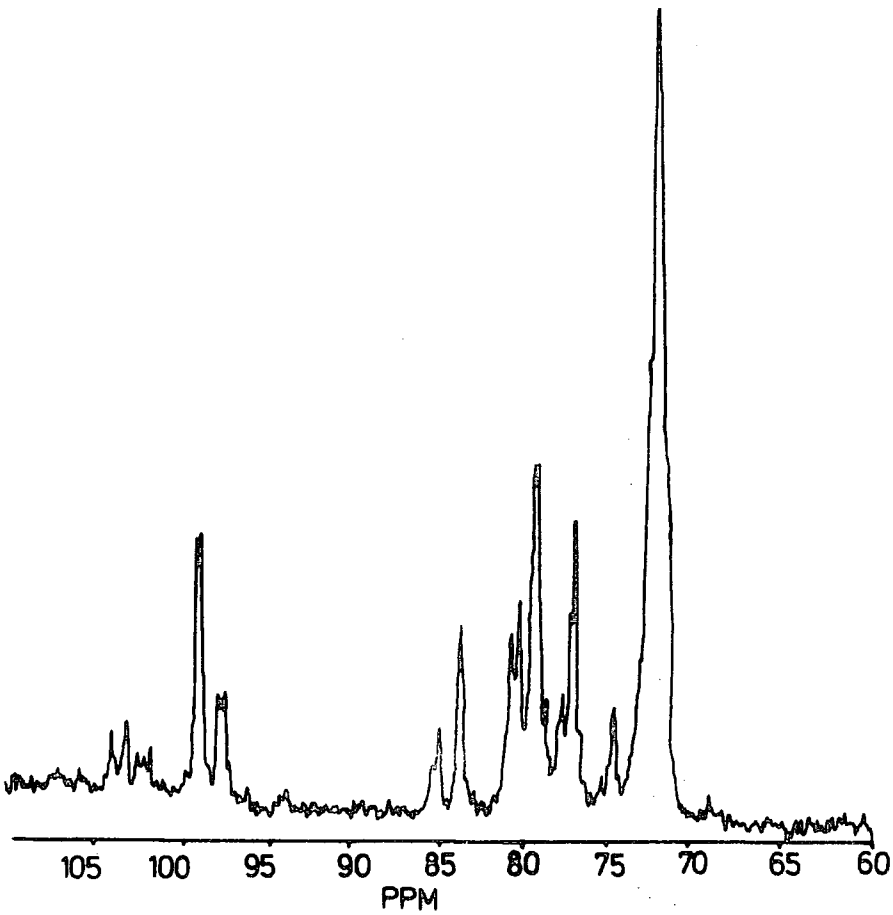

Figure 40 ^{13}C n.m.r. spectrum of a 2.8 D.O.S. NC denitrated for 5 mins. in 82% HNO_3/18 % H_2O

is of a denitrated sample (82 % HNO_3, 5 mins. reaction time), however, gives some indication of the likely difficulties in extracting such information since the considerable fine structure apparent in the anomeric region is complicated by a poor signal to noise ratio. The n.m.r. analysis gives an overall D.O.S. of 2.31 with ~50% of the β,D-glucopyranose residues being trisubstituted and ~20% being 6-monosubstituted,

the partitioning between the disbustituted derivatives being 2:1 in favour of the 2,6 compared with the 3,6 derivative. Since Wu[216] has shown that substitution at C_6 largely leaves the anomeric region unaffected, sequence distribution will be manifest from the effect of substitution at the C_3 position in adjacent rings. On this basis we might anticipate that the highest field component assigned to the anomeric carbon in the 3,6-dinitro substituted β,D-glucopyranose residues would be essentially a doublet structure since the β,D-glucopyranose units linked to C_1 will have either a nitrate ester functionality present (trinitro) or absent (2,6-dinitro, mononitro) at C_3'. It is interesting that the splitting between the doublet at high field is 0.8 p.p.m. compared to the shift in the anomeric region, 1.3 p.p.m., attributable to a nitrate ester at C_3, (taken as the average splitting between both the first 2 and the second 2 components of the anomeric region). However it is possible to explain this by the fact that C_3' is one bond further removed in the system. Since the shift at the anomeric carbon for a C_6 nitrate ester functionality is known to be small this provides a consistent overall description of the effect of long range substituents.

Consider now the derived substitution pattern for this particular sample. In an octad sequence of units we may expect approximately four trinitrate, 3-dinitrate, (1 of which would be 3,6-disubstituted), and 1 mononitrate ester β,D-glucopyranose residue. On a random basis of substitution of nitrate groups along a sequence of units we might expect a 3:2 (trinitrate vs. 2,6 dinitrate plus mononitrate) intensity ratio for the high field region. Even with the relatively poor S/N ratio for the spectra in Figure 40 it is clear that

the intensity ratio is more nearly 3:4 and this seems to indicate non-random substitution. The broadened nature of the components also indicates that although longer range effects are small they are none the less significant and this becomes even more apparent in the analysis of the component centred at 104.7 p.p.m. attributable to the anomeric carbon in β,D-glucopyranose residues with unsubstituted C_2 and C_3 positions. On an octad basis this signal originating from the anomeric carbon should primarily show splitting originating from the presence or absence of a nitrate ester group in the C_3' position at the adjacent ring (attached to the anomeric carbon). On a statistical basis there is a 5:2 probability that a nitrate ester group is present in the C_3' position however the two outside components of the triplet, (separated by 0.8 p.p.m.), are of roughly equal intensity. This indicates that the cumulative effect of longer range shift effects, (from C_2), are probably important since a third component is also observed in an intermediate shift position. It is tempting to assign these three components in decreasing shift to high field as arising from adjacent β,D-glucopyranose residues which are either the trinitrate, 3,6-dinitrate or 2,6-dinitrate derivatives; the indication being again that the substitution is non-random.

The more intense components at lower field, (99.7 p.p.m. and 98.4 p.p.m.), attributed to trinitrate and 2,6-dinitrate substituted β,D-glucopyranose residues also exhibit fine structure. Thus the latter shows a 3 component structure which might be due to the lack or presence of nitrate ester functionalities at either or both of C_3' and C_2'. The dominant component arising from the trinitrate at 99.7 p.p.m.

again suggests a rather specific sequence arrangement. In summary therefore it appears that sequence information might be accessible from detailed analysis of the anomeric carbon region which is especially sensitive to substitution pattern in the adjacent glucose residue. Major problems, however can be expected in investigating this in any great detail since the S/N ratio for the spectrum in Figure 39 is not sufficiently good and improvement with current instrumentation would not be feasible on a realistic time scale.

4.3.2 Partial D.O.S. for Nitration in Different Acid Mixes

Having considered the basis of the assignments and subject analysis of data we may now proceed to a discussion of the data for the partial D.O.S. for nitration in the three different acid mixes described in the previous section. The data is shown in Table 4.2. Considering firstly the material of highest total D.O.S., (2.83), no evidence has been detected for any monosubstituted residues and a partitioning between 83% trinitrate, 11% 2 6-dinitrate and 6% 3,6-dinitrate yields partial D.O.S. of 1, 0.94 and 0.89 for C_6, C_2 and C_3 carbons. The corresponding data for the nitrated material of lower D.O.S. reveals that only for the material of 2.37 D.O.S. is there any significant contribution from unsubstituted ß,D-glycopyranose residues.

From the limited number of nitrocelluloses studied in detail by Wu[216] a general treatment of equilibrium partial D.O.S. was suggested, the central feature of which is that the reactivity of a given hydroxyl group is independent of the substitution pattern. In the light of the crude examination of sequence distributions described above the implication

Table 4.2

Acid mix	N.m.r. DOS total	DOS partial			Percentage components				
		C_6	C_2	C_3	Tri	2,6	3,6	6 mono	Unsubstituted
18.7% HNO_3									
59.3% H_2SO_4	2.37	0.94	0.77	0.66	55	22	11	6	6
21% H_2O					(46)	(28)	(14)	(11)	
22% HNO_3									
75% H_2SO_4	2.62	1.0	0.87	0.75	62	25	13	-	-
3% H_2O					(67)	(20)	(10)	(3)	
64% HNO_3									
26% H_3PO_4	2.83	1.0	0.94	0.89	83	11	6	-	-
10% P_2O_5					(81)	(11)	(6)	(2)	

of such a model that reactivities and positions in adjacent β,D-glucopyranose residues does not depend on substitution pattern does not seem to be tenable and this raises doubts about the validity of a simplistic description of a series of complex equilibria in terms of only 3 parameters, namely the ratios of equilibrium constants for substitution at the 3 sites, (2,3, and 6), in a given β,D-glucopyranose residue. Since the nitrated materials described here fall in a D.O.S. range not explicitly examined in detail by Wu[216] but nonetheless covered by this distribution model it is of interest to compare the ^{13}C n.m.r. derived substitution pattern with those predicted by the simple equilibrium model. The data is shown in brackets in the relevant columns in Table 4.2 and reveal tolerable agreement. the main discrepancy being the overestimate of the model of the extent of unsubstituted and monosubstituted β,D-glucopyranose residues. Since a large number of samples have been investigated in this work in the total D.O.S. range 2.0-2.83 we will postpone a detailed comparison with the preductions based on Wu's model until a later section.

4.3.3 Denitration in Different Acid Mixes for Fixed Periods of Time

Table 4.3 displays the data provided from ^{13}C n.m.r. spectra of denitrated nitrocelluloses obtained from 2.83 D.O.S. starting material immersed in the 4 acid mixes described in the experimental section. The first important point to note is that denitration to a total D.O.S. of 2.0 provides no evidence for unsubstituted β,D-glucopyranose residues. The equal distribution of tri and mono nitrate substituted residues is fortuitously in agreement with Wu's simple model however

Table 4.3

Acid mix	Total DOS from n.m.r.	DOS partial			Percentage components				
		C_6	C_2	C_3	Tri	2,6-	3,6-	6-Mono	Unsubstituted
64% HNO_3 26% H_3PO_4 10% P_2O_5	2.83	1.0	0.94	0.89	83	11	6	-	-
95% HNO_3 5% H_2O	2.74	1.0	0.92	0.82	74	18	8	-	-
88% HNO_3 12% H_2O	2.43	1.0	0.77	0.66	55	22	11	12	-
83% HNO_3 17% H_2O	2.21	1.0	0.68	0.53	37	31	16	16	-
79.1% HNO_3 20.9% H_2O	2.00	1.0	0.56	0.44	31	25	13	31	

the latter predicts a substantially larger proportion of disubstituted products than are actually observed. Since the simple model essentially ignores medium effects material of the same D.O.S. produced either by nitration and denitration under different conditions should appear with the same distribution pattern. A comparison of the data in Table 4.2 for D.O.S. 2.37 with that in Table 4.3 D.O.S. 2.43 again reveals a tolerable agreement; the only major discrepancy being the partitioning between monosubstituted and unsubstituted residues. The denitration process is seen to be in the order $C_3 > C_2 \gg C_6$ and the equilibrium D.O.S. decreases rapidly on going from fuming nitric acid to 79.1% nitric acid.

4.3.4 Denitration in a Given Acid Mix as a Function of Time

Starting from a material of D.O.S. 2.83 samples have been examined by ^{13}C n.m.r. after periods of 1,5,20,300 and 400 secs. denitration in 82% nitric acid and the data are displayed in Table 4.4. In Chapter Two it has been shown by E.S.C.A. that denitration to a depth of ~100Å is at the equilibrium value for a given acid mix in a reaction time of 1 second and the fact that ^{13}C n.m.r. detects no difference with respect to the initial starting material merely reflects the small fraction of the total volume sampled by E.S.C.A. Within 5 seconds the reaction has penetrated well into the macrofibrils and significant differences are observed. The D.O.S. therefore drops mainly due to loss of nitrate ester at the C_2 and C_3 positions.

The D.O.S. at 40 mins. reaction time of 2.15 is essentially the equilibrium value and the data for samples studied after longer reaction periods, (up to 12 hours), provide

Table 4.4

Acid mix	Total DOS from n.m.r.	DOS partial			Percentage components				
		C_6	C_2	C_3	Tri	2,6-	3,6-	6-Mono	Unsubstituted
64% HNO_3 26% H_3PO_4 10% P_2O_5	2.83	1.0	0.94	0.89	83	11	6	-	-
72% HNO_3 1 s treatment	2.83	1.0	0.94	0.89	83	11	6	-	-
82% HNO_3 5 s	2.72	1.0	0.9	0.82	74	16	8	2	-
82% HNO_3 20 s	2.62	1.0	0.86	0.76	66	20	10	4	-
82% HNO_3 5 min.	2.31	1.0	0.71	0.6	47	24	13	17	-
82% HNO_3 40 min.	2.15	1.0	0.63	0.52	40	23	12	25	-

identical data. The D.O.S. is marginally lower than for the sample denitrated in 83% nitric acid; the data for which are displayed in Table 4.3. The distribution of substitution patterns are similar, the main difference being the higher percentage contribution of monosubstituted β,D-glucopyranose residues for the lower acid strength. The trend is maintained since for 79.1% acid strength the D.O.S. has dropped further to 2.0.

4.3.5 Comparison of Data

It would be expected from the simplified analysis presented by Wu[216] that material of a given D.O.S. would show the same partitioning irrespective of the equilibrium conditions under which it is produced. However it is readily apparent from a comparison of a series of denitrated and nitrated materials in the range 2.0-2.83 where the major proportion of β,D-glucopyranose residues are either di or tri substituted that this is not so.

This can be readily appreciated from the histogram plot shown in Figure 41. The striking feature of this data is that the ratio of the 2,6 to 3,6-disubstituted products does indeed appear to be largely independent of the medium as proposed by Wu[216]. It has been previously noted that the distribution of mono and unsubstituted residues is different for nitrated and denitrated materials, (2.37 and 2.43 D.O.S.), and in fact for the denitrated material there is no evidence for unsubstituted residues down to a D.O.S. of 2.0. Reference to Wu's distribution curves shows that if a simple model based on three equilibrium constants was applicable a material of D.O.S. 2.0 should have several per cent of unsubstituted

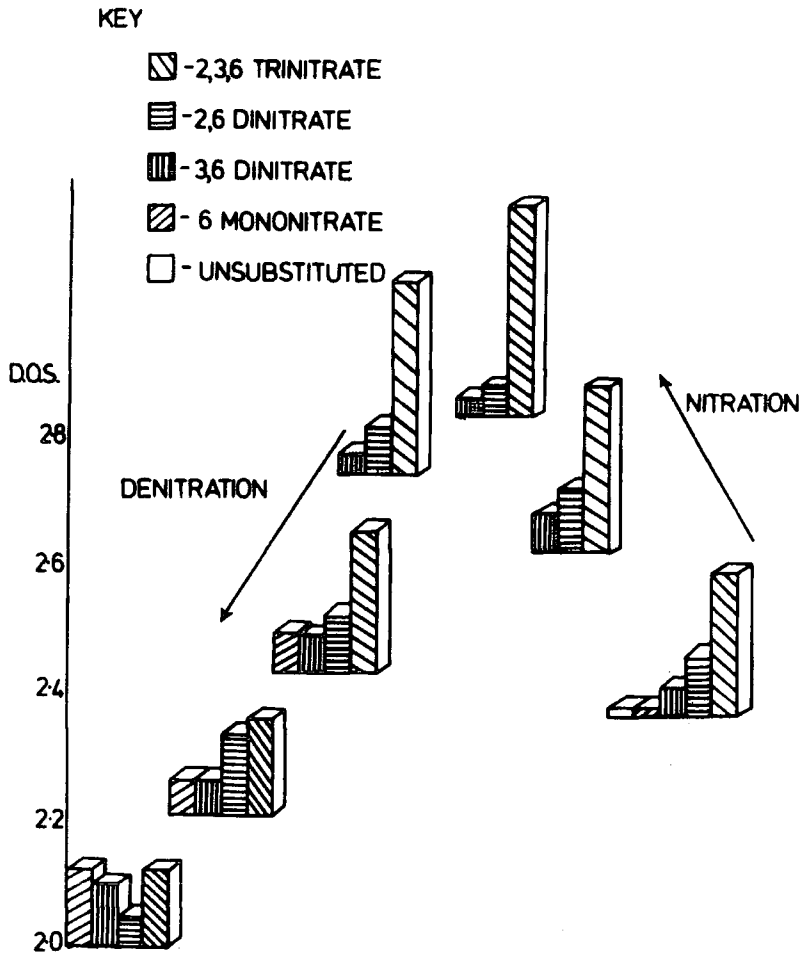

Fig. 41 Block histograms of nitrate ester distribution for given D.O.S. cellulose nitrates prepared by nitration and denitration

residues whilst for material of D.O.S. 2.37 there should be no unsubstituted residues. Figure 40 therefore illustrates in a graphical way that the situation is considerably more complex than implied by Wu's elegant but simplistic analysis.

The implication from the analysis in the introduction that substitution and sequence distribution is non random also suggests that reactions at a given site in a glucose residue are influenced by the substitution patterns in adjacent rings and this again casts doubt on the validity of a simple model which assumes that within a given ring substitution at one site is independent of the substitution pattern in the same ring. It is also interesting to note the available literature data[218] which also casts serious doubts on this assumption

since studies of denitration of simple model systems have indicated that rates are greatly influenced by structure and although these experiments were carried out under different conditions it would appear that the results from the ^{13}C n.m.r. are indeed analogous.

This denitration of ethylene glycol dinitrate, (e.g. as a model for 2,3 dinitrosubstituted β,D-glucopyranose residue) is an order of magnitude faster than for 1,4 butylene glycol dinitrate (e.g. as a model for 3,6-dinitrosubstituted β,D-glucopyranose residue). The relative rates of nitration and denitration at a given position in a substituted β,D-glucopyranose residue is therefore likely to be grossly rather than subtly dependent on substitution pattern. Published data[208] on relative rates of denitration of simple model systems shows that a primary nitrate ester is particularly stable and on the basis of this the observed behaviour in denitration of the 6-monosubstituted residue being present without any evidence for the unsubstituted β,D-glucopyranose residues is readily understandable. Although it is not possible on the data collected to quantify the situation further sufficient data is available to assess the likely ordering of relative rate and equilibrium constants and to this end we may consider the partial reaction sequences shown in Figure 42.

No evidence has been presented in the literature on rate data for the initial formation of monosubstituted derivatives other than the 6-substituted β,D-glucopyranose residues. However the fact that a significant proportion of the glucose residues are unsubstituted in nitrated material of D.O.S. 2.37 strongly suggests that the rate constants for nitration in

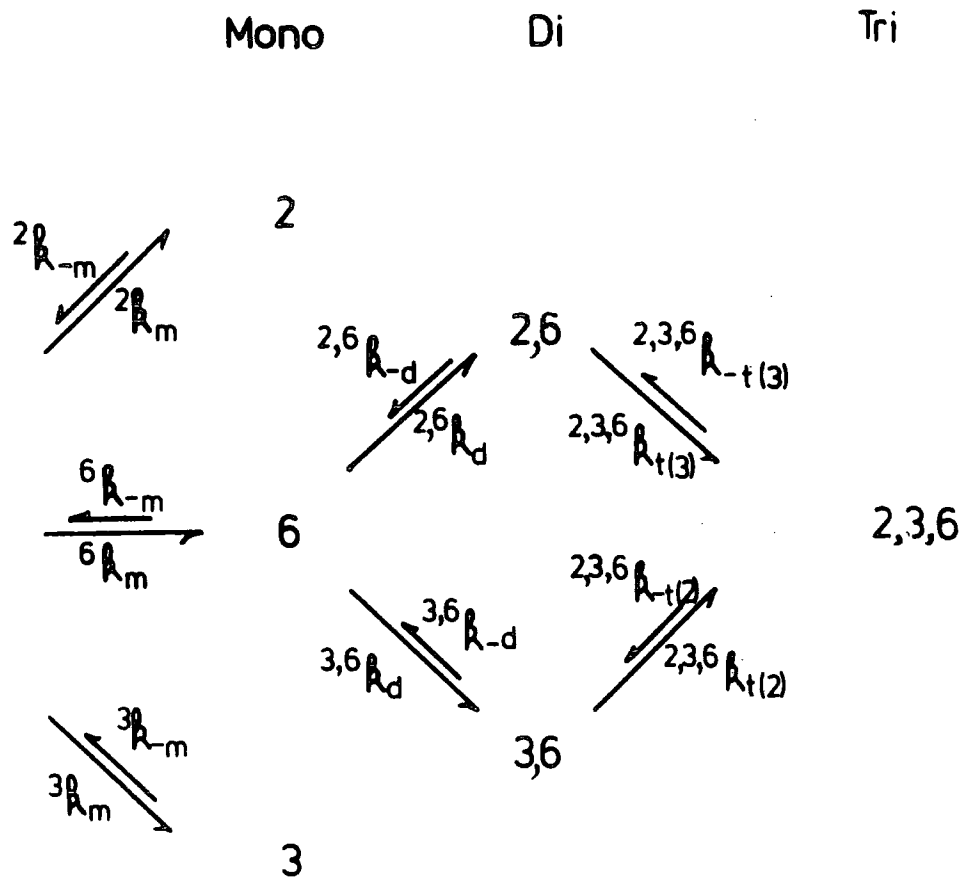

Fig. 42 Schematic showing partial reaction pathways in the nitration/denitration equilibria

the 2 and 3 sites in a given glucose residue increases with the partial D.O.S. in the particular residue in question. This is supported by literature data on model systems which indicates that the rate of a denitration step increases the more highly substituted the derivative. In terms of the partial scheme outlined in Figure 41 the rate constants for denitration of monosubstituted derivatives is certainly in the order $^{6}k_{-m} << {}^{2}k_{-m}, {}^{3}k_{-m}$. There is no available literature data on rates of nitration at primary and secondary sites in model systems, however, the equilibrium constants for formation of the mononitrate esters are undoubtedly in the order $^{6}k_{m} > {}^{2}k_{m}, {}^{3}k_{m}$. Since the order of rate constants for denitration are likely to be:

$$^{6}k_{-m} << ^{2,6}k_{-d} \quad ^{3,6}k_{-d} < ^{2,3,6}k_{-d} \quad ^{2,3,6}k_{-t}(2), \quad ^{2,3,6}k_{t}(3)$$

the order of rate constants for nitration must be

$$^{6}k_{-m} < ^{2,6}k_{d}, \quad ^{3,6}k_{d} < ^{2,3,6}k_{t}(2), \quad ^{2,3,6}k_{t}(3)$$

The constancy of the 2,6 to 3 6 disubstituted residues implies that $^{2,6}k_{d}/^{3,6}k_{d} = ^{2,3,6}k_{t}(3)/^{2,3,6}k_{t}(2)$ and this is consistent with a greater reactivity of the 2 position relative to the 3 position for a given partial D.O.S. in the residue in question. In summary therefore the nitration-denitration reactions are considerably more complex than has been implied in the past and at best a simplified model based on 3 equilibrium constants can only provide a crude qualitative picture of the partial D.O.S. in nitrated or denitrated cellulose samples. However the modifications outlined in this chapter allow a direct comparison of substitution patterns with lattice spacing data, (which will be more fully discussed in Chapter Six) and the inference that substitution is non-random is important in investigating the relationship between the D.O.S. in sequences of β,D-glucopyranose residues and the differences in 'd' spacing for nitrated and denitrated materials of the same D.O.S. prepared in different ways. It is also clearly evident from the data that the ^{13}C n.m.r. spectra provide an accurate determination of D.O.S. and if the instrument time is available provides a realistic replacement for the time-consuming Kjeldahl nitrogen analysis.

CHAPTER FIVE

E.S.C.A. STUDIES OF THE SURFACE CHEMISTRY OF CELLULOSE NITRATES AND DOUBLE BASED PROPELLANTS, WITH PARTICULAR REFERENCE TO THEIR DEGRADATION IN ULTRA VIOLET LIGHT

5.1 Introduction

The stability of cellulose nitrate and double based propellants to a number of environmental conditions is of great interest to the munitions industry.[220,221] Over extended periods of time factors such as humidity changes and exposure to solar radiation may profoundly affect the burn rate of these materials by initiating degradation of the parent nitrocellulose or through loss of plasticiser and nitroglycerin by volatilisation from the surface.[221]

In the past the degradation of cellulosic materials has been measured by monitoring changes in viscosity or tensile strength[222,226] brought about by a chain scission reaction which in cellulose itself is considered the main photolytic reaction. However the typical quantum yields for chain scission in cellulose (0.001) and cellulose nitrate (0.01) are substantially smaller by at least an order of magnitude than that reported for the photolysis of nitrate ester groups[227] and can be expected that the loss of nitrogen oxides from the photolysis of such groups will be the main reaction in cellulose nitrate. Very little work has in fact been published in the photolysis of the simple alkyl nitrates but in the wavelengths of interest to this work ($\lambda > 2900$) there is evidence for three primary processes:[223]

$$R\text{-}CH_2\text{-}O\text{-}NO_2 \xrightarrow{h\nu} R\text{-}CH_2\text{-}O\cdot + NO_2 \quad (1)$$

$$\longrightarrow R\text{-}CHO + HONO \quad (2)$$

$$\longrightarrow R\text{-}CH_2\text{-}ONO + O\cdot \quad (3)$$

Quantum yields for these reactions are in the order (1) >(3) >(2). Phillips *et al*[223] have studied the thermal degradation of alkyl nitrates and reported that the initial

cleavage (1) was followed by

$$R\text{-}CH_2\text{-}O^{\cdot} + RCH_2\text{-}ONO_2 \longrightarrow RCH_2\text{-}OH + \dot{R}CH\text{-}ONO_2 \quad (4)$$

$$\dot{R}CH\text{-}ONO_2 \longrightarrow RCHO + NO_2 \quad (5)$$

In view of what is known about possible degradation pathways it is not surprising that recent studies of the thermal degradation of cellulose nitrate and double based propellant have concentrated on monitoring the rate of evolution of nitrogen oxides at elevated temperatures as determined by chemiluminescence NOX analyser techniques.[224,225] In such measurements the loss of nitrogen oxides is monitored continuously giving direct information on rates but no information is available on the reaction of degradation products with other constituents of the propellant or indeed on any chemical changes which may occur on the photolysis of a nitrate ester group. In order to fully understand the mechanism such information is essential and since it is the very surface of these materials which interacts initially with solar rays and humidity of the environment it would be of great interest to study the nature and rate of accumulation of degradation products in the outermost few tens of Angstroms of cellulose nitrate fibres and double based propellants on exposure to controlled environmental conditions. The lack of information available in the literature in the past in this area can be traced directly to the lack of a suitable technique and it is only with the advent of E.S.C.A. (X-ray photoelectron spectroscopy) in the last few years that such information is now potentially available. Recent E.S.C.A. studies (c.f. Chapter Three) of simple model systems and detailed investigations of the surface nitration and denitration of cellulosic materials has yielded important information not only on

relative rates of reaction but also on the nature and environment of functional groups. Clearly with the extensive information now available on the surface chemistry of the cellulose nitrates it is possible, using this data as a basis for analysis, to study the degradation of such materials on exposure to U.V. light. This is not true however for the double based propellant since very little is known of the surface chemistry of such materials or indeed how the components of the propellant, (nitroglycerin, nitrocellulose and various stabilisers and additives), may interact in the bulk. It is the purpose of the work, outlined in the following pages, therefore, to carry out a detailed analysis of the surfaces of double based propellants for a range of compositions in order to establish a data base similar to that already available for the cellulose nitrates and to study the degradation occurring in the outermost few tens of Angstroms in these materials on exposure to U.V. light. In order to limit the many variables in such an investigation the photodegradation of cellulose nitrates and double based propellant (60/40 nitroglycerin(NG)/nitrocellulose (NC) composition only) has been monitored in dry atmospheres of oxygen and nitrogen for given periods of time.

5.2 Experimental

The double based propellants examined in this work were supplied by the Ministry of Defence, Waltham Abbey, in various wt/% ratios of NG/NC. Approximately 1% by weight of diethyl-diphenyl-urea stabiliser, (carbamite), was incorporated in all samples and before analysis the propellants had been stored for at least one year. The propellants in sheet

form, (3mm in thickness), were cut to probe tip size, (18 x 8mm), and mounted on a special cooling probe, the temperature of which can be accurately controlled by pumping liquid nitrogen to the probe tip. Samples considered in this work were pre-cooled to -110°C in a dry nitrogen atmosphere by the use of a glove bag attached directly to the insertion lock of the spectrometer. (In the U.V. degradation studies it was found sufficient to purge the insertion lock with nitrogen before cooling the sample in the lock). This procedure precludes the deposition of water vapour onto the propellant surface. The samples were then pumped down in the insertion lock, ($\simeq 10^{-3}$ torr), before introduction to the sample chamber, ($\simeq 5 \times 10^{-8}$ torr). It was found that the pressure of the chamber was maintained during this procedure and there was no evidence for loss of NG from the surface under normal operating conditions, (viz the spectra were independent of the typical time scale of the measurements). However it should be noted that it is possible to instigate a steady loss of NG to the chamber by increasing the temperature of the probe tip (c.f. Section 5.3.1). The spectra were run on an A.E.I. E.S.200A/B electron spectrometer using a $Mgk\alpha_{1,2}$ X-ray source operated in a fixed retardation ratio mode. Under the conditions of these experiments the Au $4f_{7/2}$ level used for energy calibration had a f.w.h.m. of 1.15ev. Spectra were analysed using a Du Pont 310 curve resolver.

All cellulose nitrates irradiated by U.V. light were prepared by standard laboratory procedures outlined in Chapter Three from dewaxed, depectinised cotton linters. 60% NG/ 40% NC propellants were used for the irradiation experiments

which were carried out in a specially designed rig described elsewhere[228] using a 500W Hanovia lamp cut off λ = 2900nm. the photon flux of the lamp is ≈ 30 watt hours per metres^2 and the most intense lines occur at 366, 546, 436, 405 and 303nm with less intense components at 254 and 265nm, in a flow or static atmosphere of dry oxygen or dry nitrogen. The sample was kept at a fixed distance from the lamp, (16 cms), and the temperature of the sample over prolonged exposure did not rise above 28°C. The exposed material was transferred directly to an A.E.I. **E**.S.200 A/B spectrometer, (c.f. Chapter Two), and analysed by the cold probe technique described earlier.

5.3 Results and Discussion

5.3.1 Surface Chemistry of the Double Based Propellants

Previous studies of both simple model systems and of nitrated and denitrated cellulosic materials has shown the distinctive nature of the C_{1s} and N_{1s} levels for structural features likely to be present in double based propellants (c.f. Chapter Three). With a knowledge of relative photoionisation cross sections and instrumental response functions it is possible to establish stoichiometries on the E.S.C.A. depth sampling scale, (~50Å using a $Mgk\alpha_{1,2}$ X-ray source). In the particular case of the double based propellants the surface chemistry could conceivably involve not only the nitrocellulose (NC) and nitroglycerin (NG) components but also the stabilising component diethyl-diphenyl urea which although only present at low levels could conceivably segregate at the surface. The surface composition is therefore defined in terms of two parameters representing the relative proportions

of the three components. The C_{1s}/O_{1s} and C_{1s}/N_{1s} intensity ratios provide the two measurable parameters which allow the surface composition to be determined.

Before considering the data for the double based propellants it is of interest to note the E.S.C.A. spectrum of N.G. itself since this has not previously been reported. The sensitivity to detonation of N.G. implies that especial caution is necessary in measuring the core level spectra. To this end a cooled sample (c.f. Section 5.2) of the 60/40 NG/NC material was slowly allowed to warm whilst the sample was maintained in high vacuum ($\sim 5 \times 10^{-8}$) in the spectrometer chamber. By monitoring the pressure in the chamber it was found possible to determine when appreciable amounts of NG/NC started to desorb from the surface. By recording the samples to $-110^{o}C$ at this stage it has proven possible to obtain the C_{1s}, N_{1s} and O_{1s} levels of an N.G. overlayer on N.C. and a typical spectrum is shown in Figure 43. For comparison purposes we also include core level spectra for the 35/65 formulation and distinctive differences in intensity ratio and in binding energies of the component of the C_{1s} levels are readily apparent. The surface compositions of the four double based propellant systems studied in this work are shown with error limits in Table 5.1 where comparison is drawn with the bulk compositions. It is clear from this that there is a close correspondence between the surface and bulk chemistries and this is best illustrated by means of the comparison in Figure 44. Several distinctive features are of note. Firstly the correspondence between surface and bulk composition is closest for the two samples which are close to 50 mole% in the two major components. For the

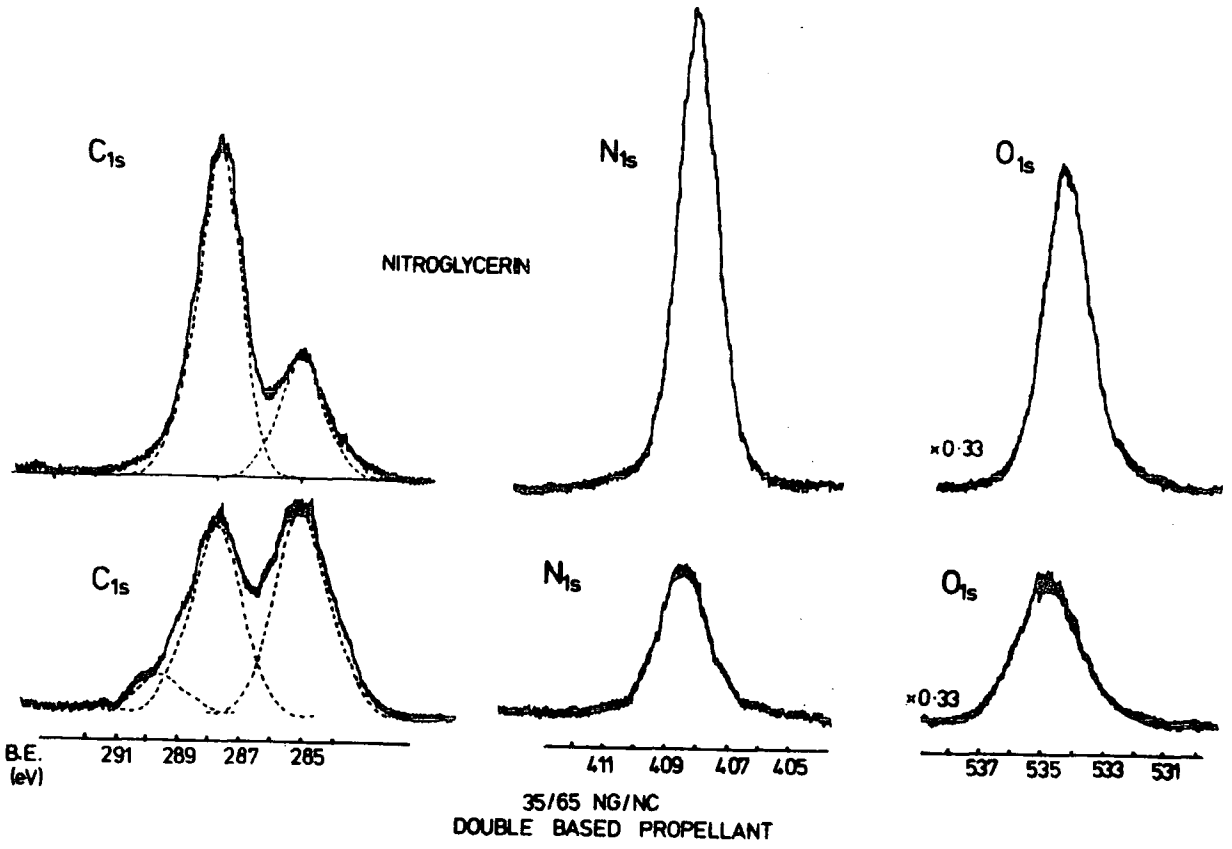

Fig. 43 C_{1s} and N_{1s} core level spectra of nitroglycerin and 65/35 NC/NG double based propellant

Table 5.1

Wt./% NG/NC Ratio		Mole %		
		NG	NC	DEDPU
35/65	Calculated	38	62	
	E.S.C.A.	31 ± 1	68 ± 1	1.0 ± 0.2
40/60	Calculated	45	55	
	E.S.C.A.	49 ± 1	49 ± 1	2.0 ± 0.2
50/50	Calculated	54	46	
	E.S.C.A.	53 ± 1	46 ± 1	1.0 ± 0.2
60/40	Calculated	63	37	
	E.S.C.A.	82 $^{+0}_{-1}$	5 $^{+0}_{-2}$	13.0 - 1

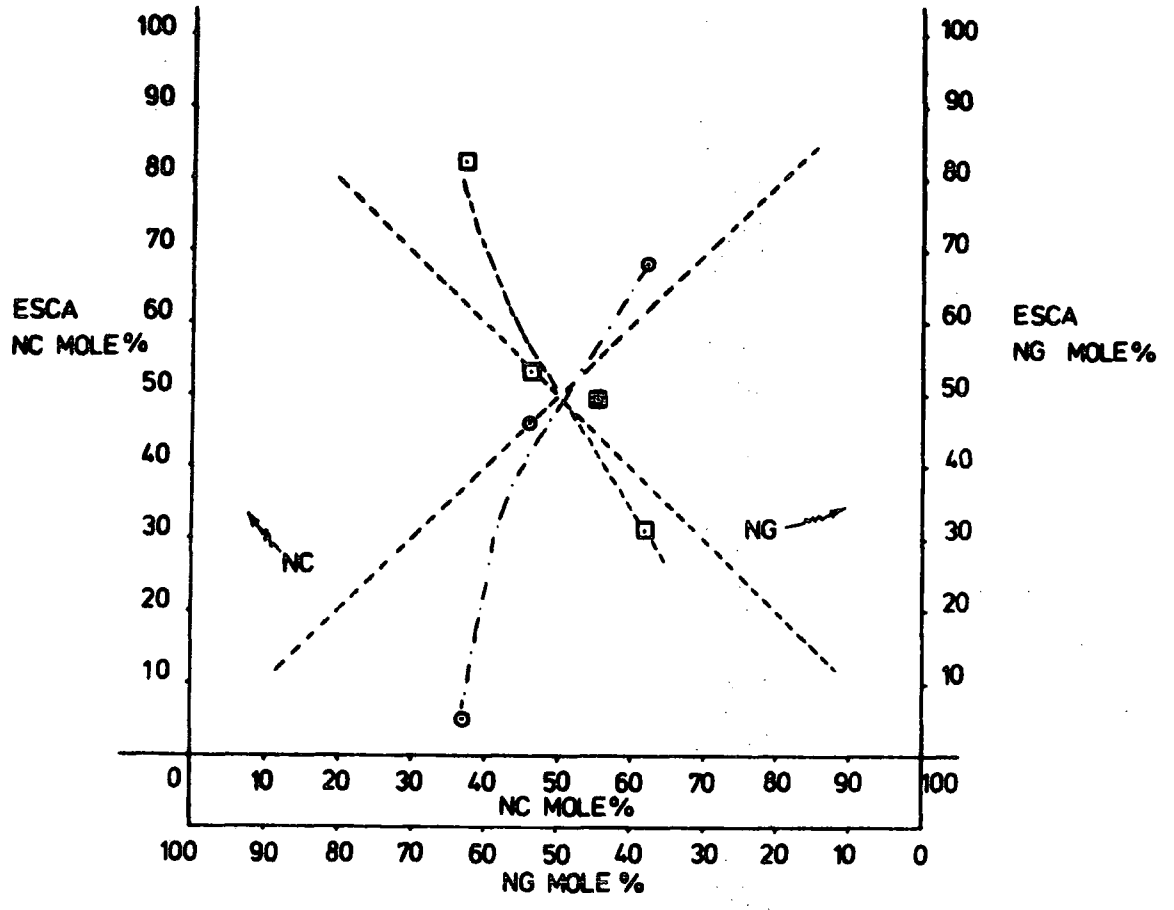

Fig. 44 Graph of Bulk mole % of NC/NG in double based propellants versus mole % NC/NG determined by E.S.C.A. (The dashed curves link the NC(O) and NG(□) data points whilst the dotted lines represent the correlations expected if surface and bulk are identical

samples with a low bulk composition in N.G. there is a tendency for the surface to be somewhat lower in this component than for the bulk. By contrast for the sample with a larger composition in N.G. there is a tendency for the surface to become comparatively enriched in this component and this is accompanied by significant surface segregation of the stabiliser. This migration in 60/40 N.G./N.C. may well influence the subsequent reactions at the surface occurring on photo irradiation in U.V. light and this important topic will now be addressed.

5.3.2 U.V. Degradation of Cellulose Nitrate and Double Based Propellant

During an early study of the surface chemistry of nitrocellulose fibres it was noticed that a degradation reaction took place in the surface regions as a result of exposure to a Mgk$\alpha_{1,2}$ X-ray source for prolonged periods (>5 hrs.). This degradation was characterised by a reduction in intensity of the N_{1s} core level corresponding to a nitrate ester group at 408.3 ev and the growth of a peak at ≈400 ev presumably corresponding to the products of this degradative process (c.f. Figure 25). In the following discussion of the irradiation of nitrocellulose and double based propellant in ultra violet light the importance of this low binding energy component will become apparent and special reference will be made to it in the next four sections which discuss the following irradiations:

(a) Irradiation of nitrocelluloses (2.6 and 1.9 D.O.S.) in N_2;

(b) Irradiation of nitrocelluloses (2.6 D.O.S. only) in O_2;

(c) Irradiation of 60/40 N.G./N.C. propellant in N_2;

(d) Irradiation of 60/40 N.G./N.C. propellant in O_2.

5.3.3 Irradiation of Nitrocelluloses (2.6 and 1.9 D.O.S.)in N_2

The degradation of 1.9 D.O.S. material in a nitrogen atmosphere is shown schematically in Figure 45 which depicts the C_{1s}, N_{1s} and O_{1s} core levels of irradiated materials. The degradation is considerably more rapid than that observed in the X-ray degradation studies previously referred to. Reference to Figure 46 shows that the C_{1s}/N_{1s} ratios for this material, (excluding in this case the hydrocarbon peak at 285.0 ev and

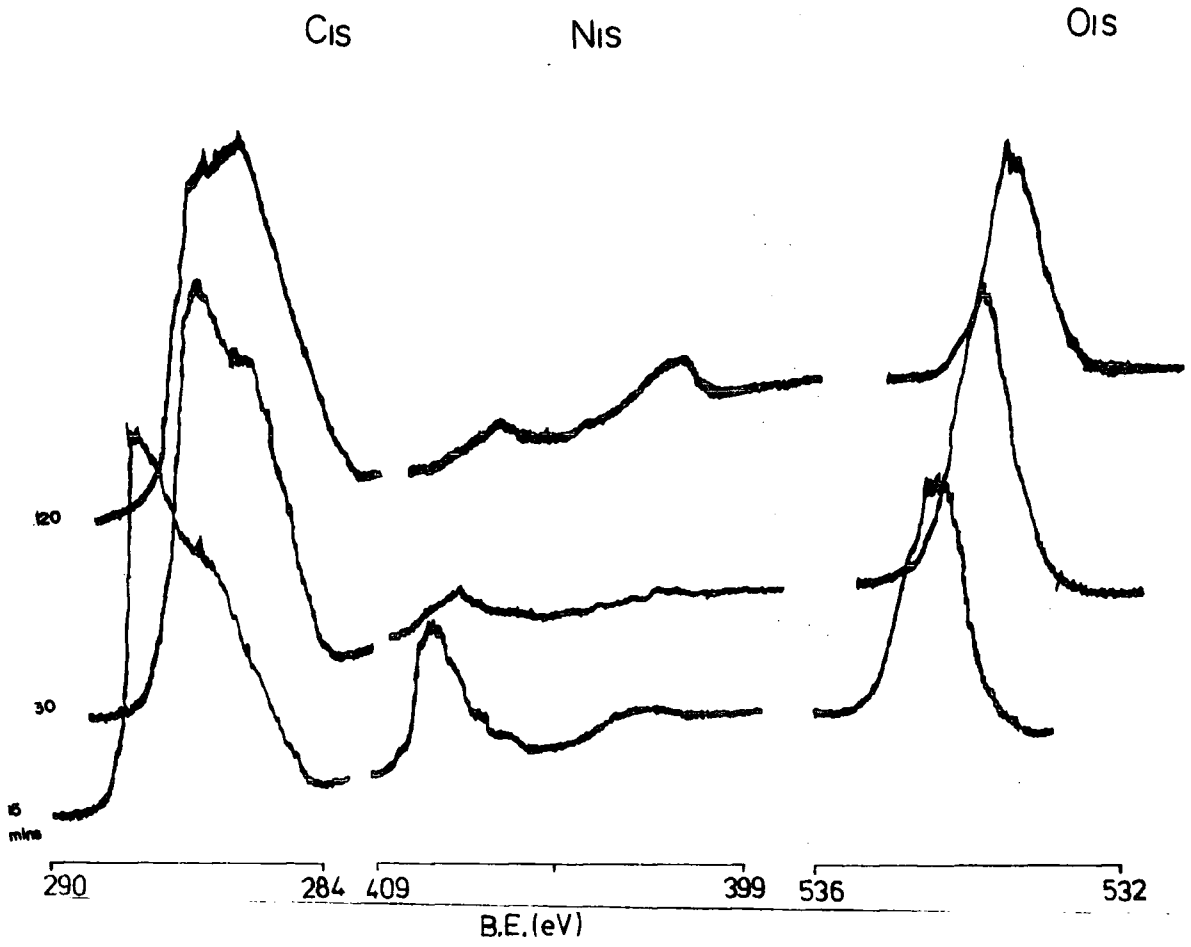

Fig. 45 Core level spectra of a 1.9 D.O.S. NC as a function of time on irradiation in U.V. light in a nitrogen atmosphere

sensitivity factors), rises sharply corresponding to a rapid loss of nitrogen from the surface regions. Surprisingly this is not associated with a similar decrease in oxygen levels, (c.f. C_{1s}/O_{1s} ratio Figure 46), although there is some evidence from the C_{1s} profiles for increased C-O or aldehydic groups.

However the increase in intensity of the N_{1s} peak at ≈400 ev is also rapid and after 2 hrs. exposure has an intensity equivalent to that of the main peak at 408 ev corresponding to the nitrate ester. It is not inconceivable that this low binding energy nitrogen containing functionality is associated with an oxygen atom perhaps in the form of an oxime

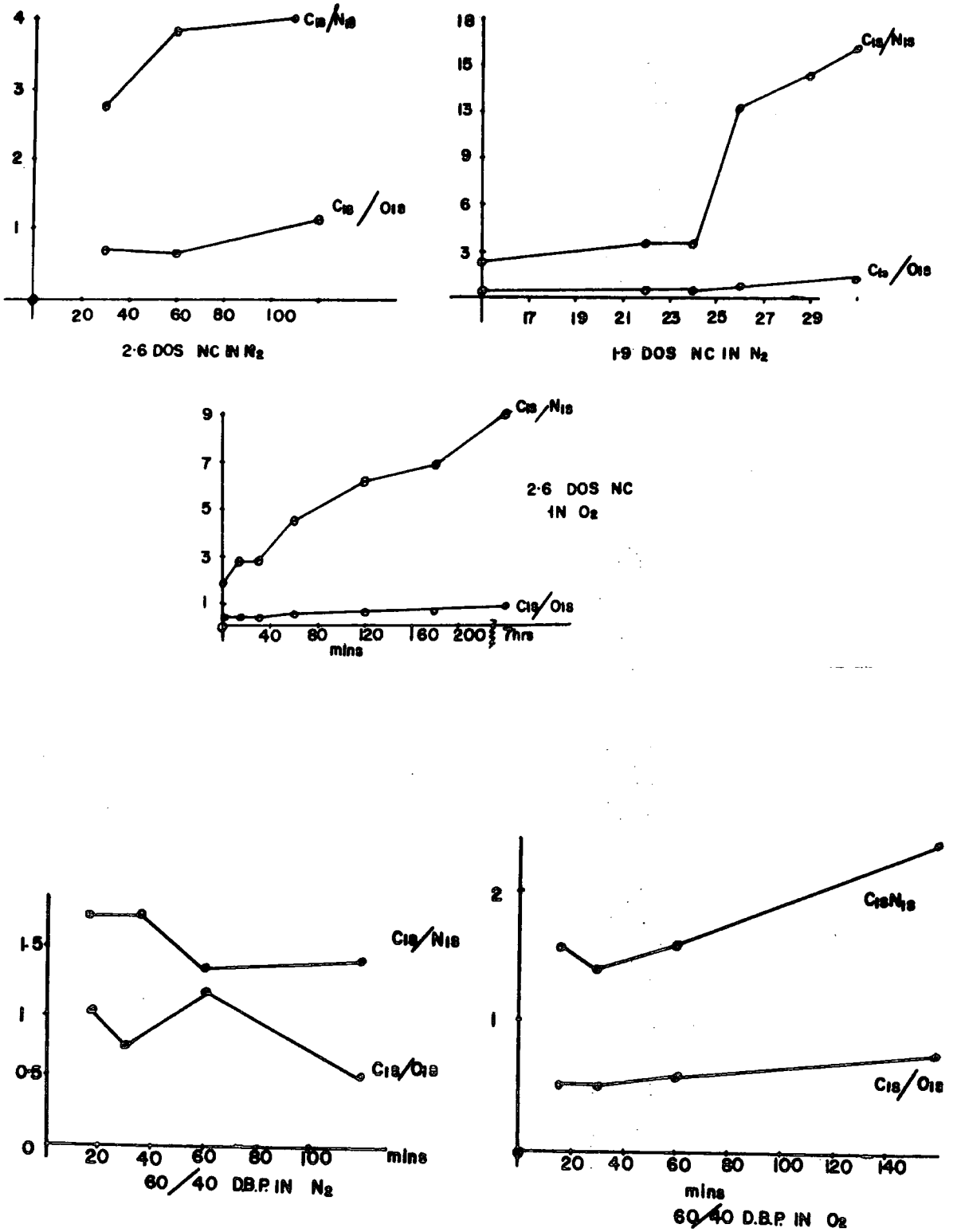

Fig. 46 C_{1s}/O_{1s} and C_{1s}/N_{1s} core level area ratios, (for a series of irradiations in U.V. light), of 1.9 and 2.6 D.O.S. NC and double based propellant in nitrogen and oxygen atmospheres

(B.E. = 400 ev)[229] which may account for the slow decrease in oxygen levels. It is also worth noting that throughout these irradiations the amount of nitrite ester. (appearing as a peak at ≈406 ev), which is known to be formed in similar irradiations on simple alkyl nitrates, (c.f. introduction), remains at a relatively constant ratio of 5% of the main nitrate ester peak.

Turning now to the data pertaining to 2.6 D.O.S. material (Figure 46) it is clear that the rate of decomposition under identical conditions is considerably reduced with a much slower loss of nitrogen and comparable decline in oxygen levels. The nitrate ester to low B.E. component area ratio, for example, falls from 6.45 to 2.0 in 2 hrs. for 2.6 D.O.S. material and from 4 to 0.5 in 2 hrs. for 1.9 D.O.S. nitro-cellulose. This difference in rate is interesting and may be explained in terms of the difference in preparation of the two nitrocelluloses. The low D.O.S. material prepared by nitration in a high sulphuric acid content acid mix is known to have a small level or residual sulphate ester group which have resisted hydrolysis, (c.f. Chapter Three), whereas the high D.O.S. nitrocellulose prepared in a low sulphuric acid content mix is essentially free of such groups. It is not inconceivable that such groups may act as a photo-initiator and promote the degradation. This is supported to some extent by the induction period of ≈20 mins. observable in the irradiation of 1.9 D.O.S. material before the rapid rise in C_{1s}/N_{1s} ratios. Another interesting observation is that nitrocelluloses prepared in mixes with a high percentage of sulphuric acid are particularly difficult to stabilise and without prolonged boiling and washing procedures will rapidly yellow and decompose.[41]

5.3.4 Irradiation of 2.6 D.O.S. Nitrocellulose in O_2

Consideration of the spectra in Figure 47 and the C_{1s}/N_{1s} and C_{1s}/O_{1s} area ratios for this irradiation reveals a rapid loss of nitrogen characterised by a rapid increase in C_{1s}/N_{1s} ratios (Figure 46). Again there is a relatively slow loss of oxygen but examination of the C_{1s} profile for such materials reveals a substantial increase in carboxyl and aldehylic groups with time. For example,

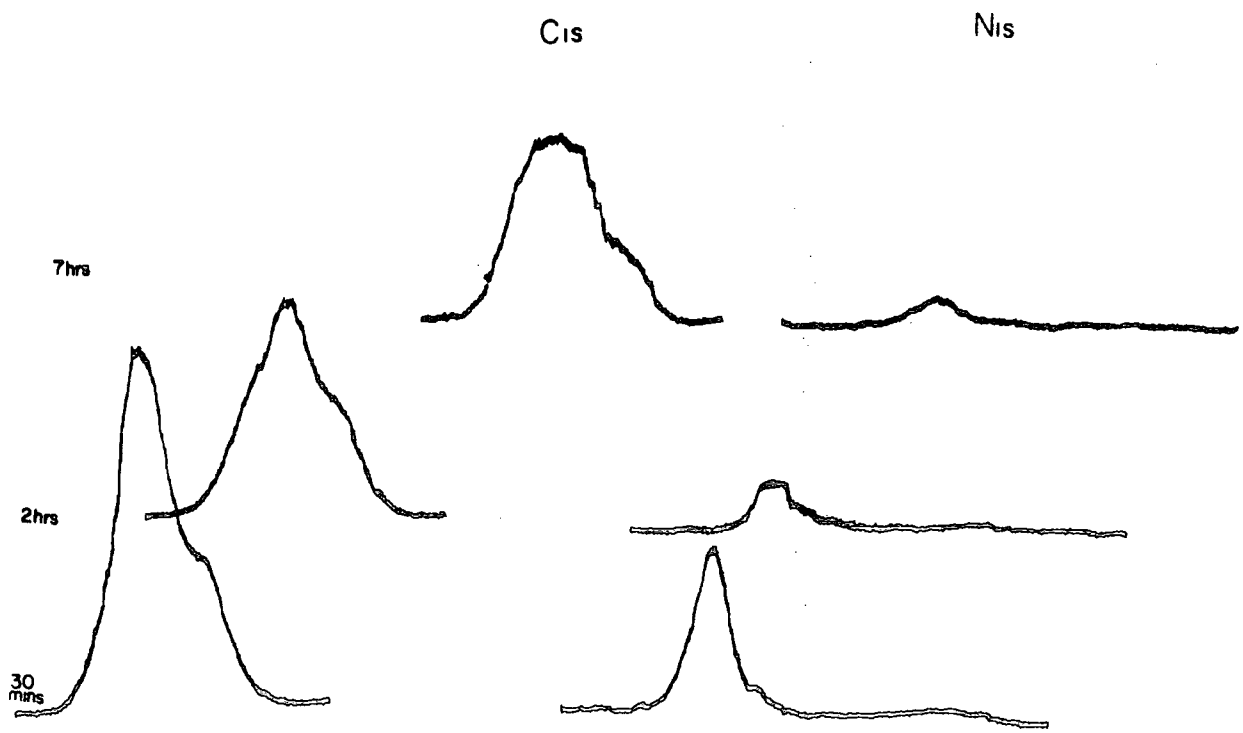

Fig. 47 Core level spectra of a 2.6 D.O.S. NC irradiated for increasing periods of time in U.V. light in an oxygen atmosphere.

the peak at 290.4 ev corresponding to a carboxyl functionality increases in intensity by a factor of 5 during the first three hours of irradiation whereas the other C-O functionalities (aldehydes. $C\lessgtr^{O}_{O}$, C-O, peroxides) increase by an overall factor of 1.5. An important point to note is the lack of a low B.E. nitrogen and it may be possible to conclude that in the presence of oxygen the free radical sites which would in a nitrogen atmosphere react to produce the low B.E. nitrogen are quickly attached by free oxygen to form peroxides[1,229] or other oxidised species.

5.3.5 Irradiation of 60/40 N.G./N.C. in N_2

The results of this irradiation at first glance may appear somewhat anomalous since the C_{1s}/N_{1s} and C_{1s}/O_{1s} ratios indicate a constant or even a slight gain in nitrogen and oxygen with irradiation time. A possible explanation would be that a significant proportion of stabiliser has migrated to the surface during the course of the experiment but this possibility is excluded by extensive time dependent studies carried out on such propellant described in a previous section. The low B.E. component in the N_{1s} spectrum is again much in evidence and after 2 hrs. irradiation has an intensity greater than that of the nitrate ester group. That some of this peak is due to the D.E.D.P.U. component is shown by the broadened nature of this peak. However it should be noted that the purpose of this stabiliser is two-fold; firstly it acts as a plasticiser and secondly is present as a stabiliser acting as a scavenger of nitrogen dioxide which is liberated. It is known to prevent autocatalytic

breakdown of nitroglycerin although little is known of the mechanisms involved.

The uptake of NO_2 in the surface regions by the enhanced levels of D.E.D.P.U. (carbamite), may tend to explain the anomalous ratios.

5.3.6 Irradiation of 60/40 N.G./N.C. Propellant in O_2

The loss of nitrogen on irradiation is not as rapid as in the 2.6 D.O.S. nitrocellulose in O_2, (c.f. Figure 47), although there is some evidence for the low binding energy component at 400 ev. The nitrate ester/low B.E. component area ratio falls from 2.95 to 1.33 during the course of the irradiation. Examination of the C_{1s} profiles of this material reveals a rise in intensity of the peak at 290.4, (corresponding to a carboxyl functionality). The area ratio of all the other C_{1s} species at lower B.E., (excluding hydrocarbon), to the carboxyl group falls from 25 to 2.6 during the irradiation indicating extensive oxidation in the surface regions.

In conclusion then to this initial study of the U.V. degradation of cellulose nitrates and double based propellants it has become apparent that the lower D.O.S. nitrocellulose has an increased rate of degradation compared with the more highly substituted residues perhaps as a result of the increased levels of sulphate esters in the surface regions. The nature of the low B.E. nitrogen component observed in most of these irradiations has not been fully elucidated since not only is it coincident in binding energy with the Mgk$\alpha_{3,4}$ satellite peaks but in the case of the double based

propellant occurs in a similar position on the binding energy scale to the D.E.D.P.U. component (see Section 5.3.1). It is evident however that in order to explain the high levels of oxygen observed in the surface regions this low binding energy component must be associated with at least one atom of oxygen perhaps in the form of an oxime. The level of nitrite ester throughout these irradiations has remained constant although one would expect from early studies of prototype systems for the level of such esters to increase on irradiation in U.V. light. It is possible that such esters once formed are continuously converted to the low B.E. component.

A photolytic mechanism for the conversion of a nitrite group to an oxime in the solid state has not been reported in the literature although in solution such conversions are well known under the name of the Barton Reaction,[230,231,232] which is known to have the following mechanism:

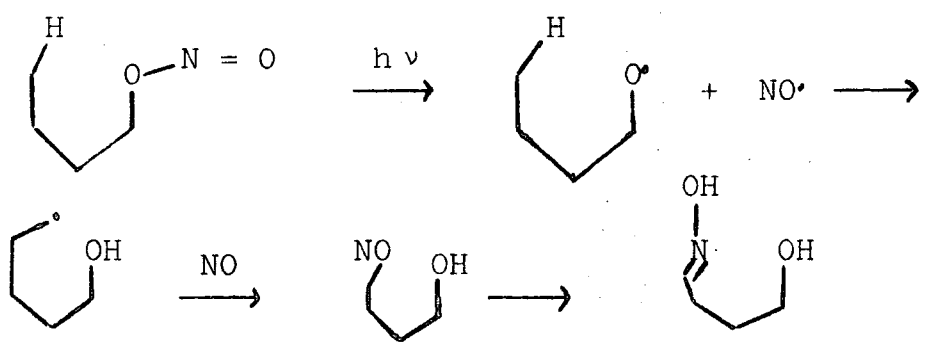

An analogue of such a reaction could occur in the surface regions of the materials studied in this work although it is clear from examination of the data presented and in particular the high level of oxygen present that the true situation is probably a complex combination of several reaction pathways. An interesting comparison can be drawn between these studies and ^{13}C n.m.r. investigations of nitrocelluloses extracted

from aged samples of double based propellants using methylene chloride. These propellants had been stored for periods of up to 21 years and although the poor signal/noise ratio of this particular set of spectra prevents the accurate determination of partial degrees of substitution at given positions on the glucopyranose residue it is possible to estimate the D.O.S. of the materials and this information is given in Table 5.2.

Table 5.2

Storage Time	D.O S.
<6 months	2.24
12½ years	2.08
21 years	1.96

There is a steady decline in nitrogen content of the extracted material with time although there is little evidence for additional features in the ^{13}C n.m.r. spectra which may correspond to degradation products. It is probable that E.S.C.A. is detecting changes occurring in the surface chemistry of cellulose nitrates and double based propellants which may affect initial burn rates that cannot be detected by other techniques.

It is obvious that E.S.C.A. has potential in the study of the degradation of cellulose nitrates and double based propellants and that this work is a fundamental basis for further work on the important topic of thermal degradation of such materials.

CHAPTER SIX

A ^{13}C N.M.R. AND X-RAY DIFFRACTION STUDY OF THE RELATIONSHIP BETWEEN THE DISTRIBUTION OF NITRATE ESTER GROUPS AND INTERCHAIN d.(101) SPACING IN A SERIES OF CELLULOSE NITRATES

6.1 Introduction

Soon after the discovery of the diffraction of X-rays by crystalline materials the technique was applied to cellulosic materials and in particular to cellulose nitrates. Much of the early work on cellulose and cellulose nitrates has been reviewed in Chapter One and it is clear that in the case of cellulose nitrates, much emphasis was placed on the measurement of the mean interchain spacing (d(101)) which is a particularly strong reflection in the X-ray powder diagram of cellulose nitrates. Miles,[41] for example, has reported that if cellulose is nitrated then, in general, the interchain distance increases with degree of substitution (D.O.S.) with the possibility of a plateau occurring between 12-13% nitrogen content, (corresponding to 2.26-2.58 D.O.S.) up to a limiting value of $\approx 7.3\text{Å}$ for the so-called "trinitrate". On denitration however the spacing is maintained over a significant D.O.S. range down to a nitrogen content of 11%, (D.O.S. 1.97). Hence cellulose nitrates of the same degree of substitution (D.O.S.) may have quite different mean interchain spacings depending on the method of preparation.

This phenomenon has been further investigated by Trommel[213,83] (c.f. Chapter One) whose results from an identical investigation are recorded in Figure 5. He came to the conclusion that this difference in mean interchain spacing could be explained in terms of a different distribution of nitrate groups in nitrated and denitrated material although sufficiently sensitive techniques at that time had not been developed to allow this hypothesis to be subjected to detailed scrutiny. Nitrated cellulose according to the Trommel[213,83]

argument had uniform distributions of nitrate ester groups along the cellulose chains due to the nitrating acid penetrating most parts of the cellulose. On denitration however it was assumed that the acid did not readily penetrate the highly crystalline trinitrated areas of the chain and denitration was far more likely at sites adjacent to lower nitrated residues. The final product therefore in this model would have large areas of relatively unsubstituted residues alongside regions of trinitrated material which were assumed to hold the chains apart despite loss of nitrate groups from other regions. This extreme model however has been shown to be untenable by the ^{13}C n.m.r. distribution data, (presented in Chapter Four), for a range of denitrated materials prepared in nitric acid-water mixes identical in composition to those used by Trommel.[213] In this work we have shown that no unsubstituted residues were present even down to a D.O.S. of 2.0. However limited sequence distribution data available from this work also suggested that there is a greater tendency for the 3,6 disubstituted residues, for example, in a denitrated sample, (D.O.S. 2.31), to be adjacent to a lower nitrate rather than a trinitrated residue. In other words the distribution of groups sequentially along a given chain is non-random.

Clearly, the mean interchain spacing in cellulose nitrates must reflect the detailed differences in microstructure in terms of distribution of nitrate groups both around a single residue and along a chain, (sequence distribution), and it is only recently, (with our full assignment of the ^{13}C n.m.r. spectra of cellulose nitrates) c.f. Chapter Four, that a comparison of mean interchain spacing and distribution of

nitrate groups has become feasible. In this chapter such a comparison is presented for a range of celluloses nitrated in nitric-sulphuric mixes and for a high D.O.S. (2.8) material denitrated in a series of nitric-acid water mixes. Improved S/N ratio for this series of ^{13}C n.m.r. spectra also allows further investigation of sequence distribution.

In the final section of this chapter the important question of the equilibrium situation in the nitration of cellulose is also addressed in the light of the new data presented in the coming pages.

6.2 Experimental

The nitrated material used in this study was prepared in mixed acids by methods described in Chapter Three. The denitrated material was prepared from 2.8 D.O.S. cellulose nitrate denitrated in nitric acid/water mixes similar to those used by Trommel.[213,83]

The X-ray diffractometer used was a Phillips P.W. 1130 3kW, X-ray generator incorporating a P.W. 1050 diffractometer assembly, (Cu tube operating at approximately 40 kV, 25ma). The recordings span from 4^{o} in 2θ to 30^{o} in 2θ and the mean 'd' spacing is taken as the centre of the peak occurring at around 12^{o} in 2θ.

The samples which had been pressed into paper form, (c.f. Chapter Three), were mounted into a glass holder. The error in such measurements is estimated at $< \pm$ 0.05 on the final reading. The ^{13}C n.m.r. spectra were obtained on a Varian Associates S.C.300 spectrometer and the distribution data calculated by methods described in Chapter Four.

6.3 Results and Discussion

The distributions of nitrate groups in the various nitrocelluloses studied are best represented in the form of block histograms set on an X-ray spacing vs. degree of substitution graph as in Figure 48. The X-ray d(101) spacings of the denitrated material across a large range of D.O.S. are shown to be consistently higher, (particularly for low D.O.S.) than those of cellulose nitrates prepared by nitration for comparable D.O.S. It is only in the high D.O.S. region that the spacings are comparable and it is interesting to note that in this area the nitrated and denitrated products have similar distribution patterns. Indeed the distribution patterns of the lower D.O.S. materials also reflect the difference in spacings; for example the difference between 2.37 nitrated and 2.43 denitrated products is 0.2Å and between 2.14 nitrated and 2.2 denitrated is 0.35Å. These changes can only be due to differences in distribution of nitrate groups and in particular to the proportion of unsubstituted residues in the samples. The denitrated nitrocelluloses have no unsubstituted residues and have a correspondingly higher X-ray spacing than their nitrated counterparts. However it would be naive to consider the problem in terms of substitutions at individual residues since the mean spacing is likely to be determined by substitutions and hydrogen bonding interactions along chains of cellulose residues. Fortunately the improved signal/noise ratios for the ^{13}C n.m.r. spectra (compared with the work reported in Chapter Four, for nitrated material allows a detailed study of the splitting of peaks in the anomeric region which reveals sequence distribution information and it is this data, Figure 49, which we

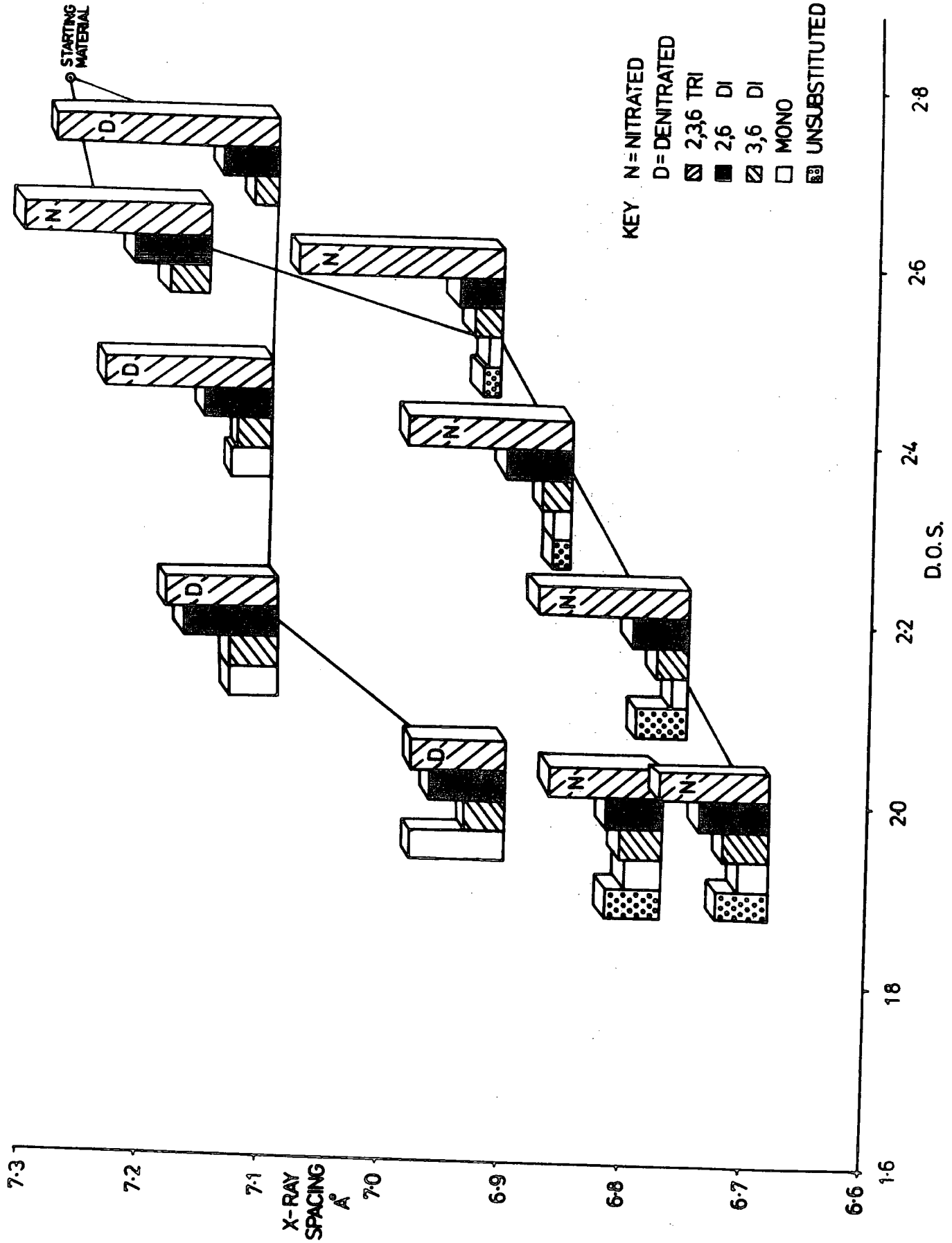

Fig. 48 Block histograms of nitrate ester distributions for given degrees of substitution against the mean interchain spacing as measured by X-ray diffraction

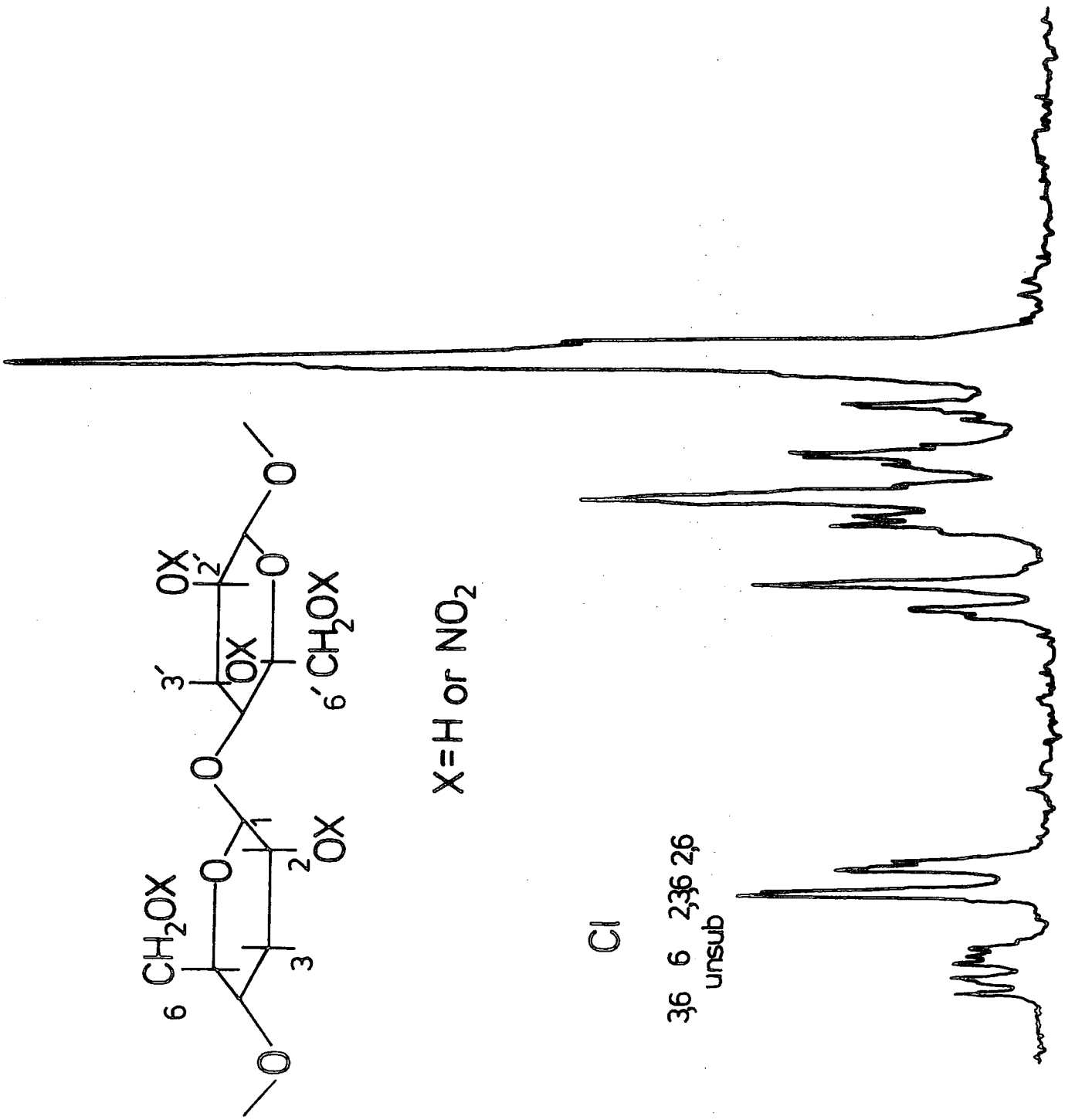

Fig. 49 ^{13}C n.m.r., (75.5 MHz proton decoupled), spectrum of a 1.9 D.O.S. cellulose nitrate prepared by nitration

shall now consider.

The 75.5 MHz ^{13}C n.m.r. spectrum is for a low D.O.S. (1.9) cellulose nitrate prepared by nitration in 53% HNO_3 20% H_2SO_4 and 27% H_2O. Taking first the lowest field peak at 104 p.p.m. due to an anomeric carbon (CI) in a 3,6 disubstituted ring it has been previously reported, (Chapter Four), that for denitrated material the splitting of 0.8 p.p.m. observed in this peak is due to the presence or absence of a nitrate group at C_3' in an adjacent* ring and that the distribution of nitrate groups along a chain is non-random. In other words the 3,6 disubstituted residues are more likely to be adjacent to other 3,6 disubstituted or 2.3,6 trisubstituted β-d-glucopyranose rings. This is again apparent for the spectra for nitrated material shown in Figure 49 and from consideration of the distribution data obtained from the ^{13}C analyses listed in Table 6.1 which, for the 1.9 D.O.S. material, can be simplified approximately in terms of a decad sequence; (viz. the ratio of tri: 2,6 di; 3.6 di: 6 mono: unsubstituted residues is partitioned approximately 4:2:1:1:2). On the basis of a random substitution pattern one would predict a probability of 0.5, (5/10), that a 3,6 disubstituted residue in this material would be adjacent to another 3,6 or trisubstituted residue. The integrated area ratios available for the spectrum in Figure 49, however, reveal a probability closer to 0.25. Repeating the calculation for the peak at highest field in the anomeric region (≈98 p.p.m.) due to C1 in 2,6 disubstituted residues we would expect a probability of ≈ 0.5, (on the basis of a random

---

* Footnote: for definition of the term 'adjacent' the reader is referred to Figure 49 where the adjacent ring is defined as that linked through the C_4' position to the ring in question.

TABLE 6.1 NITRATED MATERIAL

N.M.R. D.O.S.	TRI	2,6	3,6	MONO	UNSUBST	X-RAY d(101) SPACING
1.9	38	19	14	12	18	6.81
1.9	36	23	14	10	17	6.66
2.1	50	18	10	5	17	-
2.14	53	17	8	6	16	6.73
2.37	55	22	11	6	6	6.90
2.50	58	14	9	4	5	6.93
2.62	62	25	13	-	-	7.25
2.53	65	16	11	4	4	7.08
2.67	71	16	9	4	-	7.13
2.83	83	11	6	-	-	7.28

substitution pattern), that a 2,6 disubstituted residue would have a C_3' substituted ring, (3,6 or 2,3,6), adjacent to it. It is difficult to quantify the data from this region of the spectrum;however, it is clear that there is a very much higher probability, (≈ 0.8), that a 2,6 disubstituted residue has a C_3' substituted residue adjacent to it.

Considering also the major component of the anomeric region at ≈ 99.7 p.p.m. a random model would give an equal probability of a 2,3,6 trisubstituted residue having a 3' substituted residue adjacent to it and in this case the spectrum does indeed suggest two components of roughly equal intensity. We have previously noted the possibility of longer range effects influencing splitting patterns for the remaining component associated with unsubstituted and 6 mono-substituted residues and the probability that such residues are more

likely to be adjacent to residues which have no nitrate ester group at the C_3' position, (2,6 unsub or other mono substituted residues).

The foregoing analysis based on experimental data allows a rough model to be constructed of a likely structure for octad sequence of residues in a nitrocellulose of D.O.S. 1.9 prepared by nitration and this is indicated schematically in Figure 50. A similar analysis has been made of a sample corresponding to a higher D.O.S., (2.6), and the results are also displayed in Figure 50. The conclusions to be drawn from this is that far from being random the nitrate ester equilibrium favours short blocks of fully substituted rings with short blocks of lower D.O.S. residues. This is not unreasonable since it has been previously argued that the rate constants for nitrate ester formation at a given site in a glucose residue must increase as the D.O.S. increases in that residue. By the same token substitution in adjacent residues may well therefore increase the rate of nitration such that a block structure develops. In Chapter Four the partial D.O.S. for denitrated material was considered and the striking difference with respect to nitrated materials of the same D.O.S. (>2) is reflected in the absence of unsubstituted residues. For comparison purposes a sequence analysis has been carried out on 2.14 nitrated and 2.2 denitrated material and the most probable models are recorded in Figure 51. Despite the small difference in nitrogen content the most probable decads reveal considerable differences in sequence patterns for nitrated and denitrated materials along a given chain. This is reflected in a large difference, ($\simeq 0.35\text{Å}$), in the mean interchain spacing, (c.f. Figure 48), whereas similar analyses of sequence patterns

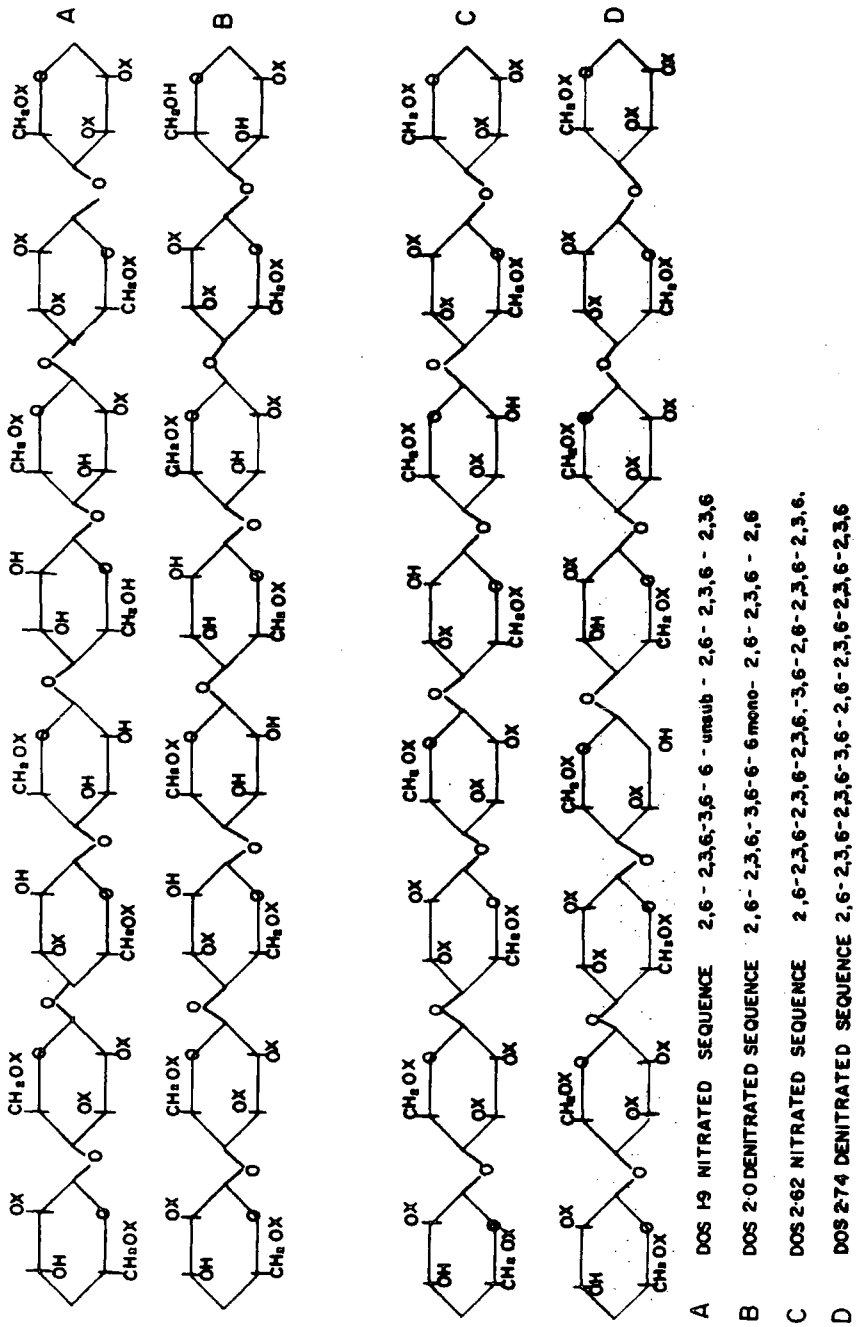

Fig. 50 Models of the most probable octad sequences in a chain of 1.9 and 2.6 D.O.S. nitrated and 2.0 and 2.7 D.O.S. denitrated materials

2,6 Mono Tri Tri 3,6 Unsub Unsub Mono 2,6 Tri

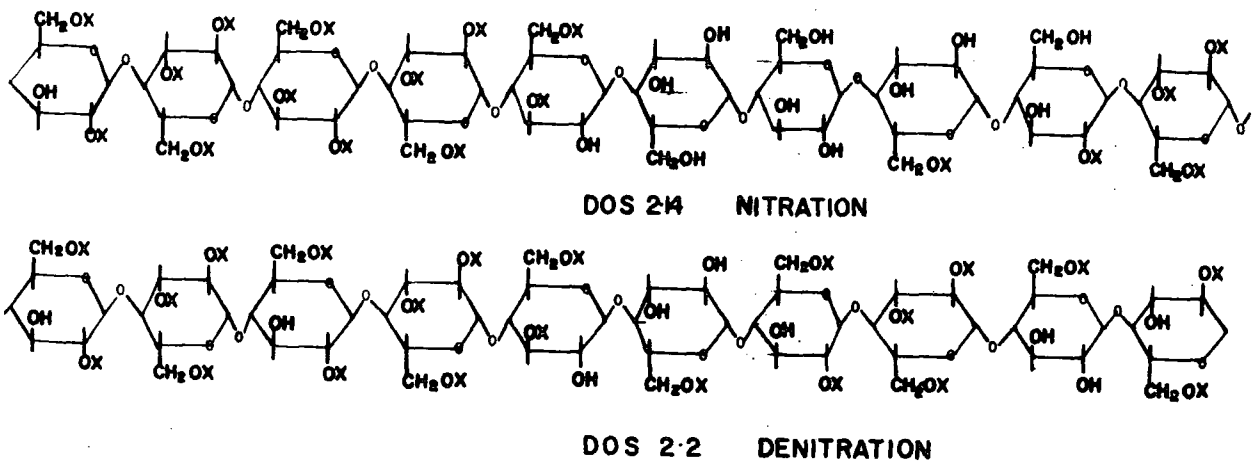

2,6 Tri 2,6 Tri 3,6 Mono 2,6 Tri Mono 2,6

Fig. 51 Models of most probable decads for 2.14 D.O.S. nitrated and 2.2 D.O.S. denitrated cellulose nitrates

drawn between materials of relatively high D.O.S.;((2,62) nitrated and (2.74) denitrated), and very low D.O.S.; ((1.9) nitrated and (2.0) denitrated), shown in Figure 50 where the difference in spacings is small (c.f. Figure 48), show strong similarities; the only changes being in the number of mono and unsubstituted residues present. To conclude this discussion on the sequence information it should be stressed that the models presented in Figures 50 and 51 are very much simplified and ideally require computer modelling similar to that presented by Atkins to determine nearest neighbour distances between chains, although it is clear that the large differences in sequence patterns between nitrated and denitrated

materials (Figure 51) must give rise to local differences in hydrogen bonding systems and indirectly to interchain spacings. The work considered here, however, has essentially dealt with nitration and denitration in different media. With respect to the important question of equilibria it would be extremely interesting to investigate materials prepared by nitration and denitration in the same medium.

Figure 52 shows the ^{13}C n.m.r. spectra of a cellulose nitrate prepared by nitration in 53.5% H_2SO_4, 20.8% HNO_3, 25.7% H_2O and denitration of a 2.8 D.O.S. material in the same mix. The striking feature of the spectra is that the final D.O.S. attained in this case is not the same for nitration and denitration. At first glance this may seem inconsistent with a pure equilibrium nitration reaction and may seem to support an accessibility argument (c.f. Chapter One). It is appropriate here therefore to review the data presented in this thesis with respect to this important question.

Clearly, the theory of accessibility, (see Chapter One), which argues for a rate controlled nitration where the final D.O.S. is dependent only on the relative accessibility of the cellulose is untenable. It is obvious, for example, that inaccessible regions in this argument should be totally unsubstituted since the nitrating acids cannot penetrate these regions and also that the degree of accessibility may be altered according to the swelling power of the nitrating acids (c.f. Chapter One). However the ^{13}C n.m.r. data discussed in Chapters Four, Six and Seven reveal that over a large D.O.S. range of denitrated materials and above a D.O.S. of ≈2.5 in nitrated materials no unsubstituted residues are

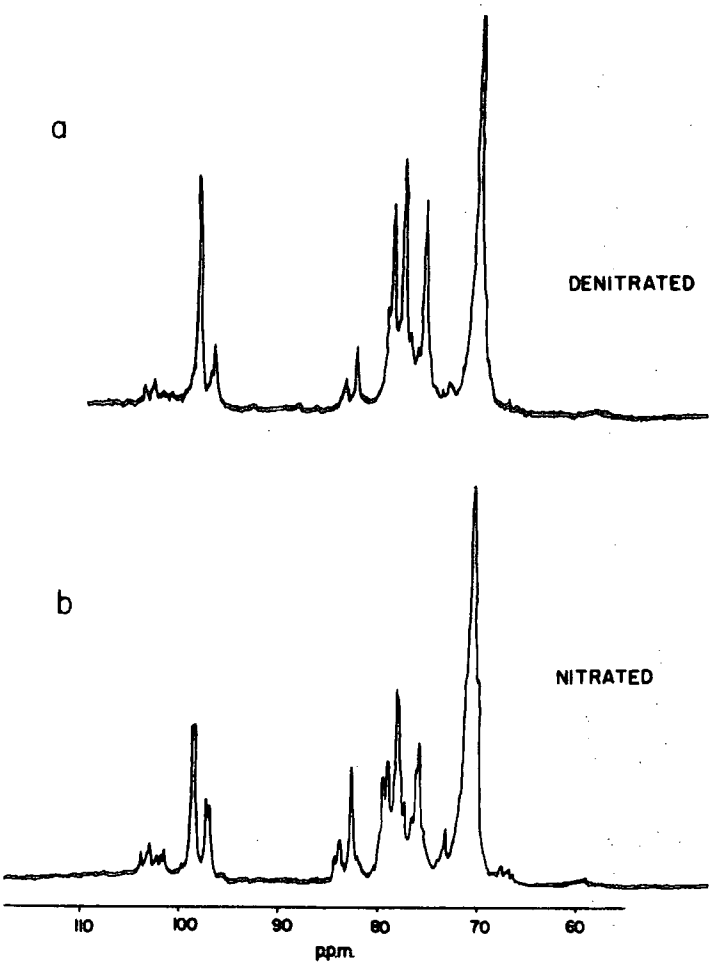

Fig. 52 ^{13}C n.m.r. (75.5 MHz, proton decoupled) spectra of cellulose nitrates prepared by (a) nitration and (b) denitration in the same mix.

present indicating that in all probability acids of some composition reach all parts of the fibre in a standard nitration time of two hours.

The E.S.C.A. data has also revealed that at the very surface of fibrils even in mixes where the sulphate ester effect, (c.f. Chapter Three), is negligible or absent, (nitric-phosphoric mixes) total substitution is not attained and the final D.O.S. at the surface is dependent on equilibria established at the surface the final position of equilibrium depending on the acid mix employed. If the top 20-50Å is to be considered totally accessible at least in comparison to the remaining several microns of a typical macroscopic fibre then the fact the reaction never goes to completion in the surface regions is impossible to explain on the basis of an extreme accessibility theory. In other reactions of cellulose, however, as has been shown in the oxidation experiments, (c.f. Chapter Three), the accessibility does play an important part.

Reference to Chapter Seven reveals also that the final D.O.S. seems unrelated to the swelling power of the reagent, (according to the Miles diagram),[41] in fact it is generally true that mixes which produce a highly swollen cellulose, nitrate to particularly low levels. Whereas according to an accessibility theory increased swelling should be related to increased D.O.S. Again we must assume that under all normal conditions of nitration the acid is able to rapidly penetrate all areas of the fibrils perhaps initially by passing through voids between fibrils reacting rapidly at the surface (within 1 sec.) and diffusing more slowly into the bulk of the fibrils.

However the other extreme of a pure equilibrium theory also has some anomalies for example one would expect in an equilibrium that a cellulose nitrated in a given mix should have the same D.O.S. as a high D.O.S. cellulose nitrate denitrated in the same mix. In one case ^{13}C n.m.r. data has shown that this is clearly not the case. Figure 52 shows such experiments and the difference in ^{13}C spectra for such material is clearly evident where the denitrated material has clearly the higher D.O.S. The explanation appears to lie in the data discussed in this chapter. It has been shown, for example. that the rate constants for nitration at a given site in a β-d-glucopyranose residue increase with the D.O.S. of the ring. Also the nitration of a given residue is dependent to a large extent on the D.O.S. of the adjacent residue and in particular on whether there is a nitrate group at the C_3' position in an adjacent ring.

Clearly, on a microscopic scale the equilibrium situation is rapidly established at individual sites along a chain but the many factors which determine the final D.O.S. on a macroscopic level are such that materials nitrated and denitrated in the same mix need not have the same D.O.S. Indeed as has already been demonstrated in this chapter nitration and denitration at a given residue will proceed according to the influence of its immediate neighbour giving rise to differences in sequence distribution and ultimately to a difference in average D.O.S. It is worth pointing out that a similar experiment carried out at high D.O.S. revealed no difference in D.O.S. between materials nitrated and denitrated in the same mix. This is consistent with the theory presented here and inconsistent with an accessibility argument which would suggest a similar difference in D.O.S.

CHAPTER SEVEN

BIREFRINGENCE AS AN ANALYTICAL TOOL FOR ESTIMATION OF DEGREE OF SUBSTITUTION IN CELLULOSE NITRATES

7.1 Introduction

The birefringence of cellulose and cellulose nitrates has been the subject of intense investigation almost since the development of this classical technique.[41,201] It has long been known, for example, that cellulose itself is positively birefringent, (in other words the refractive index for light vibrating parallel to the length of the axis of the fibre, ($n_{\parallel}$), is greater than the refractive index for light vibrating perpendicular to this axis, ($n_{\perp}$)).[201] Upon nitration however there is a gradual change and the fibres become negatively birefringent presumably due to a large increase in the number of the highly polarisable nitrate groups contributing to $n_{\perp}$ (c.f. Chapter Two and reference 187 for explanation of the phenomena in terms of electric vectors). Miles[41] has adequately reviewed the literature on the study of birefringence in cellulose nitrates up to 1955 and it is clear that the work up to and including this period was essentially qualitative with the emphasis being placed upon determination of polarisation colours of fibres between crossed nicols rather than on direct determination of path difference using optical accessories, (i.e. compensators). Table 7.1, for example, gives the expected polarisation colours for a range of nitrocelluloses as a function of nitrogen content as reported by Kohlbeck.[217]

A full understanding of the origin of such colours in fibrous materials requires a detailed knowledge of the complex optics involved, (c.f. Chapter Two), but it is sufficient to note that the path difference τ of the ordinary and extraordinary rays in the analyser of the microscope which indirectly gives rise to such colours is given by:

Table 7.1

Polarization colour	Order	%N
Grey white	1st	11.0
White	1st	11.5
Yellow white	1st	11.7
Yellow	1st	12.0
Orange	1st	12.2
Red orange	1st	12.3
Red	1st	12.4
Violet	2nd	12.5
Blue	2nd	12.6
Blue white	2nd	12.8
Pale grey	1st	13.1
Grey	1st	13.2
White	1st	13.4
Intense white	1st	13.5

$$\tau = d(n_{11} - n_1) \qquad (7.1)$$

where d is the thickness of the fibre and $(n_{11}-n_1)$ is the effective birefringence. The measurement of path difference is possible using various compensation techniques (c.f. Chapter Two), (the choice of compensator depending upon the fraction of a wavelength path differences to be measured), but the direct determination of birefringence of individual fibres has not been considered feasible due to difficulties in measuring the width of the fibre in the direction of the light. Lewis,[218] however, has recently suggested a method for such a determination of fibre thickness which depdnds upon the measurement of the temperature coefficient of path

difference by a hot stage microscope method. The method however is tedious and not well characterised. Perhaps the best way of representing path difference data for a given batch of cellulose nitrate fibres is in the form of block histograms of the distribution of path difference as reported originally by Lewis.[214] The data reproduced in Figure 53 shows such data as a function of D.O.S. for cellulose nitrates prepared by the mechanical and displacement processes.

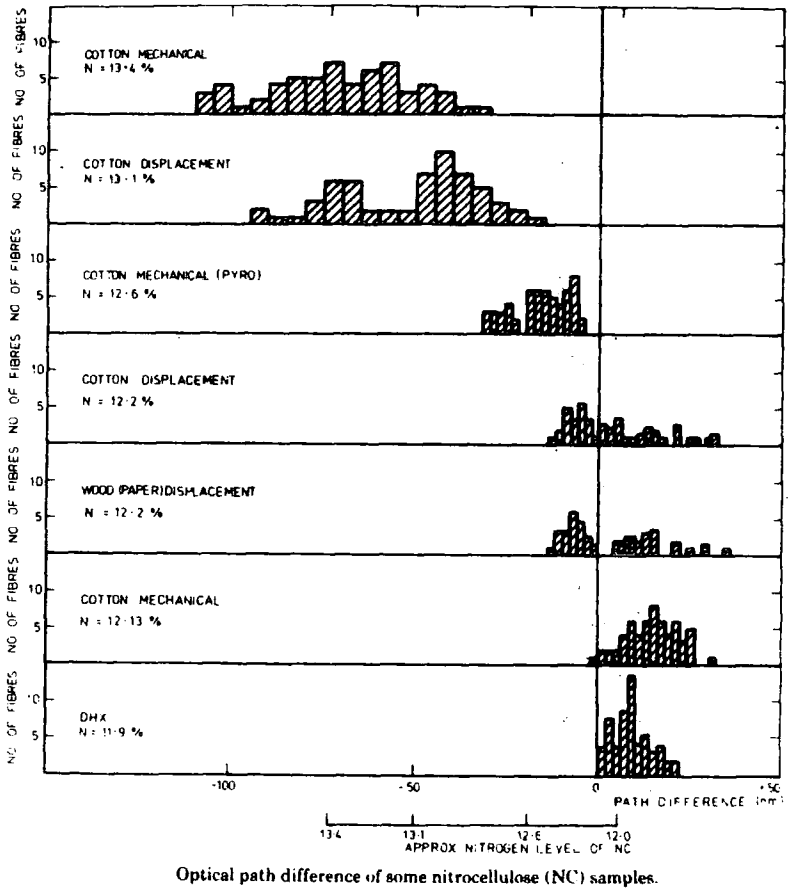

Optical path difference of some nitrocellulose (NC) samples.

Fig. 53 Block histograms of the path difference distributions for a series of cellulose nitrates (reproduced from reference 214)

The broad distribution is primarily due to the known distribution of fibre thicknesses within a given batch of cotton linters but by calibrating against known D.O.S. material and dividing through by an average value for fibre thickness, an estimation of D.O.S. can be made.[214]

How such measurements are dependent on the crystallinity of the original cellulose is a matter of great interest to cellulose chemistry since for semicrystalline polymers the birefringence is given as

$$\Delta n = Xc\ \Delta nc + (1 - Xc)\ \Delta na + \Delta nf \qquad (7.2)$$

where Xc is the degree of crystallinity determined by X-ray diffraction data; Δnc is the crystalline phase birefringence; ΔNa is the amorphous phase birefringence and Δnf is a part of the birefringence which arises from the distortion of the electric field of the light wave at the phase boundaries.[217] The value of Δnf is generally small and sometimes considered negligible although the Becke line method[200] used by Meredith[188] in the work, reported in Chapter Two, measures similar properties of the fibre. In the work of Meredith[188] and that discussed in Hartshone and Stuart[201] the spiral angle of the fibre is said to influence the birefringence (c.f. Chapter Two).

The correlation of molecular orientation with birefringence data however requires an understanding of the origin of inherent molecular anisotropy. As early as 1924 Bragg[216] showed that the birefringence of calcite and aragonite could be calculated using classical formulae for dipole-dipole interaction. Such calculations have not been reported for cellulose nitrates although they are particularly suitable for such studies. The highly polarisable nitrate group, for example, can be substituted in a controlled manner by a suitable choice of acid mix, (c.f. Figure 3). The x, y, z coordinates of the nitrate groups around a residue have been established by Atkins,[56] (c.f. Chapter One), and the distribution of nitrate groups around the residue for a

given D.O.S. have been determined in Chapter Four. Lewis[218] has recently attempted such calculations using the ^{13}C n.m.r. data reported in this thesis. Since these calculations are of relevance to the work described in this chapter they will be discussed in some detail here.

The polarisability of an atom in the presence of a polarisable neighbour is given by

$$\alpha^1 = \alpha/(1 - \sum \alpha'') \qquad (7.3)$$

where α is the polarisability of the same atom for random arrangement by neighbours; α'' is the polarisability of the influencing neighbour and is given by

$$\beta = 3x^2 - r^2/r^5 \qquad (7.4)$$

where r is the distance between the dipoles and x is the component of this distance in the direction of the electric vector.

Thus to obtain the polarisability of, for instance, a particular oxygen atom in the presence of polarisable neighbours a value of β is calculated for each neighbouring atom from equation 7.4.

The refractive index n corresponding to the particular direction of the electric vector is then obtained from the Lorentz-Lorentz equation

$$(n_2-1/(n^2 + 2) = (D/M) \sum ai\ Ri \qquad (7.5)$$

where ai is the number of atoms or ions of refractivity Ri which is itself given by

$$Ri = 4\pi N\alpha^1/3$$

N being Avogadros number. D the crystal density and M the molecular weight. The steps then of the calculation

are as follows:

(1) The total refractivity of the nitric ester group is calculated from the refractive indices and the densities of nitroglycerin nitrocellulose and diethylene glycol dinitrate. The value of Rm the molecular refractivity can be calculated from equation 7.5. These molecular refractivities may be split into their component atomic refractivities, thus,

$$RNG = 3RC + 5RH + 3RNO_3 \text{ etc.}$$

(2) The total molecular refractivity can be calculated and estimations made of the atomic refractivities.

(3) Values of β, (equation 7.4), for the three coordinate directions for all the oxygen-oxygen interactions affecting the refractivity of the nitric ester group in the (2) (3) and (6) positions can thus be calculated and used to estimate the refractivity in 3 directions of each individual oxygen atom.

The total refractivity of the nitric ester groups in (a) the average x/y direction and (b) the z direction calculated by Lewis are shown in Table 7.2.

Table 7.2

The Refractivities of the Nitrate Ester Groups

		x/y	z
$NO_3(2)$		8.81	9.92
$NO_3(3)$		10.48	7.85
$NO_3(6)$	gg	8.91	9.99
$NO_3(6)$	gt	10.87	7.75
$NO_3(6)$	tg	10.85	7.78

Lewis[218] has continued by calculating the effect of degree of substitution on total birefringence using the data in Chapter Four: for a full account of these calculations the reader is referred to the original paper[218] but for the purposes of this chapter it is sufficient to consider Table 7.2 only, which shows the refractivities of the nitrate groups in the x/y and z directions, from which it is immediately clear that it is only the (3), 6(gt) or 6(tg) which can contribute to the observed negative birefringence of the cellulose nitrate fibre. The important conclusion to be drawn is that the 6(gg) conformer of the primary nitrate group (c.f. Chapter One), (Figure 4), previously thought to be a possible orientation of the group is ruled out by birefringence data.

As can be seen however the calculations rely upon many assumptions which are described succinctly by Lewis.[218] The most important assumptions are perhaps that the oxygen atoms on one ring do not interact with those in a neighbouring ring and that substitution at a given site does not alter the orientation of neighbouring nitrate groups.

Reference to the literature reveals, for instance, that the nearest interchain and interatomic distances in cellulose trinitrate may occur between the primary nitrate group and the 3 nitrate group in adjoining rings or in rings of a parallel chain.[218] (Also using glycerol and its nitrated derivatives as model systems unpublished M.N.D.O. L.C.A.O. S.C.F., full optimisation calculations[221] carried out in this laboratory have indicated that substitution of a nitrate group at the C_2 position in

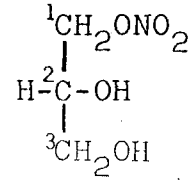

alters the orientation of the nitrate group already present although there is little evidence in the literature to substantiate this.

Clearly there is a need for independent experimental verification of the calculated results since the conclusion that the 6(gg) conformer does not occur is of some importance to cellulose chemistry. Lewis[218] himself has offered some experimental support for calculated birefringences for a range of cellulose nitrates of D.O.S. 2.37-2.62 but there is some doubt (c.f. Chapter Two) as to whether the method is reliable across a range of D.O.S. and between individual batches of fibres of different sources. In this chapter therefore a series of cellulose nitrates which were well characterised by many of the methods outlined in this thesis were analysed at the M.O.D. Waltham Abbey, and the accuracy of the degree of substitution estimation assessed.

7.2 Experimental

The cellulose nitrates used in this work were nitrated in linters form by the Mitchell method.[207] Stabilisation was carried out by the procedures outlined in Chapter Three but the drying procedures were adapted to avoid hot oven drying. Samples were initially air dried, then vacuum dried at 30°C for several hours before storage over P_2O_5 for 24 hours. (It is hoped that this mild procedure tends to preserve the lumen).

The dried fibres were immersed in glycerol on glass slides and cover slips sealed with Canada Balsam.

The higher D.O.S. materials prepared in this work were analysed using a Berek compensator, Model No. 1740, inserted

into a Swift polarising microscope. All samples were also analysed at the M.O.D. Waltham Abbey using a rotary mica compensator and for low D.O.S. materials an elliptical compensator was employed (c.f. Chapter Two). Distributors of path differences were plotted and estimations of the D.O.S. made using the method of Lewis.[214]

The ^{13}C n.m.r. distribution data, X-ray diffraction '101' spacings and E.S.C.A. D.O.S. were determined by methods reported in previous chapters. The Kjeldahl nitrogen determinations were carried out by methods described in the Appendix.

7.3 Results and Discussion

The distribution of path differences for three high D.O.S. cellulose nitrates, (determined using a Berek compensator). are shown as block histograms in Figure 54. The number of fibres analysed and the actual degree of substitution of the samples is also given. Reference to the data reproduced in Figure 53 reveals a comparable distribution range to that reported by Lewis[214] and tolerable agreement with the predicted D.O.S. At low D.O.S., however, the Berek compensator is inaccurate and no distribution data was recorded in this range in this laboratory. All samples however were analysed at the M.O.D. Waltham Abbey and the estimated D.O.S. of the samples as measured from path difference data is recorded in Table 7.3 for comparison with the well characterised cellulose nitrates prepared in this laboratory.

Before considering the accuracy of these determinations it is worth discussing Table 7.3 in some detail.

TABLE 7.3

Sample	Kjeldahl	E.S.C.A.	N.M.R.	Bire-fringence	'd' spacing	N.M.R. Distribution					Approximate Acid Mix Composition			HISTORY OF SAMPLE
						TRI	2,6	3,6	MONO	UNSUB	H_2SO_4	HNO_3	H_2O	
1	11.1(2.0)	2.1	1.90	12.1(2.3)	6.81	38	19	14	12	18	53.5	20.8	25.7^{s}	Nitrated cellulose
2	10.6(1.8)	1.8	1.90	11.5(2.1)	6.66	36	23	14	10	17	52.6	20.7	26.7^{s}	Nitrated cellulose
3	12.3(2.3)		2.14	-	6.73	53	17	8	6	16	70.3	20.7	9.0	Nitrated cellulose
4	12.2(2.3)	2.3	-	12.57(2.5)	-	-	-	-	-	-	-	-	-	Nitrated cellulose supplied by M.O.D.
5	12.0(2.3)	2.1	2.1	12.61(2.4)	6.61	50	18	10	5	17	70	15	15	Nitrated cellulose
6*	9.2(1.5)	1.0	1.5	11.68(2.1)	cellu-losic	18	12	32	13	25	70	11	19	Nitrated cellulose
7	12.2(2.3)	2.6	2.5	13.08(2.6)	6.92	68	14	9	4	5	60	20	20	Nitrated cellulose
8	-	2.2	2.65	13.2(2.6)	-	67	20	11	2	0	58	20	22^{s}	Nitrated cellulose
9	13.3(2.6)	2.6	2.62	13.15(2.6)	7.1	62	25	13	0	0	75	22	3	Nitrated cellulose
10*	13.3(2.6)	2.0	2.61†	12.92(2.5)	6.61	71	13	8	6	2	75	21	4	High D.O.S.(2.7) NC Denitrated in this mix
11*	13.3(2.6)	2.0	2.53†	13.19(2.6)	7.08	65	16	11	4	4	75	21	4	Nitrated cellulose
12	13.2(2.6)	2.6	2.67†	13.6(2.7)	7.13	71	16	9	4	0	60	25	15	Nitrated cellulose
13*	-	1.9	2.62†	13.02(2.6)	6.71	69	17	9	3	2	-	-	-	Denitration of Sample 12
14	-	-	2.14	12.51(2.4)	6.61	46	16	14	18	8	53.5	20.8	25.7^{s}	Nitrated cellulose
15	-	-	2.64	13.0(2.6)	6.7	67	18	12	3	1	53.5	20.8	25.7^{s}	Denitration of Sample 16 in this mix
16	13.7(2.8)	2.8	2.83	13.7(2.8)	7.3	83	11	6	0	0	26 H_3PO_4	64	10 P_2O_5	Nitric/Phosphoric acid nitration

*, s, ÷ (see text)

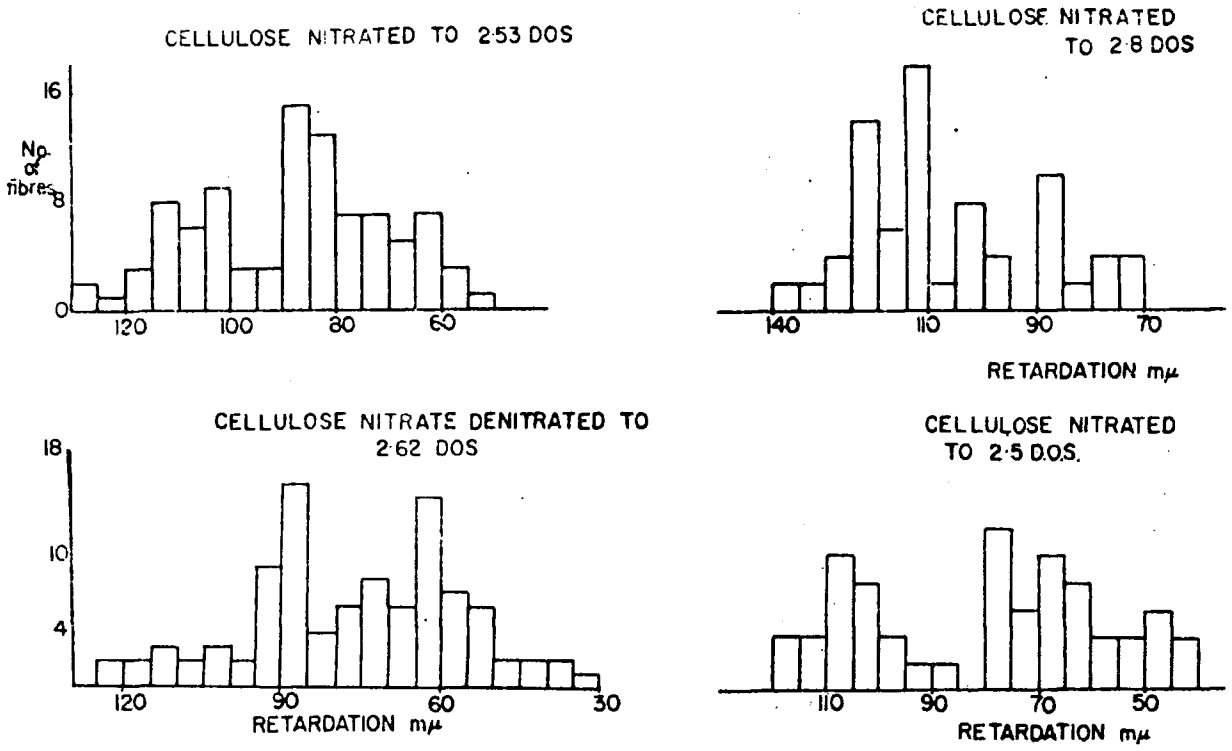

Fig. 54 Block histograms of the path difference distributions of some cellulose nitrates (measured by Berek compensator)

The Kjeldahl results are recorded as % Nitrogen with the approximate D.O.S. reported in brackets alongside. The E.S.C.A. data for each sample is also listed although the 'sulphate ester effect' referred to in Chapter Three clearly alters the surface D.O.S. In cases where this effect is particularly pronounced the sample number is marked with an asterisk.

The acid mix composition used to nitrate the sample is also shown and it is of interest to compare the actual D.O.S. of the sample with that predicted by the Miles diagram (c.f. Figure 3).

The acid mix composition was not precisely measured (i.e. by nitrometer), but the approximate composition was based on the careful mixing of acids, (sometimes using 1-1 acids to prevent excessive heating on mixing). Where the Miles diagram does not agree with the D.O.S. attained this could be either due to inaccuracy of the composition or inaccuracy of the diagram. Those mixes which lie within the swelling regions of the Miles diagram (Figure 3) are marked with an 'S'.

The ^{13}C n.m.r. data is given as total D.O.S. and as percentage components of tri, di, mono and unsubstituted residues. It should be noted that those samples marked with a (†) were run on a 90 MHz n.m.r. spectrometer housed at Waltham Abbey and the final distribution data may be less accurate due to the poorly resolved spectra obtained. It can readily be seen however that, in general, the Kjeldahl determinations are in good agreement with the n.m.r. results. In cases where this is not so it is thought that this is probably due to incomplete digestion, (c.f. Appendix), in the Kjeldahl determination due to the incorrect choice of digestion method.

Turning now to the birefringence data recorded in Table 7.3 as % nitrogen, (with approximate D.O.S. in brackets alongside), it is clear from the graph in Figure 55, which shows the actual D.O.S. of the sample against that estimated from the birefringence), that in the high D.O.S. range the correlation is very good indeed. At low D.O.S. however the nitrogen content is grossly overestimated and although this may be due to inaccurate calibration at low D.O.S. it may be that in regions close to the neutral point where the value

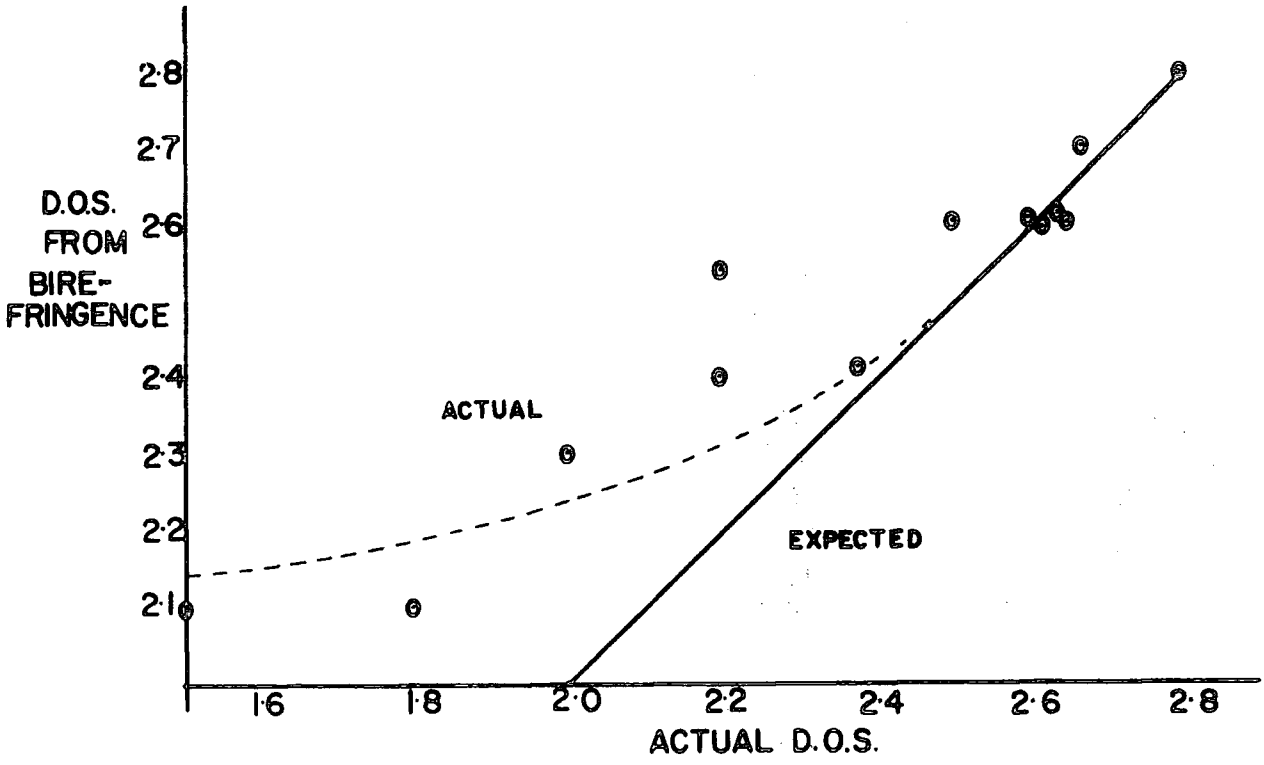

Fig. 55 Graph of the D.O.S. of cellulose nitrates estimated by a birefringence technique against the known D.O.S.

of ($n_{11} - n_{\perp}$) is very small factors such as the form of the fibre,[201] (discussed in Chapter Two), may become important.

It is evident, however, that birefringence measurements on fibres of high D.O.S., (2.4-2.8), are particularly useful for D.O.S. estimations and represent a reliable alternative to the time consuming Kjeldahl analysis. This work also supports the experimental data presented by Lewis[218] in verification of his calculated values.

It would be interesting to compare birefringence data for materials of the same D.O.S. but differing in distribution of nitrate groups (e.g. nitrated and denitrated samples used

in the work presented in Chapter Four) since reference to Table 7.2 indicates they should differ in birefringence. At the time of writing, however, this work has not yet been completed.

APPENDIX ONE

A.1 Kjeldahl Analysis for Nitrogen[211,212]

The Kjeldahl nitrogen determinations reported in this thesis were carried out according to a procedure developed at P.E.R.M.E., Waltham Abbey. As in all distillation methods the sample is first digested in alkaline or acid conditions to yield inorganic nitrates. This is then made alkaline, if necessary, and Devardas Alloy is added to reduce the nitrate to nitrite and finally ammonia which is distilled into Boric acid solution for titration with standard acid, (0.1 N HCl). The digestion stage is extremely important especially in the analysis if nitrocelluloses since some samples, (>12.7% N), may not be fully digested by standard alkaline methods. Hence two procedures designated A and B are adopted, depending on the estimated nitrogen content of the nitrocellulose. These methods are fully described below.

A.2 Method A. Alkaline Digestion for Samples less than 12.7% N

50-120mg of NC were weighed into a glass ampoule and then deposited into the base of a semi-micro flask. The ampoule was broken and 2.0mls of H_2O, 0.1mls of 30% H_2O_2 and 8mls of 20% NaOH were then added. The flask was then heated to $\approx 100^{\circ}C$ and maintained at this temperature for about 20 mins. to dissolve the sample. 20mls of water were then added and the solution was heated to $100^{\circ}C$ again to destroy the remaining hydrogen peroxide. After the mixture had cooled to $\approx 30^{\circ}C$. 1.00 ± 0.01 gms of Devardas Alloy, (weighed into a glass ampoule), were deposited into the flask. The steam inlet tube was attached to the neck of the flask, (as shown in the diagram), and the condenser outlet tube was allowed to dip

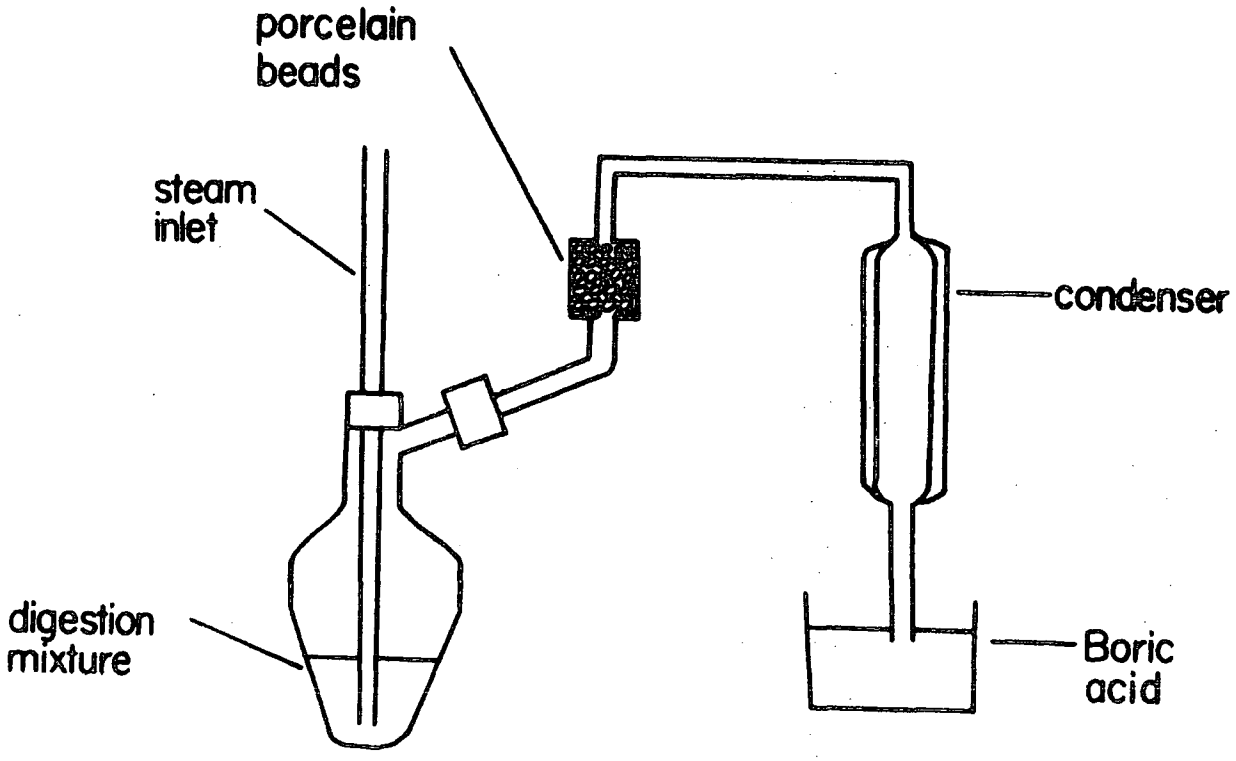

Fig. 56 Apparatus used in the Kjeldahl determination

≈10mm below the surface of the boric acid in the receiver flask. (25 mls of 4% Boric Acid). The heating of the flask was controlled to prevent excessive foaming (although it is possible to add an antifoaming agent before heating). The ammonia liberated was steam distilled over with ≈ 50 mls of H_2O and then titrated, (using bromocresol green as indicator) with 0.1 N HCl. The volume of solution in the flask should remain constant during the distillation.

A.3 Method B. Samples over 12.7% N Acid Digestion

50-120mg of NC were weighed into the reaction flask and cooled in an ice-water bath. 2 mls. of concentrated H_2SO_4 were added dropwise to the flask and left to dissolve the sample for 30-60 minutes. The solution was then carefully diluted by adding 10g of crushed ice and 15-17 mls of 30% NaOH. Continue as in A.

Since Devardas Alloy has its own nitrogen content it is necessary to carry out a blank determination using all reagents except the NC for each determination. The method is generally calibrated using Potassium Nitrate. The nitrogen content using this procedure is generally quoted to two decimal places although the choice of the wrong digestion method can give inaccurate results.

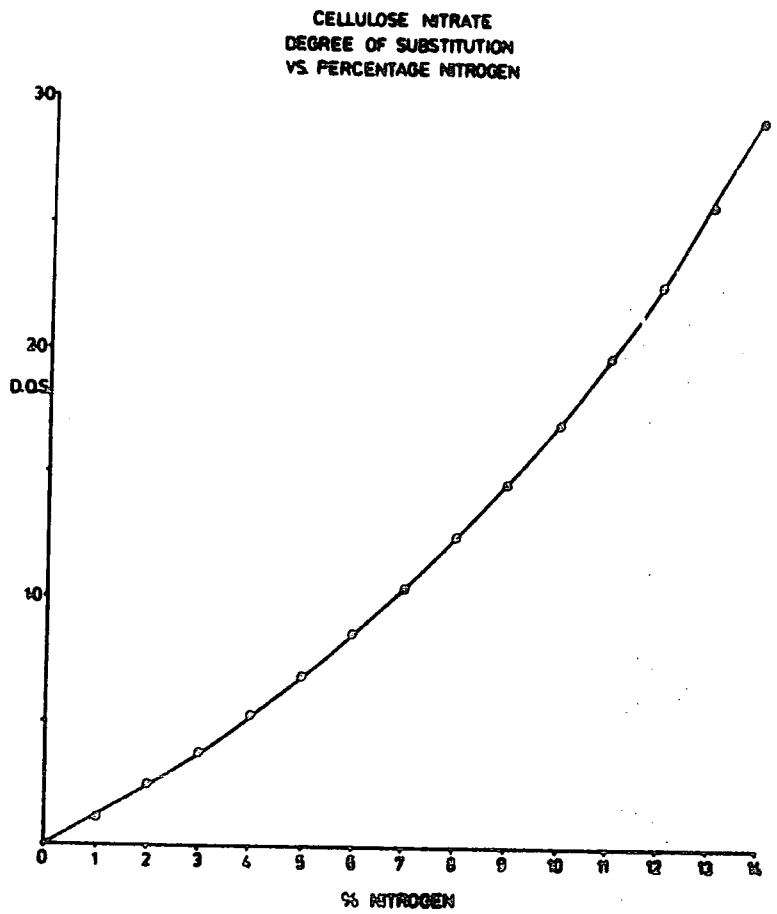

Figure 57 Graph of percentage nitrogen against degree of substitution

APPENDIX TWO

LECTURES AND SEMINARS ATTENDED DURING THE PERIOD 1978-81

15 September 1978

Professor W. Siebert (University of Marburg, West Germany), "Boron Heterocycles as Ligands in Transition Metal Chemistry".

22 September 1978

Professor T. Fehlner (University of Notre Dame, U.S.A.), "Ferraboranes: Syntheses and Photochemistry".

12 December 1978

Professor C.J.M. Stirling (University of Bangor), 'Parting is Such Sweet Sorrow' - the Leaving Group in Organic Reactions.

14 February 1979

Professor B. Dunnell (University of British Columbia) "The Application of N.M.R. to the Study of Motions in Molecules".

16 February 1979

Dr. J. Tomkinson (Institute of Laue-Langevin, Grenoble), "Properties of Adsorbed Species".

4 March 1979

Dr. J.C. Walton (University of St. Andrews), "Pentadienyl Radicals".

20 March 1979

Dr. A. Reiser (Kodak Ltd.), "Polymer Photography and Mechanism of Cross-Link Formation in Solid Polymer".

25 March 1979

Dr. S. Larsson (University of Uppsala), "Some Aspects of Photoionisation Phenomena in Inorganic Systems".

25 April 1979

Dr. C.R. Patrick (University of Birmingham), "Chlorofluorocarbons and Stratospheric Ozone: An Appraisal of the Environmental Problem".

1 May 1979

Dr. G. Wyman (European Research Office. U.S. Army). "Excited State Chemistry in Indigoid Dyes".

2 May 1979

Dr. J.D. Hobson (University of Birmingham), "Nitrogen-centred Reactive Intermediates".

8 May 1979

Professor A. Schmidpeter (Institute of Inorganic Chemistry, University of Munich), "Five-membered Phosphorus Heterocycles Containing Dicoordinate Phosphorus".

9 May 1979

Dr. A.J. Kirby (University of Cambridge), "Structure and Reactivity in Intramolecular and Enzymic Catalysis".

9 May 1979

Professor G. Maier (Lahn-Giessen), "Tetra-tert-butyltetrahedrane".

10 May 1979

Professor G. Allen, F.R.S. (Science Research Council), "Neutron Scattering Studies of Polymers".

16 May 1979

Dr. J.F. Nixon (University of Sussex), "Spectroscopic Studies on Phosphines and their Coordination Complexes".

23 May 1979

Dr. B. Wakefield (University of Salford), "Electron Transfer in Reactions of Metals and Organometallic Compounds with Polychloropyridine Derivatives".

13 June 1979

Dr. G. Heath (University of Edinburgh) "Putting electrochemistry into Mothballs - (Redox Processes of metal Porphyrins and Phthalocynanines".

14 June 1979

Professor I. Ugi (University of Munich), "Synthetic Uses of Super Nucleophiles".

20 June 1979

Professor J.D. Corbett (Iowa State University, Ames, Iowa, U.S.A.). "Zintl Ions: Synthesis and Structure of Homo-polyatomic Anions of the Post-Transition Elements".

27 June 1979

Dr. H. Fuess (University of Frankfurt), "Study of Electron Distribution in Crystalline Solids by X-ray and Neutron Diffraction".

21 November 1979

Dr. J. Muller (University of Bergen), "Photochemical Reactions of Ammonia".

28 November 1979

Dr. B. Cox (University of Stirling), "Macrobicyclic Cryptate Complexes, Dynamics and Selectivity".

5 December 1979

Dr. G.C. Eastmond (University of Liverpool). "Synthesis and Properties of Some Multicomponent Polymers".

12 December 1979

Dr. C.I. Ratcliffe (University of London), "Rotor Motions in Solids".

19 December 1979

Dr. K.E. Newman (University of Lausanne), "High Pressure Multinuclear NMR in the Elucidation of the Mechanisms of Fast, Simple Inorganic Reactions".

30 January 1980

Dr. M.J. Barrow (University of Edinburgh) "The Structures of some Simple Inorganic Compounds of Silicon and Germanium - Pointers to Structural Trends in Group IV".

6 February 1980

Dr. J.M.E. Quirke (University of Durham), "Degradation of Chlorophyll-a in Sediments".

23 April 1980

B. Grierson B.Sc., (University of Durham), "Halogen Radiopharmaceuticals".

14 May 1980

Dr. R. Hutton (Waters Associates, U.S.A.), "Recent Developments in Multi-milligram and Multi- gram Scale Preparative High Performance Liquid Chromatography".

21 May 1980

Dr. T.W. Bentley (University of Swansea), "Medium and Structural Effects in Solvolytic Reactions".

7 October 1980

Professor T. Tehlner, "Metalloboranes Cages or Coordination Compounds?"

16 October 1980

Dr. D. Maas (Salford University) "Reactions a Go-Go".

30 October 1980

Professor N. Gassie, (Glasgow University), "Inflammability Hazards in Commercial Polymers".

6 November 1980

Professor A.G. Sykes (Newcastle University), "Metalloproteins: An Inorganic Chemists Approach".

12 November 1980

Dr. M. Gerloch (University of Cambridge), "Magnetochemistry is about Chemistry".

13 November 1980

Professor N.N. Greenwood (Leeds University). "Metallborane Chemistry".

19 November 1980

Dr. T. Gilchrist (University of Liverpool) "Nitrosoolefins as Synthetic Intermediates".

4 December 1980

Reverend R. Lancaster "Fireworks".

18 December 1980

Dr. R. Evans (University of Brisbane. Australia). "Some Recent Communications to the Editor of the Australian Journal of Failed Chemistry".

22 January 1981

Professor E. Dawes (Hull University), "Magic and Mystery through the Ages".

29 January 1981

Mr. H. Maclean, (I.C.I. Ltd.), "Managing in the Chemical Industry in the 1980's".

5 February 1981

Professor F. Stone (Bristol University), "Chemistry of Carbon to Metal Triple Bonds".

18 February 1981

Professor S. Kettle (University of East Anglia) , "Variations in the Molecular Dance at the Crystal Ball".

25 February 1981

Dr. K. Bowden (University of Essex), "The Transmission of Polar Effects of Substituents".

11 March 1981

Dr. J.F. Stoddart (I.C.I. Ltd.), "Stereochemical Principles in the Design and Function of Synthetic Molecular Receptors".

17 March 1981

Professor W. Jencks (Brandeis University, Massachusetts), "When is an Intermediate not an Intermediate?".

7 May 1981

Professor M. Gordon (Essex University), "Do Scientists Have to Count?".

10 June 1981

Dr. J. Rose (I.C.I. Plastics), New Engineering Plastics.

CONFERENCES ATTENDED DURING THE PERIOD 1978-1981

1. Quantitative Surface Analysis Conference at the National Physical Laboratory, October 1979.

2. Royal Institute of Chemistry/Chemical Society Annual Congress, Durham, April 1980.

3.* Nitrocellulose and Double Based Propellants Conference, Waltham Abbey, Essex, 1980.

4. Polymer Characterisation Symposia, Durham, July 1981.

* Paper presented 1980.

REFERENCES

1. Hon, N.S. J.Polym.Sci (Polym.Chem.Ed.) 1976, 14, 2497
2. Schonbein, C.F. History of Explosives 2nd.Ed.London 1917
3. Warwicker J. and Jeffries R., Shirley Pamphlet No. 93, 1966, Shirley Institute, Manchester.
4. Whistler, R. National Bureau of Standards Paper RP 1299 Vol. 24, 1940.
5. Roelofsen T., Biochim Acta 1954, 13, 155.
6. Tripp V. Text Res.J., 1954, 24, 956.
7. Sisson W.A. Contr.Boyce Thompson Inst. 1937. 9, 239.
8. Sisson W.A., Contr.Boyce Thompson Inst., 1937, 9, 389.
9. Ruska H., Kolloid Z. 1940, 92, 276.
10. Ruska H. Kolloid Z 1940 93, 163.
11. Hess K. Melliand Textilfiber 1943, 24, 289.
12. Hess K., Kiessig H. and Gundermann J. Z.Phys.Chem. 1941, B49, 64.
13. Preston R.D. Discuss,Faraday Soc. 1951, 11, 165.
14. Preston R.D. Molecular Architecture of Plant Cell Walls, Chapman and Hall, London 1952.
15. Hodge A. and Wardrop A., Nature, 1950, 165, 272.
16. Vögel A. Makromol.Chem., 1953, 11, 111.
17. Frey Wyssling A. Makromol.Chem. 1951, 6, 7.
18. Muhlethaer K. Papier Darmstadt 1963, 17, 546.
19. Das D., Mitra M. and Wareham J.F. Nature 1954, 174, 1058.
20. Kratky O. and Sembach H. Angew Chemie 1955, 67, 603.
21. Nägeli C. Die Stärkekorner Publ.Schultess K. Zurich, 1858.

22. Herzog R.O., Janke W., Z.Physik, 1920, 3 196.

23. Meyer K. and Misch L. Helv.Chim.Acta. 1937, 20, 232.

24. Freudenberg K. J.Chem.Educ.1932, 9, 1171.

25. Bergmann M. Ber. 1930, 63, 316 and 2304.

26. Staudinger H., Mohr R., Ber, 1937, 70, 2296.

27. Grälen N., T.Svedberg Nature 1943, 152, 625.

28. Kate, J.R. Trans.Faraday Soc. 1933, 29, 279.

29. Frey Wyssling R. Protoplasma 1937, 25, 261.

30. Mann J., Meths of Carb.Chem. 1963 3, 114.

31. Conrad C.C. Scroggie A.G. Ind.Eng.Chem.1945, 37 592.

32. Tarkow H., Stamm J., J.Phys.Chem. 1955, 56, 262.

33. Atalla R.H., Gast J.C., Macromolecules, 1980, 7.

34. c.f. Shafizadeh, F. Adv.Carb.Chem. 1971, 26, 297.

35. Muhlethaer K. Z.Schweiz Forstv. 1960, 30, 55.

36. Manley R.S.J., Nature, 1964, 204, 1155.

37. Frey Wyssling A., Protoplasma, 1937, 27, 372.

38. Bracconot H. Annl.Chim.Phys., 1819, 12, 185.

39. Knecht E. J.Soc.Dyers Col. 1896, 12, 89.

40. Hausermann C. Z.Angew Chem. 1910, 23, 1761.

41. Miles F.D., Cellulose Nitrate Publ.Interscience London 1953.

42. Bikales N.S., Segal, Cellulose and Cellulose Derivatives, High Polymers, Part V, Publ.Interscience, New York, 1972.

43. Clibbens D.A., Ridge, B.P., J.Textile Inst.1927, 18, 135.

44. Nevell T.P. in 'Methods of Carbohydrate Chem.', Vol.III Ed.Whistler R.L. London,1963.

45. Allen T.C., J.Polym.Sci., Macro Reviews, 1973, 7, 184-262.

46. Wilson, Mandell. Tappi, 1961 44(2) 131-137.

47. Davidson T., J.Text.Inst. 1955, 46, 407.

48. Putnam, Tappi 1964, 47(9), 549.

49. Sookne A. Harris, Am.Dyestuff Reptr. 1941, 30, 107.

50. Davidova, Rachinskii, Russ.Chem.Rev. 1965, 34(2), 104.

51. Guthrie, Bullock, Ind.Eng.Chem. 1960, 52(11), 935.

52. Head, F.S. J.Text.Inst. 1955, 46. 400 and 584.

53. Davidson, J.Text.Inst. 1948, 39, 65-86.

54. Heyes, T.F. J.Soc.Chem.Ind. 1928, 47, 90T.

55. Schweizer, J. J.Prakt.Chem. 1857, 72, 109.

56. Atkins, E.D.T., Polymer, 1979, 20, 145.

57. Fowler, J.R., Unruh C.C., J.A.C.S. 1947, 69, 1636.

58. c.f. Bikales, N.S., Segal, L., Cellulose and Cellulose Derivatives, High Polymers, Part V, Publ.Interscience,1972.

59. Jayme, G. Neuschaffer T. Naturwissenschaften. 1957,62, 44.

60. Jayme G., Papier, 1951, 5. 244.

61. Jayme G., Verburg W., Reyon Zellwolle Chemiefasern 1954, 32, 143 and 275.

62. c.f. Whistler R.L. in "Methods in Carbohydrate Chemistry, Vol.III, Academic Press, London 1963.

63.) Green, J.W., "Drying and Reactivity of Cellulose in
64.) Ref. 62, p.95.

65. Merchant M.V., Tappi 1957, 40, 771.

66. Bikales N.S., Segal L. Cellulose and Cellulose Derivatives, High Polymers Part IV, Publ.Interscience 1972.

67. Kuhn L.P., J.A.C.S. 1952, 74, 2492.

68. Rowen J.W., *et al*, J.Natl.Bur.Std. 1947, 39, 133.

69. Mitchell J.A. Annal.Chem.1957, 29, 499.

70. Marriann H., Mann, J. J.Appl.Chem. 1954, 4, 204.

71. Barker S. *et al* , J.Chem.Soc. 1954, 3468.

72. Higgins H.G., J.Aust.Chem.Soc. 1957, 10, 496.

73. Higgins H.G., J.Polym.Sci. 1961, 51, 59.

74. Kuhn, L. Annal.Chem. 1950, 22, 276.

75. Siegbahn, K. E.S.C.A. Applied to Free Molecules Uppsala 19.

76. Millard, M. Surface Characterisation of Biological Materials by X.P.S. West Regional Res.Centre, Albany, California.

77. Soignet, D. Reps.U.S. Agric.Res.Services. S.Region, 1975, ARS 5-60, 6-18.

78. Gray, D. Cell.Chem.and Tech. 1978, 12, 735.

79. c.f. Macdonald, Historical Papers on Modern Explosives, London and N.Y. 1912.

80. c.f. Marshall, History of Explosives, 2nd Ed.London 1917.

81. Parkes, c.f. Miles F.D. in Cellulose Nitrate (ref. 41).

82. Lewis, T.J., J.Appl.Polym.Sci. 1979, 23. 2661-2671.

83. Trommel J. Commun. N.V. Konninkl.Ned. Springstaffenfabrieken Amsterdam, No. 13.

84. Bouchonnet, Trombe, Petitpas, Mem Des Poudres, 1938, 28, 277.

85. Berl E., Smith, Ber.Der Deutsch Chem.Ges. 1908, 41, 1837.

86.)
87.) Bouchonnet, Mém Des Poudres et Saltpetre, 1838, 28. 295.
88.)
89.)

90. Chedin, Mém Des Services Chem. de L'Etat, 1944, 31, 113.

91. Blay, N.J. in 'Chemical Problems Connected with the Stability of Explosives', Ed. Hansson J. Proceedings 1973 at Sektionen F. Detonik Forbranning, Sundyberg, Sweden.

92. Gagnon, P. Can.J.Chem. 1958, 36, 212.

93. c.f. Worden, E.C. "Technology of Cellulose Esters" Eschenbach Printing Co. Easton Pennsylvania, 1928, Vol.I, Part 3, p.2325.

94. c.f. Ref. 93, page 2354.

95. Smith, A.C. Ardeer 1947.

96. Kullgren T. Svensk Kem Tidskr 1944, 56 221.

97. Gagnon, P. Can.J.Chem. 1958, 36, 212, 673, 695 and 1041.

98. Clark, D.T., Stephenson, P.J. Proceedings of Waltham Abbey Conference 1980, publ.Plenum Press, Ed. T.J. Lewis.

99. c.f. Jones D. in ref. 66.

100. Atkins E.D.T. Polymer, 1978 19, 1371.

101. Jones D. in 'Cellulose and Cellulose Derivatives', Part IV High Polymers Vol.V. Wiley Interscience, 1971, London.

102. c.f. Bragg, W.H. Bragg W.L. in X-rays and Crystal Structure, G. Bell and Sons, London, 1924.

103. c.f. Mathieu M. 1936, l.c. p.41 c.f. F.D.Miles, J.Phys. Chem. 1930, 34, 2607.

104. Clark, D.T. Stephenson, P.J., Polymer 1981 in press.

105. Matthieu Trans.Far.Soc. 1932, 24, 132.

106. Manley, R.St.J., J.Polym.Sci., 1965 B3 691.

107. Frey Wyssling A. Biochim.Biophys.Acta 1955, 18, 166-8.

108. Sponsler O.L. Protoplasma 1931, 12, 241.

109. Lewis T.J. Unpublished data.

110. Berl E. Klaye R. Z.des Gesamte Scheiss-und Springstoffen-wessen. 1907.

111. Fabel K. Nitrocellulose, 1934, 10, 3-5 and 24-26.

112. Demougin P. Mém Des Poudres, 1930, 24. 147-156.

113. Bonnet J. Mém Des Poudres, 1930, 24, 157-173.

114. Waltham Abbey Report No. TR109, pg. 22.

115. Lewis T.J. M.O.D. P.E.R.M.E. Report TR109. Waltham Abbey Essex and Polymer 1978, 19(3).

116. Desmaroux M. Mém des Poudres 1931, 24, 265.

117. History of Modern Explosives, R.I.C. Lectures 1958-60, No. 5.

118. Scott K.T.B. A.R.D., Explosives Report. 53/43. 1943.

119. Lewis T.J. Unpublished work, P.E.R.M.E.

120. Ayerst, R.P., A.D.P.A. Conference, 1977.

121. Lemanceau L., Stephan, N., Proceedings of Waltham Abbey Conference, 1980 Publ.Plenum Press.

122. Soignet, D.M., J.A.P.S. 1976, 20 2483-2495.

123. Millard, M. West Regional Labs., Agric.Res. Services, Dept. of Agric. Berkely California, 94710.

124. Dorriss G. Gray, D. Cell.Chem. and Tech. 1978, 12, 722-734.

125. Davidson, G. 1940, 31, T81-96, J.Text.Inst.

126. Sookne A. Am.Dyestuff Reptr., 1940, 29 333.

127. Head, F.S., J.Text.Inst. 1953. 44, T209-23.

128. Herzog, R.G., J.Phys.Chem. 1926, 30 458.

129. Kratky O. Kolloid Z. 1955, 70, 14.

130. Dolmetsch, H. Kolloid Z. 1962, 185, 106.

131. Schweiger, R.G. 1974, 57, 86-90, J.Polym.Sci.

132. Assaf, A.G. Haas, R.H., J.A.C.S. 1944, 66, 59.

133. Wu, T.K. Macromolecules 1980, 13, 74-79.

134. Sobue H. Tappi, 1956, 39, 415.

135. Schlatter. H. Chem.Met.Eng. 1921, 25, 281-86.

136. Heuser, Chemistry of Cellulose, Chapman and Hall, London, 1944.

137. Dorée, M. Methods of Cellulose Chemistry, Chapman and Hall, London, 1947.

138. Connor, R.T., High Polymers Part V Cellulose and Cellulose Derivatives, Part IV 51-87, 1971.

139. Hallwachs, W., Wied,Ann., 1888, 33, 301.

140. Broglie M. de. Compt. Rend, 1921, 172, 274.

141. c.f. Robinson, H. Phil.Mag., 1914, 28, 277.

142. Siegbahn, K. *et al* , Nucl.Phys. 1956, 1, 137.

143. Nordling C., *et al*, Phys.Rev. 1957, 105, 1676.

144. Siegbahn, K., Nordling, C. Fahlman, A.. *et al* ,'E.S.C.A. Atomic, Molecular and Solid State Structure Studied by Means of Electron Spectroscopy', Almquist and Wiksells, Uppsala, 1967.

145. Siegbahn K., Nordling C., Johansson, G., *et al*, "E.S.C.A. Applied to Free Molecules", North-Holland Publ.Co., Amsterdam, 1969.

146. Clark, D.T., 'Structure and Bonding in Polymers as Revealed by E.S.C.A.' in 'Electronic Structure c.f. Polymers and Molecular Crystals', Eds. J. Ladik and J.M. Andre, Plenum Press, New York, (1975).

147. Wagner, C.D., Anal.Chem. 1979, 51, 466.

148. Rosen, A. and Lindgren, I., Phys.Rev. 1968, 176, 114.

149. Bagus, P.S., Phys.Rev. 1965, 139A, 619.

150. Shirley, D.A. in 'Advances in Chemical Physics', 23, 85, Ed. I. Prigogine and S.A. Rice, Wiley, New York, 1973.

151. Gelius, U. and Siegbahn, K., Farad.Disc.Chem.Soc., 1972, 54, 257.

152. Snyder, L.C., J.Chem.Phys. 1971, 55, 95.

153. Adams, D.B. and Clark, D.T., Theoret.Chim.Acta., 1973, 31, 171.

154. Clark, D.T., 'Chemicals Aspects of E.S.C.A.' in Electron Emission Spectroscopy', Ed. W. Dekeyser and D. Reidel. D. Reidel Publishing Company, Dordrecht, Holland, 373, 1973.

155. Murrell, J.N. and Ralston, B.J., J.Chem.Soc.Farad.Trans. II, 1972, 68, 1393.

156. Schwartz, M.E., Chem.Phys.Lett., 1970, 6, 631.

157. Shirley, D.A. Chem.Phys.Lett. 1972, 15, 325.

158. Jolly, W.L. and Hendrickson, D.N., J.Amer.Chem. Soc., 1970 92, 1863.

159. Clark, D.T., Cromarty, B.J., Dilks, A. J.Polym.Sci. Polym.Chem., Ed. 1978, 41, 193.

160. Koopmans, T.A., Physika, 1933, 1, 104.

161. Ascarelli, P. and Missoni, G. J.Electron Spec. 1974, 5 417.

162. Carlson, T.A. and McGuire, G.E., J.Elect.Spec. 1972. 1, 161.

163. Fadley, C.S. Baird, R.J. Siekhaus W., J.Elect.Spec. 1974, 4, 93.

164. Schofield, J.H., Laurence Livermore Laboratory Report U.C.R.L.-51326, Jan. 1973.

165. Schofield, J.H., J.Elect.Spec. 1976, 8, 129.

166. Giese, A.T. and French, C.S., Appl.Spectr. 1955, 9, 78.

167. Vanderbilt, J.M. and Henrich C., Appl.Spectr., 1963, 7, 171.

168. Gunden, E. and Kaplam, B. J.Opt.Soc.Amer. 1965, 55, 1094.

169. Smith, H.F., P-E, UV/FL Prod.Dept.Tech. Memo No. 34, 1980.

170. Dilks, A. Ph.D. Thesis, University of Durham 1977, in 'The Application of E.S.C.A. to Structure Bonding and Reactivity of Some Polymer Systems'.

171. Wagner, C.D., Farad.Disc.Chem.Soc. 1975. 60, 306.

172. Drummond, I.W. and Errock, G.A. Gec.J.Sci.Tech. 1974, 41. 94.

173. Purcell. E.M., Phys.Rev. 1938, 54, 818.

174. Helmer, J.C. and Weichert. N.H., Appl.Phys.Lett. 1968, 13. 268.

175. Pople, J.A. and Scheider, W.G.: High Resolution N.M.R. McGraw-Hill New York, 1959.

176. Becker, E.D., High Resolution, N.M.R. Academic Press, New York 1969.

177. Bovey, F.A. Nuclear Magnetic Resonance Spectroscopy Academic Press, New York. 1969.

178. Emsley, J.W. High Resolution N.M.R. Spectroscopy vols. 1 and 2, Pergamon Press, Oxford, 1965.

179. Breitmaeir, W., Voelter, ^{13}C N.M.R. Spectroscopy, Verlag Chemie GmbH. Weinheim/Bergstrasse, 1974.

180. Lamb, W.E., Phys.Rev. 1941, 60, 817.

181. Cooley, J.W., Math.Comput. 1965, 19, 296.

182. Noggle, J.H. and Schirmer, R.E., The Nuclear Overhauser Effect, Chemical Applications, Academic Press, New York, and London 1971.

183. Kaplan, J.I. J.Chem.Phys. 1957, 27, 1426.

184. Perlin, A.S. and Casu, B., Canad.J.Chem. 1970 48 2599.

185. Dormann, D. J.A.C.S. 1871, 93, 4463.

186. Bragg, W.L., The Crystalline State, 1-2, Bell & Sons, London 1933.

187. Kerr, Optical Mineralogy, McGraw-Hill, New York, 1959.

188. Meridith, R., J.Appl.Phys. 1953, 4, 369.

189. Kohlbeck, J., J.A.P.S. 1976 20(1), 153-6.

190. Briggs, D. 'Handbook of Photoelectron Spectroscopy', Heyden 1975.

191. Henke, B.L. Adv.X-ray Analysis 1969, 13, 1.

192. Manne, R. and Åberg, T. Chem.Phys.Lett. 1970, 7, 282.

193. c.f. Shuttleworth, D. Ph.D. Thesis 1978. University of Durham.

194. Pauli, W., Naturwisschaften, 1924. 12. 741.

195. Huang, J.J. Rabelais, J.W. and Ellison, F.O., J.Elect. Spec. 1975, 6, 85.

196. Einstein, A., Ann Phys. 1905, 17 132.

197. Perlin A.S. and Hamer, G K. in ^{13}C N.M.R. in Polymer Science'. Ed. W.M. Pasika, Publ.Chem. Inst. of Canada, 1979.

198. Pyfe, C. Marchessault, R., unpublished work.

199. Wright, F.E. The Transmission of Light Through Transparent Inactive Crystal Plates. Am.J.Sci. 4th ser.Vol.31, pp.193-211, 1911.

200. c.f. Optical Crystallography, Wahlstrom, J.Wiley and Sons. New York, 1979.

201. c.f. Crystals and the Polarising Microscope, Hartshone, N.H. and Stuart, A. Publ.Arnold 3rd.Ed. 1960.

202. Clark, D.T., "E.S.C.A. Applied to Polymers" in Advances in Polymer Science, 1978, 24, 126. Springer-Verlag, Heidelberg.

203. Clark, D.T. and Harrison, A., J.Polym.Sci. Polym.Chem.Ed. in press.

204. Clark, D.T. in "Characterisation of Polymers by Means of Photon, Ion and Electron Probes", A.C.S. Symposium Series, Ed. H.R. Thomas and D.W. Dwight, 1980, in press.

205. Trommel, J., Communication No. 15, 1959 of the N.V. Koninklijke Nederlandsche Springstoffen-Fabrieken Henengrucht 204, Amsterdam-C. The Netherlands.

206. Murray, G.E. and Purves, C.B., J.A.C.S., 1940, 62, 3197.

207. Mitchell, R.L. Analytical Chem., 1949, 21 1496.

208. Svetlov, B.S., Kinet Katal 1972, 13, 792.

209. Penn, D.R., J.Elect.Spec. and Rel.Phen. 1976, 9, 29.

210. Clark, D.T. and Thomas, H.R., J.Polym.Sci.Polym.Chem.Ed. 1977, 16.

211. Kirk, P.L., Analytical Chem. 1950 22(2) 354.

212. Bradstreet R.B., in 'Kjeldahl Method for Organic Nitrogen' Academic Press, 1965. New York.

213. Trommel, J. Communication No. 13 1955 of the N.V. Koninklijke Nederlandsche Springstoffen-Fabrieken, Henengrucht 204, Amsterdam-C, The Netherlands.

214. Lewis, T.J., J.A.P.S. 1979, 23, 2661-2667.

215. Leader, B. Analyt.Chem. 1973. 45(9), 1700-1706.

216. Bragg, W.L., Proc.Roy.Soc.A. 1924, 105, 370

217. c.f. Rabek, J.F. 'Experimental Methods in Polymer Chemistry', Wiley Interscience. New York, 1980.

218. Lewis, T.J. in preparation, 1981.

219. Clark, D.T., Munro, H., Stephenson. P.J. unpublished work.

220. Schubert, H., Proceedings of conference on Lifetime of Rocket Propellants and Explosive Charges, 1971, Inst.Fur Chemie der Treib-und Exposivstoffe Jahrestagung 71, Karlsruhe, Germany.

221. Hansson, J. Chemical Problems Connected with the Stability of Explosives, Symposium Proceedings 1973. Sket.F.Detonik och Forbranning. Jonköping. Sweden.

222. Desai, R.L. Dept. of Forestry and Rural Development of Canada, Ottawa, Technical Paper T322.

223. Phillips, L. Nature 1950, 165 564.

224. Wallace, I.G., and Powell, R.J., 5th Symposium on Chemical Problems Related to Stability of Explosives, Bastad, Sweden, 197..

225. Stuart, R.D., Ahad, E., and Perrault, G., "Conference on Standardisation of Safety and Performance Tests for Energetic Materials", U.S. Arradcom Dover, N.J. 21-23. June 1977.

226. Baugh, P.J. in Cellulose and Cellulose Derivatives Part V, Eds. Bikales N.S., Segal L. High Polymers vol.5, Wiley Interscience, 1971.

227. Ranby, B, and Rabek, J.F. 'Photodegradation, Photo-oxidation and Photostabilisation of Polymers', Wiley Interscience 1975, London.

228. Clark, D.T., and Munro, H.S. in preparation.

229. Robinson, J.W., Handbook of Spectroscopy, vol.I. C.R.C. Press 1974.

230. Hesse, R.H., Adv.Free Radicals 1967, 3. 83.

231. Heusler, K., Agnew Chem.Intermat.Edn. 1964, 3, 525-538.

232. Akhtar, M., Adv. Photochem. 1966, 2, 263.